Characterisation of the differentiation process of induced pluripotent stem cells (iPSCs) into mesenchymal stem cells (iMSCs)

University of Oxford

Nuffield Department of Orthopaedics, Rheumatology and Musculoskeletal Sciences (NDORMS)

St Catherine's College

Florentine Timmer

Submitted in partial fulfilment of the requirements for the degree of Master of Science by Research

Trinity Term 2018

Abstract

Mesenchymal stem cells (MSCs) are adult stem cells derived from soft tissue or bone marrow (BM) and are widely investigated due to their multi-potential differentiation and immunomodulatory abilities. They are skeletal lineage progenitors, being able to differentiate into various cell types including osteoblasts, adipocytes, chondrocytes, myocytes and more. However, MSCs are limited for use in clinical settings and for *in vitro* purposes. The main limitation for *in vitro*-based research is cell senescence, which occurs during sub-culturing of MSCs. MSC-like cells, termed induced MSCs (iMSCs), are derived from induced pluripotent stem cells (iPSCs) and display similar characteristics as MSCs. Yet, these iMSCs are not restricted by senescence, making them an attractive alternative source. The differentiation of iPSCs into iMSCs has been recently described, however mechanisms that underlie this process and the comparison between iMSCs and BM-MSCs are largely lacking.

This study aimed to identify a suitable protocol for the differentiation of iPSCs into iMSCs. The chosen protocol consists of a 14-day phase 1 followed by a passaging protocol, thus selecting for cells primed for stable differentiation into the mesenchymal lineage. Detailed characterisation of the mechanistic actions during the differentiation was documented. Moreover, iMSCs were compared to BM-MSCs on a proteomic and transcriptomic level. Known mesenchymal stem cell (MSC) and pluripotency markers expression levels were measured using mass cytometry (CyTOF) and RNA sequencing techniques. Results display a gradual loss of pluripotency gene and protein expression as well as an upregulation of MSC markers, indeed indicating a shift towards a more mesenchymal-like stem cell type. However distinct features between bone-marrow derived MSCs and iMSCs are observed, including an apparent lack of adipogenic differentiation in iMSCs despite osteogenic differentiation potential.

Acknowledgements

I would like to express my sincere gratitude to Professor Udo Oppermann for taking me on as a student, Dr. Martin Philpott for his daily supervision and both for their guidance and encouragements throughout the project. I am very grateful to all present and past members of the Oppermann group for the useful discussions in group meetings, sharing their expertise and creating a fun and friendly work environment. In particular, I would like to thank Martin for teaching me lab techniques, Jim for helping with the RNA sequencing library preparation and Graham for his assistance regarding qPCR and many other things. Thank you to Manman for teaching me how to use FACS and CyTOF, Ruth for iPSC-related enquiries and Steph for helping me with the immunofluorescence. Also, a big thank you to Reshma, for helping me with all of the RNA seq analysis. During my time in the Botnar Research Centre, I am grateful to have met many amazing and inspiring students and staff. I would also like to thank Dr. Sally Cowley (the James Martin Stem Cell Facility, Sir William Dunn School, Oxford) for supplying me with iPSCs and for teaching me how to culture them.

I feel extremely fortunate to have been given the opportunity to study at the University of Oxford, particularly to execute my project at the Nuffield Department of Orthopaedics, Rheumatology and Musculoskeletal Sciences. A special thank you to Afsie and Sam for their kind and welcoming attitude and for answering all technical questions regarding the MSc(Res). Importantly, this research would not have been possible without generous funding from Arthritis Research UK and the VSBfonds.

During the last two years, I have been privileged to meet wonderful people making my time in Oxford so special. To my co-students Chao and Henry, thank you for helping me with lab

related enquiries, but more importantly thank you for making my time in the lab so much more fun. To my best Botnar buddy Quitterie, I am happy we came to Oxford at the same time. I have had so much fun with you, talking about anything over tea or a pint (a pint more often than we would like to admit). I will miss our late-night lab sessions, drinks at the Butchers Arms and the many times we've gone out for a party. Of course, thank you to my college friends and Oxford hockey club Ladies 1s for being a source of support, encouragement and entertainment. And to my favourite Dutchies Linda, Anne and Karlijn, I have had so much fun with you and feel very fortunate to have met you during my time in Oxford. Finally, I would like to thank my parents, brothers and David for always being supportive and providing counsel.

Contents

Chapter 1 Introduction……14

1.1 Stem cells……..14

1.2 Induced pluripotent stem cells (iPSCs)…….16

1.2.1 Signalling pathways and mechanisms of pluripotency maintenance ……..17

1.2.2 Epigenetic mechanisms in iPSCs……..21

1.3 Mesenchymal stem cells (MSCs)……...……..24

1.3.1 Clinical and *in vitro* applications and limitations of MSCs……..27

1.4 Induced mesenchymal stem cells (iMSCs)……...…30

1.4.1 iMSC derivation……30

1.5 Differentiation of iMSCs…….....36

1.5.1 Osteogenesis…….....36

1.5.2 Adipogenesis…….37

1.6 Tools for characterisation of iMSCs…….....39

1.7 Study aims……41

Chapter 2 Materials and Methods……...42

2.1 Cell culture……42

2.1.1 hiPSCs cell culture…….……...42

2.1.2 Production of Geltrex-coated plates……..…….....43

2.1.3 Passaging of iPSCs…….....43

2.1.4 Thawing and freezing down of iPSCs…….…….....44

2.1.5 hBM-MSCs cell culture…….……...45

2.1.6 Passaging BM-MSCs…….……...46

2.1.7 Thawing and freezing of BM-MSCs……..……...…46

2.2 Differentiation conditions……47

2.3 Immunofluorescence…….50

2.4 Fluorescence-activated cell sorting (FACS) ……53

2.5 Colorimetric assays……...55

2.5.1 Alizarin Red Staining……....55

2.5.2 Oil Red O……..55

2.6 Alkaline phosphatase (ALP) assay……..…….56

2.7 Mass cytometry (CyTOF) ……..……...57

2.7.1 Metal conjugation of FACS antibodies……....59

2.8 RNA sequencing (RNA-seq) ……..……60

2.8.1 RNA extraction ……61

Chapter 3 Results……...……...62

3.1 Comparison of iMSC differentiation protcols……...……..….62

3.1.1 Cell viability……..62

3.1.2 Cell morphology……...63

3.1.3 Immunofluorescence……69

3.1.4 Summary……...73

3.2 Continuation of protocol comparison – Focus on two conditions: αMEM and MesenPro……..75

3.2.1 Assessment of morphology and viability……..75

3.2.2 Immunofluorescence ……....79

3.2.3 Alkaline phosphatase (ALP) assay……...82

3.2.4 Alizarin Red Staining (ARS) and Oil Red O (ORO) ……...85

3.2.5 Summary……...89

3.3 In-depth analysis using CyTOF and RNA sequencing…….90

3.3.1 Protein expression measurements using CyTOF……..90

3.3.2 Gene expression profiling using RNA sequencing…….....98

3.3.2.1 Gene expression changes during iPSC to iMSC differentiation

……...98

3.3.2.2 Gene expression comparison of iMSCs and BM-MSCs…….104

3.3.3 Summary…….....107

Chapter 4 Discussion…….....110

4.1 Future work…….118

Supplemental Data……...…119

References…….....128

List of Figures

1.1 Stem cell hierarchy……...15

1.2 Schematic overview of reprogramming methods for iPSCs……....17

1.3 Maintenance of pluripotent state through FGF2……..18

1.4 Endogenous maintenance of pluripotency in human iPSCs…….19

1.5 Waddington's epigenetic landscape……....21

1.6 Schematic iMSC usage……28

1.7 Cellular mechanism of dexamethasone (Dex)-induced osteogenesis……...37

1.8 Schematic overview of somatic cell reprogramming to iPSCs and differentiation of iPSCs into iMSCs……....41

2.1 Schematic overview of the three phases and experiments executed per phase……....49

2.2 Schematic overview of the RNA sequencing experiment……...….60

3.1 Cell morphology of various donor-condition combinations I……..65

3.2 Immunofluorescence staining I…….71

3.3 Cell morphology of various donor-condition combinations II……...…..77

3.4 Immunofluorescence staining II……...…80

3.5 Alkaline phosphatase (ALP) assay performed at day 7 after the start of differentiation into osteoblasts using a dexamethasone-based medium……...…84

3.6 Alizarin Red Staining (ARS) and Oil Red O (ORO) staining for detection of mineralized nodules and lipid fat droplets, respectively I……...…..86

3.7 Alizarin Red Staining (ARS) and Oil Red O (ORO) staining for detection of mineralized nodules and lipid fat droplets, respectively II……...88

3.8 Protein expression levels during the iPSC into iMSC differentiation process…...…..93

3.9 Heatmap representing gene expression changes during the iPSC into iMSC differentiation process. ……...…...102

3.10 Principal Component Analysis (PCA) plot representing iPSC into iMSC differentiation……103

3.11 Principal Component Analysis (PCA) plot comparing iMSCs with BM-MSCs……104

3.12 Heatmap of differentiatlly expressed genes (DEGs) between iMSCs and BM-MSC……..……...…105

S1 Clustered heatmap of gene expression changes during iPSC into iMSC differentiation…….....119

S2 Clustered Gene Ontology (GO) Enrichment Analysis for the iPSC into iMSC differentiation process I……..119

S3 Clustered Gene Ontology (GO) Enrichment Analysis for the iPSC into iMSC differentiation process II…….120

S4 Clustered Gene Ontology (GO) Enrichment Analysis for the iPSC into iMSC differentiation process III……...120

S5 Epigenetic Factors (EFs) differentially expressed per cluster during the iPSC into iMSC differentiation process……..121

S6 Transcription Factors (TFs) differentially expressed per cluster during the iPSC into iMSC differentiation process……..122

S7 Gene Ontology (GO) Enrichment Analysis “pathway maps” comparing iMSCs with BM-MSCs……...126

S8 Gene Ontology (GO) Enrichment Analysis “process networks” comparing iMSCs with BM-MSCs……...126

S9 Gene Ontology (GO) Enrichment Analysis “GO processes” comparing iMSCs with BM-MSCs……...127

List of Tables

1.1 A list of pluripotency marker ……...20

1.2 A list of mesenchymal stem cell markers……...26

2.1 Medium conditions for iPSC into iMSC differentiation I……47

2.2 Medium conditions for iPSC into iMSC differentiation II……...48

2.3 Osteoblast and adipocyte differentiation conditions ……...48

2.4 Pluripotency and mesenchymal stem cell-related antibodies for immunofluorescence ……52

2.5 Pluripotency and mesenchymal stem cell-related antibodies for FACS…….....53

2.6 Antibody list for mass cytometry (CyTOF)…….58

3.1 Cell viability of differentiating iPSCs induced through various protocols……..63

3.2 List of genes related to epithelial-mesenchymal transition (EMT) and their function ……...101

Abbreviations

(h)ESC	(human) embryonic stem cell
(h)iPSC	(human) induced pluripotent stem cell
(h)MSC	(human) mesenchymal stem cell
iMSC	induced mesenchymal stem cell
(h)BM-MSC	(human) bone marrow mesenchymal stem cell
PGC	primordial germ cell
ICM	inner cell mass
Oct4/POU5F1	octamer-binding transcription factor 4
Sox2	sex-determining region Y-box2
Klf4	kruppel like factor 4
Lin28	lin-28 homolog A
Nanog	nanog homeobox
OSKM	Oct4, Sox2, Klf4, c-Myc
FGF2/bFGF	fibroblast growth factor 2/basic fibroblast growth factor 2
MAPK	mitogen-activated protein kinase
ERK	extracellular-signal-regulated kinase
BMP	bone morphogenetic protein
IGF	insulin-like growth factor
SSEA-4	stage-specific embryonic antigen-4
TRA-1-60/PODXL	podocalyxin
TRA-1-81/PODXL	podocalyxin
TNAP	tissue non-specific alkaline phosphatase
ALP	alkaline phosphatase
PPi	pyrophosphate
Pi	organic phosphate
HA	hydroxyapatite
DNA	deoxyribonucleic acid
TrxG	Trithorax-group
PcG	Polycomb-group
H3K4me3	trimethylation of lysine 4 on histone 3
H3K36me3	trimethylation of lysine 36 on histone 3
H3K9me3	trimethylation of lysine 9 on histone 3
H3K27me3	trimethylation of lysine 27 on histone 3
Jhdm	Jumanji domain-containing histone demethylase
PRC2	polycomb repressive complex 2
Ehmt2	euchromatic histone-lysine N-methyltransferase 2
DNMT	DNA methyltransferase
CpG	cytosine-phosphate-guanine
ISCT	International Society for Cellular Therapy
CD	cluster of differentiation
GvHD	graft-versus-host disease
CRISPR	clustered regularly interspaced short palindromic repeats
FACS	fluorescence activated cell-sorting
EB	embryonic body
ECM	extracellular matrix
ROCK	Rho-associated, coiled coil containing protein kinase
p-MLC	myosin-light-chain phosphatase

AA	L-ascorbate-2-phosphate
PDGF	platelet-derived growth factor
TGF-β	transforming growth factor β
Dex	dexamethasone
RGD	Arg-Gly-Asp
MMP	matrix metalloproteinase
EMT	epithelial-mesenchymal transition
FBS	fetal bovine serum
GTP	guanosine triphosphate
FN1	fibronectin-1
SNAI	snail family transcriptional repressor
LEF1	lymphoid enhancer binding factor 1
GR	glucocorticoid receptor
FHL-2	four and a half LIM protein 2
MKP-1	mitogen-activated protein kinase phosphatase 1
TAZ	tafazzin
RUNX2	runt-related transcription factor 2
TCF	T-cell factor
Col1	type I collagen
IBMX	3-isobutyl-1-methylxanthine
PPARγ2	peroxisome proliferator-activated receptor γ2
C/EBPβ	CCAAT-enhancer-binding protein β
cAMP	cyclic adenosine monophosphate
RNA seq	ribonucleic acid sequencing
CYTOF	mass cytometry
TOF	time-of-flight
cDNA	complementary deoxyribonucleic acid
mRNA	messenger ribonucleic acid
NGS	Next Generation Sequencing
E8	Essential 8
P/S	penicillin/streptomycin
DMEM	Dulbecco's Modified Eagle Medium
KO	Knock-Out
EDTA	ethylenediaminetetraacetic acid
DMSO	dimethylsulfoxide
PBS	phosphate-buffered saline
αMEM	Minimum Essential Medium Eagle – Alpha modification
KOSR	knockout serum replacement
NEAA	nonessential amino acids
IMDM	Iscove's Modified Eagle Medium
MP	MesenPro RS
OSM	Oncostatin M
ARS	Alizarin Red S
ORO	Oil Red O
IF	immunofluorescence
NGS	normal goat serum
RT	room temperature
PBST	PBS Tween20
Ig	immunoglobuline
MQ	MilliQ

pH	potential of hydrogen
EtOH	ethanol
4-MUP	4-Methylumbelliferyl phosphate
TRIS	tromethamine
CSB	Cell Staining Buffer
PFA	paraformaldehyde
bp	basepair
RNA	ribonucleic acid
P	passage
ng	no geltrex
g	geltrex
AD	adipocyte
D	day
tSNE	T-distributed stochastic neighbor embedding
PCA	principal component analysis
PC	principal component
DEG	differentially expressed gene
TF	transcription factor
EF	epigenetic factor
GO	gene ontology
HIF1A	hypoxia-inducible factor 1A
ZEB	zinc finger E-box binding homeobox
EGFR	epidermal growth factor receptor
CTNNB1	catenin-β1
CDH1	E-cadherin
ILK	integrin linked kinase
TWIST1	twist-related protein 1
IGF1R	insulin-like growth factor receptor 1
ERBB2	proto-oncogene tyrosine kinase 2
MET	MET proto-oncogene, receptor tyrosine kinase
AKT1	protein kinase B
BSP	bone sialoprotein
OPG	osteoprotegerin

Chapter 1. Introduction

1.1 Stem cells

Stem cells are specialized cells characterized by their unlimited self-renewal capacities and their ability to differentiate into multi-lineage cells (Wei et al., 2013; Ullah et al., 2015) They are categorized by their potency – the ability of a stem cell to differentiate into other cell types. Totipotent cells are the most potent stem cells, followed by pluripotent stem cells and multipotent stem cells. Cells with the lowest potency are termed terminally differentiated 'somatic' cells (figure 1.1). Totipotent stem cells are the most potent cells, albeit they do not exist in the human body, as they refer to a fertilized egg cell - a zygote. Totipotent stem cells are thus known for their ability to differentiate into both embryonic stem cells (ESCs) and trophoblasts, the latter forming the outside layer of the blastocyst. The next level of stemness contains pluripotent stem cells, which includes embryonic stem cells (ESCs), primordial germ cells (PGCs) and induced pluripotent stem cells (iPSCs). The common feature of pluripotent stem cells is their ability to differentiate into any cell type of the three embryonic germ layers; ectoderm, endoderm and mesoderm (Romito and Cobellis, 2016). The blastocyst with its inner cell mass (ICM) comprises of ESCs, which later develops into an embryo. Induced pluripotent stem cells (iPSCs) are *in vitro* reprogrammed somatic cells representing a cell type similar in characteristics to the ESCs.

Multipotent stem cells, including mesenchymal and hematopoietic stem cells, represent a population with less differentiation potential compared to pluripotent stem cells. Even though multipotent stem cells were originally thought to have the capacity to solely differentiate into

one specific germ lineage, it remains ambiguous whether multipotent stem cells are actually limited to this one germ layer or that they have the ability to transdifferentiate into other lineages. Recent research points out that MSCs do indeed seem to be able to differentiate along all three lineages, although a difference in potency is present depending on their tissue of origin (Krabbe et al, 2015). BM-MSCs are able to differentiate along all three lineages *in vitro*, technically making them pluripotent stem cells (Ullah et al., 2015). However, it remains unknown whether this process occurs *in vivo* and/or whether this potentially means only a subset of the MSCs have this capability, referring to their known heterogeneous characteristics as a cell population (Ullah et al., 2015). Upon differentiation of the multipotent stem cell a terminally differentiated somatic cell presents.

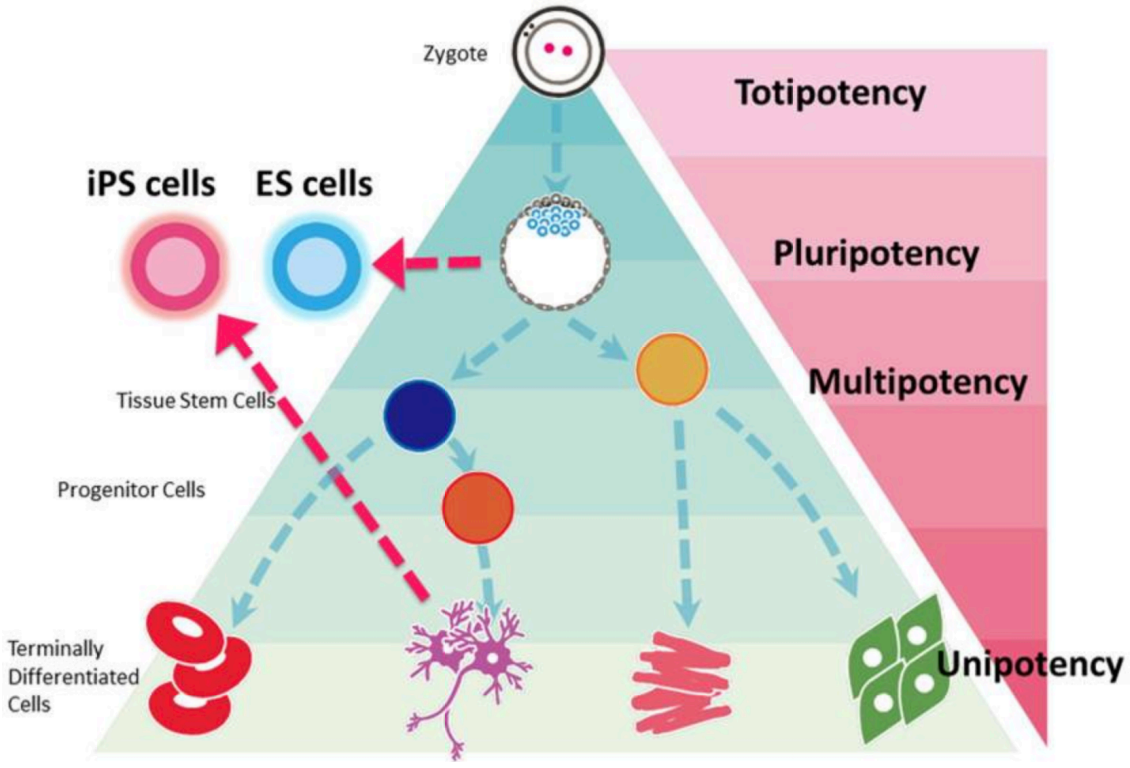


Figure 1.1 Stem cell hierarchy. At the top of the stem cell landscape, totipotent cells can form an entire new living organism. Moving down this ladder, every potency level lost is a specificity gained. Pluripotent stem cells include iPSCs (induced Pluripotent Stem Cells) and ESCs (Embryonic Stem Cells), which form the inner cell mass of the early blastocyst. Multipotent stem cells are less potent than pluripotent stem cells and upon differentiation form unipotent cells (Sugawara et al., 2012).

1.2 Induced pluripotent stem cells (iPSCs)

Induced pluripotent stem cells (iPSCs) were first introduced in 2006 by Takahashi and Yamanaka. They reprogrammed a somatic cell back into a stem cell. Mouse fibroblasts served as the precursor cell source for the first reprogrammed iPSCs. A cocktail of reprogramming factors - now referred to as the Yamanaka factors - containing the transcription factors Oct4 (octamer-binding transcription factor 4), Sox2 (sex-determining region Y-box2), c-Myc and Klf4 (kruppel like factor 4) (OSKM) were integrated into the mouse genome through retroviral transduction upon which the 3-4 week long reprogramming process started. After the first documentation of the successful reprogramming of somatic cells into pluripotent stem cells, other transduction tools including lentiviral transduction as well as non-viral reprogramming methods were introduced (figure 1.2) (Gonzalez et al., 2011; Warren et al., 2010). Moreover, other cell types such as blood cells, T cells and stem cells were also successfully tested as precursors for the iPSCs (Gonzalez et al., 2011). At present, the original OSKM factors or other varieties - including addition of Lin28 (lin-28 homolog A) and Nanog (nanog homeobox) - are used to initiate the reprogramming process. Furthermore, supplemental small compounds can be added to facilitate the reprogramming, thereby increasing the efficiency (Huangfu et al., 2008). These chemical compounds can alter the chromatin environment through various mechanisms, improving the time needed to complete reprogramming as chromatin remodelling is the rate limiting step during iPSC generation (Huangfu et al., 2008).

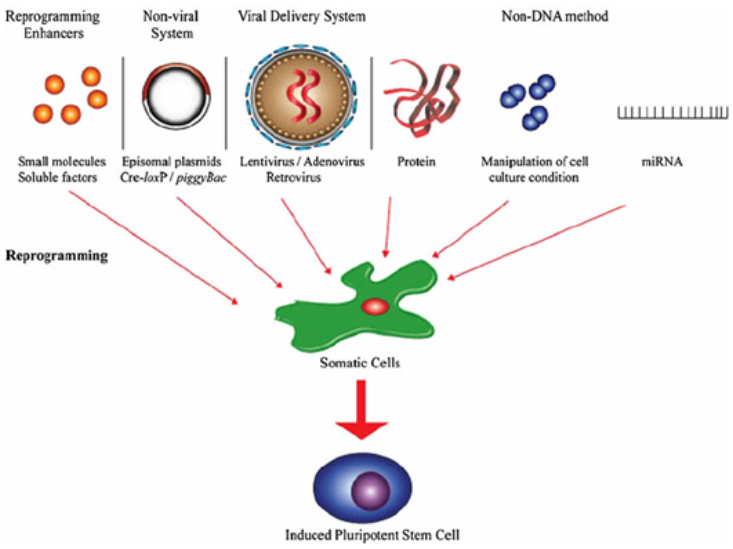


Figure 1.2 Schematic overview of reprogramming methods for iPSCs. These include both viral and non-viral as well as integrative and non-integrative methods. Furthermore, current reprogramming methods may be enhanced using small compounds. Reprogramming can be accomplished by use of a variety of somatic cell types (Lai et al., 2011).

1.2.1 Signalling pathways and mechanisms of pluripotency maintenance

Pluripotency in itself is thought to be an unstable state *in vitro* as specific culture medium composition, an extracellular matrix and exogenous growth factors are required to keep cells in such a state. This indicates that pluripotent cells might be primed for rapid differentiation (Johnson et al., 2008). In human pluripotent cells, fibroblast growth factor 2 (FGF2 or bFGF) is the main pluripotency maintenance element, exercising its function through three intracellular pathways (figure 1.3). FGF2 directly activates the MAPK/ERK (mitogen-activated protein kinases/extracellular signal-regulated kinases) pathway which in turn causes upregulation of the three main pluripotency transcription factors Nanog, Oct4 and Sox2. Moreover, it also activates downstream transcription of Nanog through the Activin/Nodal pathway by phosphorylation of Smad2/3. This pathway can also be directly activated through binding of Activin A to the receptor. FGF2 is responsible for the inhibition of Smad1/5

phosphorylation – both of which are part of the downstream signalling cascade of the BMP (bone morphogenetic protein) pathway (Pauklin et al., 2015; Bieberich et al., 2013). Without inhibition, the Smad-BMP pathway results in differentiation along the mesendodermal lineage. Other signalling pathways suggested to be involved in human cell pluripotency maintenance are the Wnt pathway through β-catenin activation, insulin-like growth factor (IGF) pathway, Notch pathway and Hedgehog pathway (Xue et al., 2011; Greenow et al., 2012; Dejosez et al., 2012; Chen et al., 2008; Xu et al., 2005). These pathways are, however, by themselves not sufficient to maintain pluripotency.

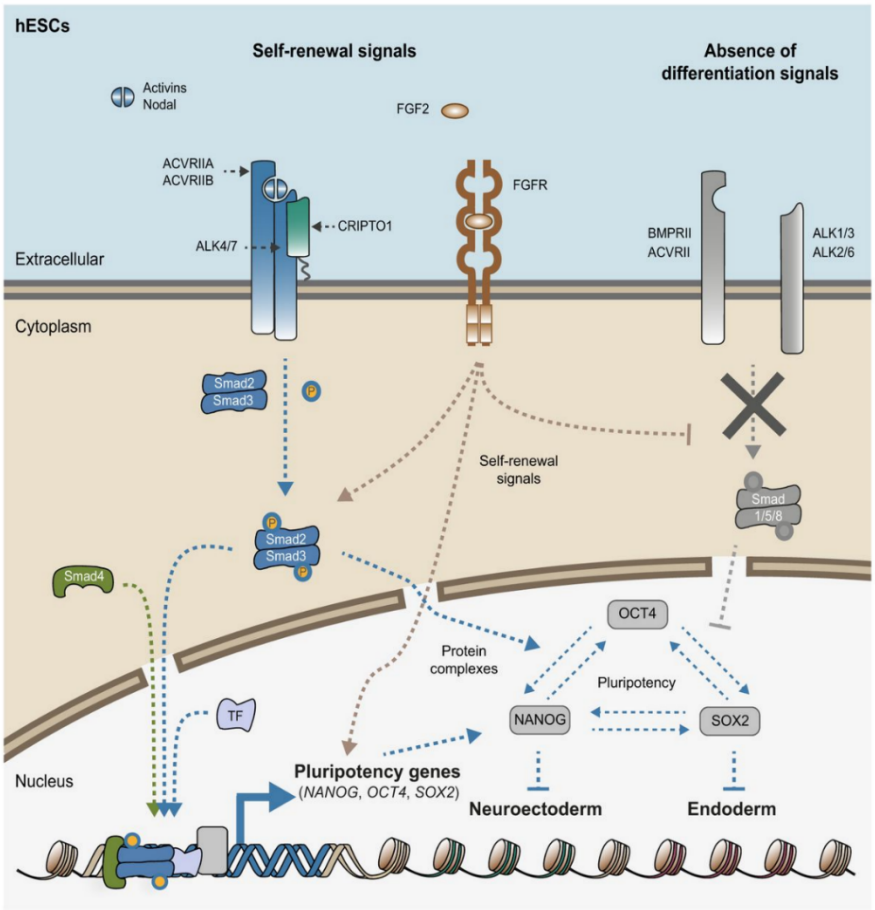


Figure 1.3 Maintenance of pluripotent state through FGF2. Pluripotent stem cells require upregulation of pluripotency transcription factors through exogenous FGF2. FGF2 exercises its functions through three intracellular pathways, either direct or indirect, affecting the gene expression of Nanog, Oct4 and Sox2. (Paukliin et al., 2015).

Acquiring a state of pluripotency is initiated through the activation of the before-mentioned signalling pathways and upon this, three main master regulators, the transcription factors Oct4, Sox2 and Nanog are activated. These transcription factors in turn initiate the expression of a cascade of genes needed to support the endogenous mechanisms underlying pluripotency. This establishes an auto- and cross-regulatory control of these transcription factors and related proteins. Other factors involved in the pluripotency cascade include Klf4 and c-Myc in human pluripotent stem cells (figure 1.4) (Johnson et al., 2008, Bieberich et al., 2013).

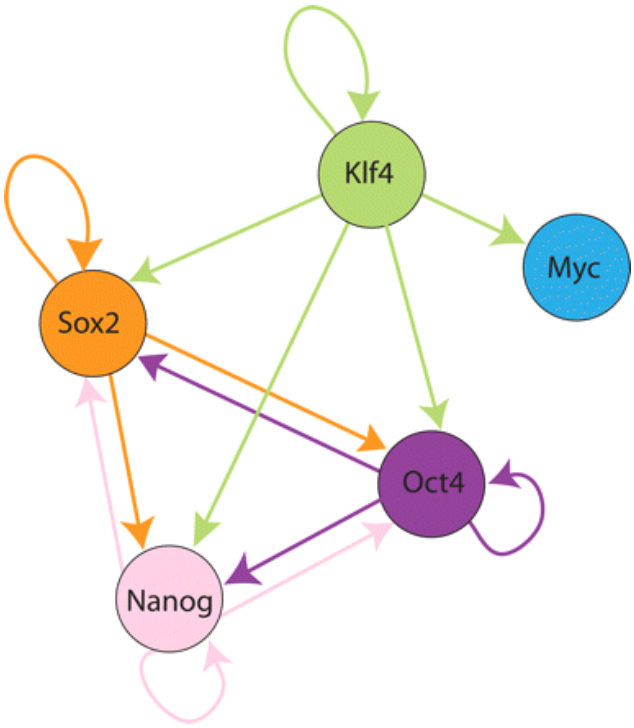


Figure 1.4 Endogenous maintenance of pluripotency in human pluripotent stem cells. The main regulators in pluripotency (Sox2, Nanog, Oct4 and others) need to become auto- and cross-regulated (Johnson et al., 2008).

Nanog, Oct4 and Sox2 are often used as defining factors in analysing the pluripotency state of a cell through immunofluorescence staining or flow cytometry. In addition to these three factors, more proteins can be used as a measure of pluripotency. Many of these markers were originally used in identifying human embryonic carcinoma cells, including stage-specific embryonic antigen-4 (SSEA-4), podocalyxin (TRA-1-60 and TRA-1-81) and tissue non-

specific alkaline phosphatase (TNAP) (International Stem Cell Initiative, 2007; Wright and Andrews, 2009). SSEA-4 is a glycosphingolipid and podocalyxin a sialoglycoprotein. Pluripotent cells are known to maintain a highly glycosylated profile, which distinguishes them from other cell types (Draper et al., 2002; Venable et al., 2005; Wearne et al., 2006, 2008; Satomaa et al., 2009). Alkaline phosphatase (ALP), specifically TNAP, is detectable during development of several tissues, although its role is most dominant in the developing skeleton where it acts as a catalyzer of the hydrolysis of pyrophosphate (PPi) into inorganic phosphate (Pi) for the formation of hydroxyapatite (HA) (Štefková et al., 2015). A list of these pluripotency markers can be found in table 1.1.

Pluripotency markers

	Full name	Localization	Function
Oct4/POU5F1	Octamer-Binding Transcription Factor	Nucleus	Transcription factor
Sox2	SRY-Box 2	Nucleus	Transcription factor
Nanog	Homeobox Transcription Factor	Nucleus	Transcription factor
SSEA-4	Stage Specific Embryonic Antigen	Cell surface	Glycosphingolipid – present in ESCs, iPSCs, EC, subset of MSCs
TRA-1-60/PODXL	T Cell Receptor Alpha 1-60	Cell surface	Glycoprotein - present in ESCs, iPSCs, EC
TRA-1-81/PODXL	T Cell Receptor Alpha 1-81	Cell surface	Glycoprotein - present in ESCs, iPSCs, EC
TNAP (ALP)	tissue nonspecific alkaline phosphatase	Cytoplasm	Several developmental processes, most dominant role in skeletal development

Table 1.1 A list of pluripotency markers. These markers are often used in gene and protein expression experiments to determine pluripotential capacities (Štefková et al., 2015; Hynes et al., 2014; Pomery et al., 2016; Sokolov et al., 2010).

1.2.2 Epigenetic mechanisms in iPSCs

Conrad Waddington coined the term epigenetics and thereby introduced the so-called Waddington epigenetic landscape (figure 1.5) (Waddington 1940; 1968). Epigenetics can be defined as ‘’the study of changes in gene function that are mitotically and/or meiotically heritable and that do not entail a change in DNA sequence’’ (Wu et al., 2001).

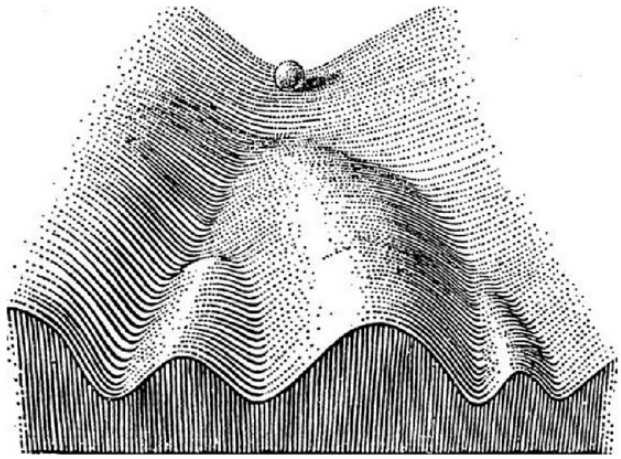


Figure 1.5 Waddinton's epigenetic landscape. This figure simulates a cellular hierarchical system whereby the ball at the top depicts a totipotent cell. As the cell differentiates along a certain lineage, it loses some of its potency irreversibly, here represented by the troughs and hills. Originally, it was thought a cell would not be able to go back to a higher potency level or transdifferentiate into a different lineage. However, it has been shown that cells are reprogrammable (e.g. iPSCs) and that (stem) cells are able to transdifferentiate into cells of other germ layers (Waddington 1940; 1968; Lin et al., 2014; Ullah et al., 2015).

Epigenetic modifications comprise many different processes, the most well-known being DNA (deoxyribonucleic acid) (de)methylation and histone modifications including methylation and acetylation (Huang et al., 2013; Dupont et al., 2016). Epigenetic mechanisms in chromatin modification - readers, writers and erasers - are needed to read, apply and erase these marks in order to control gene transcription orchestrated by transcription factors and the transcriptional machinery.

Upon reprogramming somatic cells into iPSCs, epigenetic marks are reorganized by inducing upregulation of pluripotency-related transcription factors (Lewitzky and Yamanaka, 2007; Godini et al., 2018). This reorganization places the somatic cells back into a ground state, creating pluripotent cells that move back to the top of the Waddington epigenetic landscape. iPSCs present many similar features compared to ESCs. ESCs barely contain epigenetic residue from their original cell types, referring to the near complete loss of DNA methylation patterns. This is followed by application of new tissue-specific epigenetic marks. iPSCs, in contrast to ESCs, are thought to retain certain marks related to their tissue of origin (Bar-Nur et al., 2011; Hu et al., 2010; Kim et al., 2011; Ohi et al., 2011).

iPSCs show, similar to ESCs, a distinct chromatin profile compared to tissue specific cells. Pluripotent stem cells, and thus iPSCs, are characterised by their more accessible euchromatin. This chromatin can be modified, as mentioned before. Histone modifications are mediated by Trithorax-group (TrxG) proteins and Polycomb-group (PcG) proteins (Boland et al., 2015). The most well-known include H3K4me3 (trimethylation of lysine 4 on histone 3), H3K36me3, H3K9me3 and H3K27me3. TrxG proteins catalyse trimethylation of H3K4, enhancing the reprogramming of somatic cells into iPSCs. Moreover, specific demethylation of H3K36me3 also enhances the efficiency of dedifferentiation mediated by Jhdm a1 and 1b (Jumanji domain-containing histone demethylases). H3K4me3 and H3K36me3 are both activating histone modifications. On the other hand, H3K9me3 and H3K27me3 are repressive histone modifications. PRC2 (polycomb repressive complex 2) deposits a trimethylation mark on H3K27 and is associated with gene silencing. Loss of PCR2 components reduce reprogramming efficiency of iPSCs (Onder et al., 2012; Buganim et al., 2012). Trimethylation of H3K9 results in a heterochromatin state, a more condensed version of chromatin, consequently resulting in the silencing of genes. Repression of

methyltransferases (including Ehmt2, Setdb1 and Suv39h1/2) related to the methylation of H3K9 in the histone complexes thus results in an increased reprogramming efficiency of somatic cells into iPSCs (Soufi et al., 2012; Sridharan et al., 2013). Reverse actions for the above-mentioned histone H3 domain modifications consequently result in a priming of pluripotent stem cells to start differentiating. DNA methylation is a heritable, yet reversible process and is guided by DNA methyltransferases (DNMTs) that catalyse the addition of a methyl group onto the DNA (Christman, 2002). There are two subtypes of DNMTs to be distinguished. DNMT3a and DNMT3b are *de novo* methyltransferases, applying new methyl groups to chromatin areas, most commonly in CpG rich areas also known as CpG islands. DNMT1 maintains the methylated sites rather than applying new groups (Altun et al., 2010). iPSCs are characterised by their hypomethylated chromatin profiles, methylating certain areas as differentiation into tissue-specific somatic cells occurs (Gladych et al., 2015).

1.3 Mesenchymal stem cells (MSCs)

Mesenchymal stem cells (MSCs) are a multipotent adult stem cell type that can be found throughout the body in many postnatal tissues including bone marrow (BM-MSCs), adipose tissue or umbilical cord. They also exercise their regulatory functions systemically through the controlled release of different factors (da Silva Meirrelles et al., 2006). First mentioned by Friedenstein and colleagues, they described these cells as an adherent fibroblast-like subset of the bone marrow microenvironment, specifically mentioning their capability of supporting haematopoiesis (Friedenstein et al., 1970; Jung et al., 2013). They later coined the term marrow stromal cells after identifying their stem cell properties as they were shown to be able to differentiate into numerous mesodermal tissues including fat, bone, cartilage and tendon (Parekkadan et al., 2010). The reason for their diverse set of characteristics is related to their heterogeneity as a cell population (Ullah et al., 2015). Even though the literature often describes these MSCs as one specific stem cell type, they most likely contain different subsets of cells within the larger population. Their heterogeneity is also the reason why MSC panels contain a broad range of markers. The International Society for Cellular Therapy (ISCT) have developed minimal criteria for defining multipotent mesenchymal stem cells (Dominici et al., 2006). These include upregulation (>95% of the population) of the three MSC-positive markers CD44 (sometimes interchangeably switched for CD73), CD90 and CD105, and no more than 2% of the population should express MSC-negative markers such as CD14, CD34 and CD45 - also known as hematopoietic stem cell markers. However, the expression of these cell surface markers is not limited to mesenchymal stem cells. Often, larger and more elaborate marker panels are used to further analyse the MSC population, including CD44, CD73, CD90, CD105, CD106, CD144, CD146, CD166, CD271 and Stro-1 as positive markers and CD14, CD34 and CD45 as negative (hematopoietic) cell markers. Also, because of cell surface marker similarities between MSCs and fibroblasts, it remains

difficult to distinguish between these two cell types. Within this panel, CD106 and CD146 have been suggested to discriminate between the two (Halfon et al., 2011). MSCs of early passage are known to possess higher levels of CD106 and CD146 cell surface markers compared to later passage MSCs. At a later passage, the heterogeneous MSC population is believed to contain a higher ratio of fibroblasts which would be related to the gradual loss of osteogenic potential of late passage MSCs (Halfon et al., 2011). Other MSC surface markers are not known to change throughout the serial passaging. Hence, the cell surface markers CD106 and CD146 could be used to distinguish between actual MSCs and their terminally differentiated fibroblast counterpart. A complete list of commonly used MSC markers can be found in table 1.2.

Mesenchymal stem cell markers

Marker	Full name	Localization	Function
CD44/HCAM	Homing Cell Adhesion Molecule	Cell surface	Receptor for OPN, collagens, MMPs
CD73/NT5E	Ecto-5'-Nucleotidase	Cell surface	Catalyses conversion of mononucleotides to nucleotides
CD90/Thy1	THYmocyte Differentiation Antigen 1	Cell surface	Cell-cell, cell-matrix interactions, motility
CD105/ENG	Endoglin	Cell surface	Part of TGF-β receptor complex
CD106/VCAM1	Vascular Cell Adhesion Protein 1	Cell surface	Critical in MSC-mediated immunosuppression
CD146/MCAM	Melanoma Cell Adhesion Molecule	Cell surface	Related to self-renewal and multipotency potential
CD166/ALCAM	Activated Leukocyte Cell Adhesion Molecule	Cell surface	Cell adhesion, motility
CD271/NGFR	Low-Affinity Nerve Growth Factor Receptor	Cell surface	Immunosuppressive, cell adhesion
Stro-1	Stromal Cell Surface Marker 1	Cell surface	Adherence, proliferation
CD14		Cell surface	Hematopoietic stem cell marker, detects LPS
CD34		Cell surface	Hematopoietic stem cell marker, cell-cell adhesion
CD45/PTPRC	Protein Tyrosine Phosphatase Receptor	Cell surface	Hematopoietic stem cell marker, variety of processes

Table 1.2 List of mesenchymal stem cell markers. These markers are often used in gene and protein expression experiments to determine pluripotential capacities (Halfon et al., 2011; Li et al., 2013; Enes et al., 2017).

Besides conforming to minimal requirements related to cell surface markers, MSCs should also possess the ability to differentiate along the osteogenic, chondrogenic and adipogenic lineage, known as tri-lineage differentiation. Tissue of origin can, however, lead to a difference in propensity of MSCs to differentiate along a certain lineage (Pizzute et al., 2015). Although not a constituent of the minimum requirements as set by the ISCT, immunomodulatory capabilities are considered an important feature in MSCs (Abdi et al., 2008; Gao et al., 2016; Zhao et al., 2016). This is executed through the release of growth factors and cytokines, influencing both immune cells from the adaptive and innate immune system. MSCs have been shown to inhibit immune cell proliferation and maturation both *in vitro* and *in vivo* (Le Blanc et al., 2003).

1.3.1 Clinical and *in vitro* applications and limitations of MSCs

MSCs have received significant attention in recent years due to their variety of capabilities including self-renewal, multi-potential differentiation for use in tissue engineering and regenerative medicine, as well as their immunomodulatory role both within local tissue and systemically (Horwitz et al., 2005). Applicable *in vitro* and *in vivo* use cases of MSCs are divided into three categories: Drug and compound screening, molecular and cellular process modelling (healthy/disease), and personalised cell therapy (figure 1.6) (Sabathy and Kumar, 2016).

Importantly, the *in vivo* use of MSCs has been regarded as safe as they do not show any sign of teratoma formation after transplantation. This - together with their multi-potential use - makes them excellent therapeutic candidates in several clinical applications including cardiovascular disease, neurodegenerative disease, graft-versus-host disease (GvHD), autoimmune disease, liver disease and illnesses related to the musculoskeletal system (Ripa et

al., 2007; Joyce et al., 2010; Le Blanc et al., 2008; Horwitz et al., 1999; Mohamadnejad et al., 2007). They have already been shown to regenerate bone *in vivo* in multiple animal models, indicating the potential of gene- and cell-mediated therapies of this cell type in the future (Knight and Hankenson, 2013). Moreover, MSCs are employed in a variety of regenerative and immunomodulatory *in vitro* assays, as well as specific assays on molecular and cellular process modelling (Otto et al., 2011). For example, MSCs can be utilised in the identification of epigenetic regulators during bone formation, both in healthy and pathological environments, e.g. osteoarthritis (Johnson et al., 2016). Upon identification, compounds can be tested to see if they have the potential to reverse or even prevent such disease phenotypes.

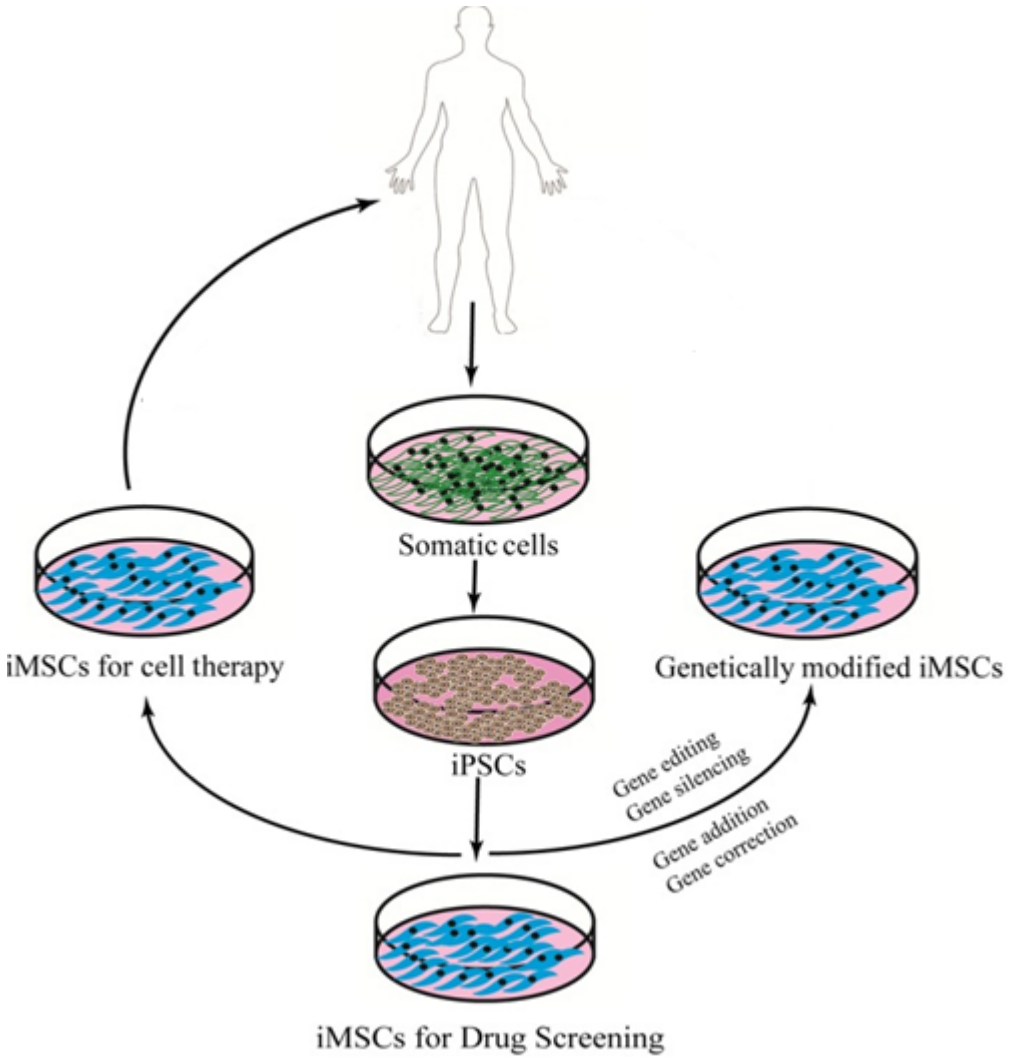


Figure 1.6 Schematic iMSC usage. iMSCs can be directed to clinical use via personalized cell therapy and used for lab-related research. This in vitro research includes drug and compound screening, molecular and cellular process modelling, and potential genetic modifications of iMSCs (Sabathy and Kumar, 2016).

It must be noted, however, that even though these cells show great promise both for *in vivo* and *in vitro* use cases, there are still limiting factors at play before they can be widely implemented (Liu et al., 2017; Hynes et al., 2014). First, the self-renewal capacity of MSCs is impaired in older people when compared to younger donors, which presents problems when looking at clinical applications. Most often, it is the elderly population that suffer from bone-related diseases such as osteoarthritis or osteoporosis. This means they will possibly have to undergo treatment whilst their mesenchymal stem cell source lack the ability to help in the regenerative process (Stolzing et al., 2008; Zhou et al., 2008). Second, the current methods for obtaining MSCs from patients are invasive, expensive and labour intensive. More specifically, MSCs harvested from sources such as bone marrow or fat make up a mere 0.001% - 0.01% and 0.05% of the total cell population, respectively (Kern et al., 2006; Bieback et al., 2008).

At present, MSCs are used in a wide variety of experiments in order to obtain a better understanding of physiological and pathophysiological processes. However, the *in vitro* culture of MSCs is associated with cell senescence. Proliferation slows down and differentiation capacity is significantly lowered over time (Bonab et al., 2006; Wagner et al., 2008; Gu et al., 2016). This means that for autologous clinical applications it would be extremely difficult to achieve sufficiently high cell numbers for specific therapies, potentially having to harvest MSCs more than once in order to obtain sufficient amounts. Large cell numbers are difficult to attain and reproducibility of experiments is hindered due to their limited proliferative capacity. Moreover, gene editing tools such as the CRISPR/Cas9 system are nearly impossible to use on MSCs as this requires selection of colonies that present stable knock-out of a specific gene, followed by serial passaging to generate a stable cell line (Zhang et al., 2017).

1.4 Induced mesenchymal stem cells (iMSCs)

For the above mentioned reasons it is important to find a source of MSCs with sufficient proliferative and differentiation capacity to be used as a substitute for endogenous MSCs. A potential solution is to derive so-called induced MSCs (iMSCs) which are obtained from induced pluripotent stem cells (iPSCs). iPSCs are known for their inexhaustible nature, capable of remaining pluripotent through as many as 40 passages as reported by Lian et al (2010). iPSCs might provide a solution for the senescence-related problems in *in vitro* cultured MSCs. Specifically, they allow for the generation of large adult cell numbers by setting up a continuous flow of iMSC production. The iMSCs resulting from iPSC differentiation have been shown to hold greater proliferation and self-renewal capacity compared to bone marrow-MSCs (BM-MSCs) whilst retaining the ability to differentiate into adipose, cartilage and bone tissue, making them an attractive alternative source for endogenous MSCs (Kang et al., 2015; Hynes et al., 2014; Sabathy and Kumar, 2016).

1.4.1 iMSC derivation

The derivation of iMSCs from pluripotent stem cells was first described by Barberi et al (2005), who co-cultured hESCs with murine OP9 stromal cells in alpha-MEM containing FBS to initiate the mesodermal differentiation. CD73+ cells were subsequently selected using fluorescence activated cell-sorting (FACS), followed by serial passaging without the stromal cell feeders. Since then, similar and adjusted protocols have emerged, mainly to be divided into four strategies: Co-culture with endogenous MSCs, embryonic body (EB) formation, spontaneous differentiation or treatment with MSC medium (Diederichs et al., 2014).

The first strategy utilises endogenous MSCs and their extracellular matrix (ECM) such that the factors released will lead to differentiation of iPSCs along the mesodermal lineage (Barberi et al., 2005).

The second strategy describes how colonies of iPSCs are utilised to form embryonic bodies (EBs). These EBs can be plated onto 0.1% gelatin-coated culture dishes in the presence of MSC medium for up to two weeks in order to reach confluence. The outgrowths can subsequently be passaged in flasks until a MSC-like morphology appears. This strategy is, however, not as time- and cost- effective as the last two strategies, which utilise the iPSCs in a feeder cell-free condition. The method describing spontaneous differentiation utilises the inherent labile feature of iPSCs able to differentiate along a certain lineage. As mentioned before, iPSCs are thought to be primed for rapid differentiation. For this to happen, frequency of medium changes is lowered and undifferentiated cells are discarded, leaving only differentiated cells. For the last strategy, as well as the most used in the literature due to its ease, iPSCs are partially dissociated into single cell colonies and plated onto 0.1% gelatin coated plates in iPSC medium including Rho-associated, coiled coil containing protein kinase (ROCK) inhibitor. ROCK inhibitor is added to single cell iPSC suspensions to avoid anoikis through inhibition of myosin-light-chain phosphatase (p-MLC) activation (Emre et al., 2010; Watanabe et al., 2007). To initiate the mesenchymal differentiation process, the medium is switched from iPSC to MSC culture medium after formation of medium-sized colonies. Several groups have used slight variations of MSC medium, ranging from basic MSC medium (Hynes et al., 2013; Frobel et al., 2014; Zou et al., 2013; Deyle et al., 2012; Diederichs et al., 2014), to additions containing L-ascorbate-2-phosphate (AA), dexamethasone (Dex) (Liu et al., 2012), platelet-derived growth factor (PDGF), transforming growth factor β (TGF-β) (Sheyn et al., 2014) and TGF-β pathway inhibitors (Chen et al., 2012; Whitworth et al., 2014). Recently, more variations have been explored in the literature

to aid the differentiation process including fibrillar collagen, fibronectin or RGD (Arg-Gly-Asp) coatings (Lui et al., 2012; TheinHan et al., 2013). The initial phase is subsequently followed by selection of cells with MSC-like features either by serial passaging or through FACS.

The main initiator of differentiation is the release of the pluripotency maintenance factor FGF2, which subsequently lowers expression of Nanog, Oct4 and Sox2, and lifts the BMP pathway block which in turn promotes differentiation along the mesodermal and endodermal lineage. However, this alone does not explain why the iPSCs would differentiate into an MSC-like cell. In the process of iPSC into iMSC differentiation it appears that the cells lose their epithelial cell characteristics and transition into a more mesodermal cell type. Epithelial cells are characterized by their adhesiveness to other cells and the ECM through cell-cell junctions, tight junctions, adherens junctions and desmosomes, and their apical-basolateral polarity. All these features are lost during the differentiation into iMSCs. There appears to be actin reorganization, matrix metalloproteinase (MMP) upregulation and loss of junctions followed by migration (Xu et al., 2009). This greatly resembles epithelial-mesenchymal transition (EMT), a process important during the developmental phase, but one that can also occur in adult tissue including fibrosis and cancer metastasis (Kalluri, 2009). Boyd et al (2009) found that the intermediate cell type in the differentiation of pluripotent stem cells to iMSCs are CD90low, indicating a shift towards an even more epithelial-like state as both pluripotent and mesenchymal stem cells are CD90 positive. Interestingly, most factors to be added in the different iMSC generation protocols are known to play a role in epithelial-mesenchymal transition (EMT). PDGF, for example, is a known mitogenic protein important in the directed migration of MSCs (Donovan et al., 2013). The effects of factors related to the

TGF-β pathway are highly dependent on the activation of specific receptors and/or components in this pathway (Sheyn et al., 2014; Chen et al., 2012).

However, this still does not explain how protocols using basal MSC medium (αMEM + L-glutamine + FBS) would be able to generate iMSCs from iPSCs, making it seem as though these extra factors are not a necessity but rather work in a complementary way. Recently, Maldonado and colleagues (2016) found that the ROCK inhibitor Y-27632 used for culturing iPSCs primes them to selectively differentiate along the mesodermal lineage via EMT in an exposure-dependent manner. ROCK is a downstream factor of Rho GTPases, activated through the non-smad TGF-β pathway or through changes in cell-cell adhesion. Specifically, EMT markers FN1 (fibronectin-1), SNAI1 (snail family transcriptional repressor 1) and LEF1 (lymphoid enhancer binding factor 1) were upregulated with increased exposure to this compound. Moreover, both the cell-cell adhesion molecule E-Cadherin was disrupted and actin bundling was changed, generating a cell morphology different from non-ROCK inhibitor-exposed iPSCs. These results suggest priming of iPSCs with an exposure to ROCKi Y-27632 towards a mesodermal lineage. This in turn could explain why primed iPSCs can differentiate into MSC-like cells with only a change of iPSC to MSC medium. Paradoxically, other research suggests that ROCK upregulation corresponds to an EMT-like process (Korol et al., 2016; Leonel et al., 2017; Sharbati et al., 2015), as ROCK initiates cell dissociation through loss of E-cadherin. This would propose the opposite of what Maldonado (2016) observed in that iPSCs will be sensitive to mesodermal lineage commitment upon activating ROCK. These contradicting results indicate the diverging effects of the TGF-β family members based on other elements including environmental cues.

An alternative explanation on how iPSCs can differentiate along a mesodermal lineage with only a change to basal MSC medium could be related to epigenetic memory. There is currently no consensus when it comes to epigenetic memory from the tissue of origin of iPSCs and how this could possibly affect the propensity of these cells to differentiate back into this lineage. Originally, studies suggested that iPSCs do retain a tissue specific epigenetic profile, but that this was lost over time through serial passaging or chromatin-modifying drugs, yielding a cell-type similar to ESCs (Kim et al., 2011; Lee et al., 2012; Polo et al., 2010). Diederichs and Tuan (2014) did observe some significant differences between iMSCs from iPSCs that had different parental tissue, although to a minimum degree. However, other research shows that DNA methylation patterns of reprogrammed somatic cells are retained even after subsequent sub-culturing of the iPSCs, with them favoring differentiation into cell types of their tissue of origin (Bar-Nur et al., 2011; Hu et al., 2010; Kim et al., 2011; Ohi et al., 2011). DNA methylation specifically is being analysed due to their stable nature in mitotic and meiotic divisions (Huang et al., 2013; Godini et al., 2018).

These results would suggest that the type of somatic cell and tissue of origin of iPSCs will have an effect on their differentiation preference towards a certain lineage. This feature could advantageously be used in experimental designs, by employing a somatic cell type for reprogramming that closely resembles the cell wanted for experiments. For this reason, BM-MSCs have already been reprogrammed into iPSCs, followed by differentiation back into iMSCs, keeping the epigenetic profile most similar to actual BM-MSCs, but with the advantage of resetting the age and senescence-related marks (Frobel et al., 2014; Deyle et al., 2012; Diederichs et al., 2014).

DNA methylation profiles of the respective donor of the somatic cells were retained upon reprogramming into iPSCs and subsequent differentiation into iMSCs (Frobel et al., 2014). The reorganization of epigenetics associated with age and senescence is the main reason these iPSCs, and subsequent iMSCs, are popular tools for *in vitro* experiments and may one day be used for therapeutic applications. However, iMSCs did re-acquire senescence-associated DNA methylation patterns upon extensive serial passaging. Specifically, known hypomethylated CpGs in late-passage and senescent MSCs were reversed to high DNA methylation in iPSCs, but subsequently lost this hypermethylation again after differentiation into iMSCs upon sub-culturing (Frobel et al., 2014). This indicates that iMSCs enter cell senescence after *in vitro* culturing, however at a significantly later stage compared to MSCs.

1.5 Differentiation of iMSCs

MSCs are characterised by their ability to differentiate into osteoblasts, adipocytes and chondrocytes. In this thesis work, iMSCs have been generated from iPSCs, differentiated along the osteogenic and adipogenic lineage and compared to BM derived MSCs.

1.5.1 Osteogenesis

The differentiation of MSCs towards the osteoblast lineage *in vitro* is accomplished by using osteogenic medium, which contains the synthetic glucocorticoid receptor (GR) agonist dexamethasone together with ascorbic acid and β-glycerophosphate. The dexamethasone-GR complex binds to the promoter regions of *FHL-2 (four and a half LIM protein 2), MKP-1 (mitogen-activated protein kinase phosphatase 1)* and *TAZ (tafazzin)*, all three supporting the activation of the osteogenic transcription factor RUNX2 (runt-related transcription factor 2). FHL-2 acts through the Wnt/β-catenin pathway by stabilizing β-catenin which translocates to the nucleus and binds to LEF-1/TCF (lymphoid enhancer binding factor 1/ T-cell factor) complex, which in turn activates transcription of *RUNX2*. MKP-1 and TAZ both facilitate the activation process of RUNX2 which in turn initiates later-stage osteogenic gene transcription (Langenbach and Handschel, 2013). Ascorbic acid (vitamin C) promotes col1 (type I collagen) synthesis and secretion, which is an essential part of bone ECM and is also an important initiator of *RUNX2* upregulation through integrins. β-glycerophosphate is a phosphate source for the production of hydroxyapatite (HA) minerals. However, it also appears to act as an intracellular signalling molecule, activating several osteogenic genes (Foster et al., 2006; Fatherazi et al., 2009; Tada et al., 2011). Calcium is the other constituent

of HA and is stored in intracellular organelles including mitochondria and endoplasmic reticula.

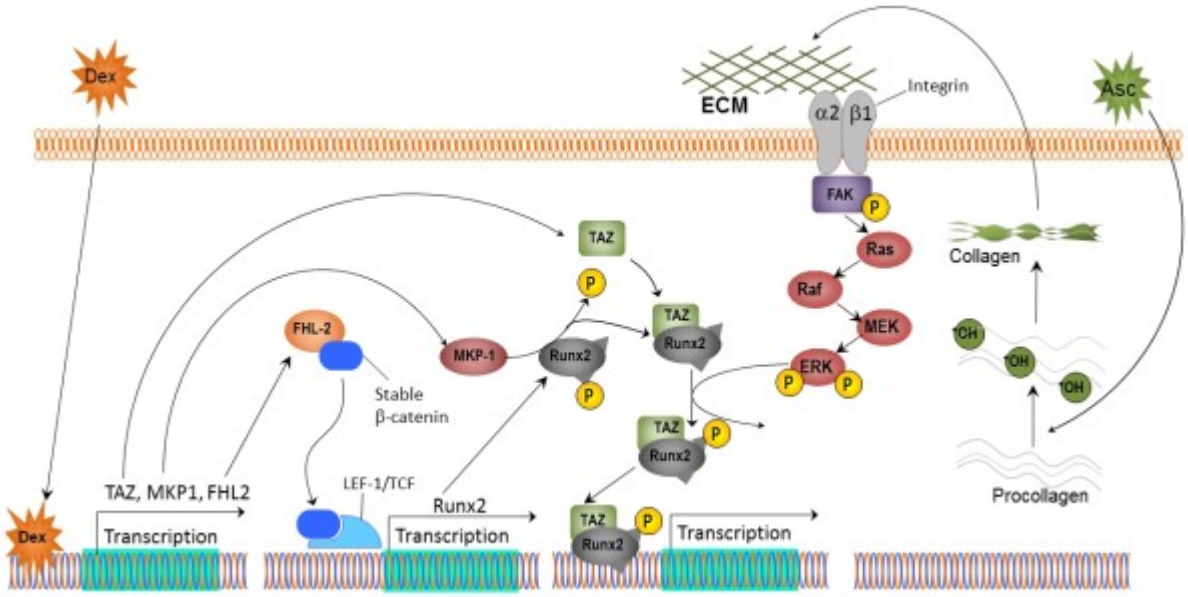


Figure 1.7 Cellular mechanism of dexamethasone (Dex)-induced osteogenesis. Dex directly affects transcription of TAZ, MKP1 and FHL2 – important factors in the process of in vitro osteogenesis. Ascorbic Acid (Asc) is also important in establishing osteogenesis through production of collagen (Langenbach and Handschel, 2013).

1.5.2 Adipogenesis

Adipose tissue contains mainly adipocytes, whose primary function entails the regulation of energy homeostasis and lipid storage (Galic et al., 2010). The directed differentiation of MSCs towards the adipogenic lineage *in vitro* includes the addition of several adipogenic-related factors. Specifically, dexamethasone, indomethacin, IBMX (3-isobutyl-1-methylxanthine) and rosiglitazone have been used to induce upregulation of adipogenic differentiation programs. Interestingly, dexamethasone is also used for osteogenic lineage differentiation however at a significantly lower concentration, indicating the time- and concentration dependent feature of this synthetic glucocorticoid (Scott et al., 2011) and the synergistic nature of other stimulatory components used. Indomethacin upregulates

peroxisome proliferator-activated receptor γ2 (PPARγ2) and CCAAT-enhancer-binding protein β (C/EBPβ), both key transcription factors in adipogenesis (Styner et al., 2010). IBMX is a factor that increases cellular cAMP (cyclic adenosine monophosphate). An increase in cAMP is associated with crucial processes that take place during the early phase of adipogenic differentiation. These processes include inhibition of Wnt10b (Bennet et al., 2002) and Sp1 (Tang et al., 1999), as well as induction of C/EBPβ and PPARγ (Hansen et al., 2001; Cao et al., 1991). Rosiglitazone is a widely prescribed type II diabetes drug and is linked to loss of bone mass in post-menopausal women that use this drug. *In vitro* studies show a decrease in osteogenesis and increase in adipogenesis upon differentiating from MSCs using this drug. This is in part due to a lowered RUNX2 expression and an increase in apidogenic markers (Benvenuti et al., 2007). Rosiglitazone-induced adipogenic differentiation of MSCs did not significantly upregulate PPARγ2, whereas indomethacin-stimulated adipogenesis did (Styner et al., 2010).

1.6 Tools for characterisation of iMSCs

A variety of methods including immunofluorescence, colorimetric assays, enzymatic assays, mass cytometry (CyTOF) and transcriptomics such as RNA sequencing (RNA seq) have been employed in the context of this thesis.

The derivation of iMSCs from iPSCs can be characterised by employing and combining several techniques. Protein and gene expression were analysed through a series of experiments. Immunofluorescence, colorimetric assays, enzymatic assays and CyTOF were used for identification and/or quantification of specific proteins. RNA sequencing targeted identification of differential gene expression patterns. Of these techniques, CyTOF and RNA sequencing are considered tools for more in-depth analysis.

CyTOF is a combination of mass spectrometry and flow cytometry, utilising a time-of-flight measurement system. This hybrid approach replaces fluorophores with stable metal elements. Where fluorophores limit the use of multiple antibodies due to spectral overlap, metal ions do not encounter this issue thus allowing for the creation of larger panels. Inside the machine, cells are nebulized and sent through an argon plasma, ionizing the metal attached to an antibody, followed by a time-of-flight (TOF) mass spectrometer measurement. The TOF measurements are subsequently linked to the metal's mass (Bendall et al., 2011).

RNA sequencing provides insights into gene expression profiles of cells. Specifically, it can analyse differentially expressed genes between a set of samples. In contrast to many other available techniques, RNA seq can be used without prior knowledge of targets, making it highly effective in the discovery of novel genes related to cellular processes. For this thesis, mRNA was selected, converted to cDNA and subsequently fragmented. Constructed libraries

are sequenced using High-Throughput Next Generation Sequencing (NGS) (Bentley et al., 2008). The generated sequences are mapped to the genome or transcriptome and thereupon gene expression levels are estimated (Costa-Silva et al., 2017; Kukurba and Montgomery, 2015).

1.7 Study aims

The objective of this thesis was to establish a standardized protocol for production of induced mesenchymal stem cells (iMSCs). Well characterised iMSCs could substitute regular hBM-MSCs, as the latter have limiting *in vitro* capabilities. Specific aims are as follows:

1) Identification of best protocol to generate MSCs from iPSCs. Selection of the best working protocol/method according to cell morphology, MSC marker expression and differentiation specific assays.

- Techniques used: immunofluorescence, light microscopy, enzymatic assays, colorimetric assays.

2) Understanding of molecular mechanisms of iPSC to iMSC lineage differentiation. Detailed molecular analysis of the iPSC to iMSC differentiation process, using the chosen protocol/method from 1).

- Techniques used: immunofluorescence, light microscopy, enzymatic assays, colorimetric assays, CyTOF, RNA Sequencing.

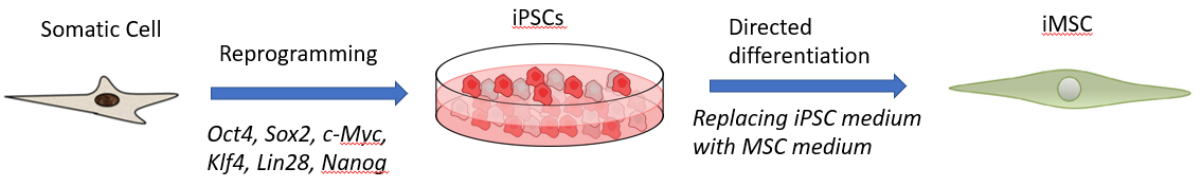


Figure 1.8 Schematic overview of somatic cell reprogramming to iPSCs and differentiation of iPSCs into iMSCs. This thesis focusses on the iPSC into iMSC differentiation to create a stable alternative cell type to be used as a substitute for BM-MSCs.

Chapter 2. Materials and Methods

2.1 Cell culture

2.1.1 hiPSCs cell culture

Human induced pluripotent stem cells (hiPSCs) were obtained from the James Martin Stem Cell Facility in the Sir William Dunn School of Pathology, University of Oxford. In total 3 hiPSC lines, consisting of 2 donors were used in the experiments described in this thesis. Designations are SFC840-03-01(Cytotune, LifeTech) (Fernandes et al., 2016) and SFC840-03-03 (Cytotune, LifeTech) (Fernandes et al., 2016) from a 67 year old female, and SFC841-03-02 (Cytotune, LifeTech) (Beevers et al., 2017) from a 36 year old male. iPSC clones were obtained from somatic cells reprogrammed with Sendai virus containing the OSKM genes used for reprogramming. All lines were derived from dermal fibroblasts from healthy donors recruited through the Oxford Parkinson's Disease Centre, having given signed informed consent, which included derivation of hiPSC lines from skin biopsies (Ethics Committee: National Health Service, Health Research Authority, NRES Committee South Central, Berkshire, UK, REC 10/H0505/71). Cells were cultured feeder-free on Geltrex®-coated plates in Essential 8 (E8) medium (A1517001, ThermoFisher) to which the accompanying supplement, 1% L-glutamine (Thermofisher, 25030081) and 1% penicillin/streptomycin (P/S) (Thermofisher, 15140122) had been added. Medium was changed every day to ensure sufficient available nutrients.

2.1.2 Production of Geltrex-coated plates

Geltrex® (LDEV-Free hESC-qualified Reduced Growth Factor Basement Membrane Matrix; Life Technologies; A1413302) was used as a basement membrane for growth of iPSCs. Upon arrival, Geltrex® was aliquoted in volumes of 400 ul in 50 ml falcon tubes and stored in the -20°C freezer. When needed, 40 ml of KO-DMEM (KnockOut™ DMEM) (Thermo Fisher; 10829018) had to be added to the aliquot to make a working stock of Geltrex® that could be stored in the 4°C fridge for up to 2 weeks. Thorough mixing is needed, avoiding air bubbles before use as this might affect the polymerization of the gel. In a 6-well cell culture plate, 1 ml of Geltrex® is added and incubated for at least 45 minutes (37°C) in order for the gel to polymerize. After usage, the Geltrex® working stock is immediately placed in the fridge to prevent instant hardening of the gel. Plates coated with Geltrex® can also be made in advance and stored in the fridge (sealed with parafilm) for a few days. Before usage, plates needed be warmed up in the incubator (37°C) for 30 minutes.

2.1.3 Passaging of iPSCs

Before passaging, plates coated with Geltrex® were prepared as per instructions from paragraph 2.1.2. The iPSCs were passaged using 0.5M ethylenediaminetetraacetic acid (EDTA) (Life Technologies; 15575-038) diluted 1:1000 in PBS to create a working stock of 0.5 mM EDTA. E8 medium was aspirated off and the 0.5 mM EDTA (1 ml in a 6-well plate) was added to the wells for 4-5 minutes (37°C) - until cells were about to detach from the matrix. The 0.5 mM EDTA solution was aspirated and cells were subsequently removed from the well using fresh E8 medium and transferred to a new Geltrex®-coated plate. After passaging, 10 uM ROCK inhibitor from a 10 mM stock in DMSO (dimethylsulfoxide) was added to the wells to prevent anoikis of cells through the downstream effects of cell

dissociation. If iPSCs displayed spontaneous differentiation, this could be circumvented in two manners; either manually removing the differentiated cells with a pipette tip before passaging, or by precisely timing the addition of the detachment solution (0.5 mM EDTA). iPSCs are most likely to randomly differentiate to a state similar to their tissue of origin, fibroblasts in these donors. Fibroblasts are more adherent to plastic and Geltrex® membranes and thus need longer to detach from their respective base compared to iPSCs. This means that iPSCs should start floating before the differentiated cells and this is how the iPSCs could be collected. To this 0.5 mM EDTA solution with cells, 10x phosphate-buffered saline (PBS) had to be added after which it could be centrifuged at 400 x g for 5 minutes. Cells were resuspended in E8 with 10 uM ROCK inhibitor and seeded in fresh Geltrex®-coated plates.

2.1.4 Thawing and freezing down iPSCs

Before iPSCs were thawed, 2 wells in a 6-well plate were coated with Geltrex®. Transport of iPSCs in cryovials from the liquid nitrogen was done on dry ice. Cells were put in a water bath (37°C) immediately to avoid crystal formation. The entire contents of the vial (1 ml) was mixed with 9 ml of pre-warmed PBS in a 15 ml falcon tube. The tube was placed in the centrifuge and spun down at 400 x g for 5 minutes. The supernatant was removed and the cells were resuspended in 2 ml E8 medium. Cells were plated at different cell densities; 80% (1.6 ml) in 1 well and 20% (0.4 ml) in the other (see figure below). If cell recovery was poor this meant the high density well would have a higher chance of survival. Medium was topped up to 2 ml and 10 uM ROCK inhibitor (ROCKi) (Y-27632; Abcam; ab120129) was added.

Freezing of iPSCs. iPSC 2x freezing medium consists of 20% KO-DMEM + 20% DMSO + 60% Embryonic Stem Cell (ESC) FBS (Thermo Fisher; 10439024) and was kept at 4°C. iPSCs were washed twice with PBS before freezing. 1 well in a 6-well plate was used for a

single cryovial. 1ml 0.5 mM EDTA was added to each well and left to incubate for 4-5 minutes or until cells were about to detach. EDTA was removed and cells were left for 30 seconds. Similar to passaging, cells were subsequently detached from the plates using 0.5-1 ml cold E8 medium and transferred to a falcon tube. To this, an equal amount of cold iPSC 2x freezing medium had to be added slowly after which cells could be stored in cryovials. Cells were kept at -80°C in freezing containers (Mr. Frostys; Thermo Fisher; 5100-0001) for 24 hours and subsequently stored in liquid nitrogen.

2.1.5 hBM-MSCs cell culture

Human bone marrow-mesenchymal stem cells (hBM-MSCs) were purchased from Lonza (female, black, 24) and Millipore (male, non-Hispanic, 27 (SCC034)). Cells used for experiments were between passage 6 and 15 depending on the donor and rate of senescence. They were cultured in MesenPro RS medium (Thermofisher, 12746012) supplemented with the accompanying MesenPro RS Growth Supplement, 1% L-glutamine and 1% P/S in either T-75 or T-175 flasks. Medium was changed every 3 days.

2.1.6 Passaging BM-MSCs

BM-MSCs were split 1:3 or 1:4 upon reaching confluency. Cells were washed with PBS, after which 10 mL of trypsin solution (TrypLE, Gibco, 12605028) was added. This was followed by an incubation time of 5 minutes at 37 °C in order to detach the cells. Upon cells reaching a state of single cell solution, 10 mL of MesenPro culture medium was added to inactivate the detachment enzymes. The contents of the flask were transferred to a 50ml falcon tube and centrifuged for 5 minutes at 300 x g. Supernatant was removed and cells were resupended in MesenPro medium, followed by seeding into new flasks.

2.1.7 Thawing and freezing of BM-MSCs

BM-MSCs were transported from the liquid nitrogen storage to the water bath (37°C) on dry ice. The entire contents of the vial (~1ml), directly after reaching a liquid state, were transferred into 15 ml falcon tubes together with 9 ml PBS. Cells were centrifuged for 5 minutes at 300x g. Supernatant was removed and cells were resuspended in MesenPro medium. Depending on the cell numbers in the vial, they were either seeded into a T-75 or T-175 flask.

Freezing of BM-MSCs: BM-MSCs were washed once with PBS before being frozen. Similar to passaging, cells were detached using trypsin at 37°C for 5 minutes and centrifuged at 300 x g for 5 minutes. 0.5 ml of BM-MSC 2x freezing medium (20% MesenPro + 20% DMSO + 60% FBS) was slowly added per roughly 1-2 million cells. This was topped up with an equal amount of MesenPro medium so as to reach 1ml per 1-2 million cells per vial.

2.2 Differentiation conditions

For the first set of experiments, 5 protocols/medium conditions were tested for the differentiation of iPSCs into iMSCs. In table 2.1 below, their exact compositions can be found. The medium was switched to either one of these conditions to initiate differentiation of iPSCs into iMSCs. The complete differentiation protocol consisted of 3 phases, of which the differentiation of iPSCs into iMSCs was covered by the first 2 phases. Phase 1, the initial differentiation phase, lasted for 14 days, as suggested by the literature from which these protocols were extracted. During this time cells remained in the same well, allowing for a change in gene expression to take place. At day 14, cells were transferred and passaged onto fresh Geltrex-coated plates, initiating the start of the maturation phase (phase 2). This phase switch selects for cells with the desired proteomic features, as only stable and viable cells are able to differentiate into MSC-like cells. This passaging protocol allowed the newly formed iMSCs to increase expression levels of typical MSC-related marker proteins. It was found that upon reaching phase 2 they had stably upregulated these MSC proteins.

Condition 1	DMEM (Thermofisher, 11965092) + 10% FBS (Thermofisher, 10500064) + 1% P/S + 1% L-glutamine	Kang et al., 2015
Condition 2	αMEM (Thermofisher, 12561056) + 10% FBS + 1% P/S + 1% L-glutamine	Hynes et al., 2014
Condition 3	αMEM + 10% FBS + 1% P/S + Ascorbic Acid + Dexamethasone	Liu et al., 2012
Condition 4	DMEM + 20% knockout serum replacement (Thermofisher, 10828028) + 1% P/S + 1% L-glutamine + 1% nonessential amino acids (NEAA) + 10 μM SB431542	Chen et al., 2012
Condition 5	IMDM (Thermofisher, 12440053) + 17% knockout serum replacement + 1% P/S + 1% NEAA + 10 ng/ml TGF-β1	Sheyn et al., 2014

Table 2.1 Medium conditions for iPSC into iMSC differentiation I.

For the second set of experiments, condition 2 and a commercial MSC medium, MesenPro, were used for the differentiation of iPSCs into iMSCs. The table 2.2 below describes their compositions. This time, however, phase 1 of the differentiation protocol was shortened to either 7 days (sample III) or to a split-upon-confluency (sample IV) protocol. The phase 1 was adjusted in order to circumvent a senescence-related issue occurring in freshly generated iMSCs around P3. Phase 2 remained the same. During the course of this experiment, the results suggested shortening phase 1 was not critical and thus a decision was made to keep growing the iMSCs on Geltrex-coated plates. This eventually resulted in iMSCs that continued proliferation over 20 passages.

MesenPro RS	MesenPro basal medium + MesenPro growth supplement + 1% P/S
Condition 2	αMEM + 10% FBS + 1% P/S + 1% L-glutamine

Table 2.2 Medium conditions for iPSC into iMSC differentiation II.

Further differentiation of iMSCs and BM-MSCs along the osteoblast and adipocyte lineages required specific differentiation medium. Both medium compositions for osteogenic and adipogenic differentiation can be found in table 2.3. Both protocols lasted for a maximum of 3 to 4 weeks, depending on the assay. Medium was changed every 3 days.

Osteoblast (1)	αMEM + 10% FBS + 1% P/S + 1% L-glutamine + 10 nM dexamethasone + 50 μM ascorbic acid + 10 mM β-glycerophosphate
Osteoblast (2)	αMEM + 10% FBS + 1% P/S + 1% L-glutamine + 10ng/ml Oncostatin M (OSM) + 50 μM ascorbic acid + 10 mM β-glycerophosphate
Adipocyte	αMEM + 10% FBS + 1% P/S + 1% L-glutamine + 1 μM dexamethasone + 0.5 mM IBMX (3-isobutyl-1-methylxanthine) + 50 μM indomethacin

Table 2.3 Osteoblast and adipocyte differentiation conditions.

To summarize the overall workflow, the differentiation process of iPSCs into iMSCs comprises two phases; the initial phase and the maturation phase. As part of their assessment, iMSCs were subsequently differentiated along the osteogenic and adipogenic lineages (phase 3). During these three phases, several experiments including immunofluorescence (IF), Alkaline Phosphatase (ALP) assays, colorimetric assays (Alizarin Red Staining and Oil Red O), as well as CyTOF and RNA sequencing were employed. Figure 2.1 displays a schematic overview of all the phases and experiments executed per phase.

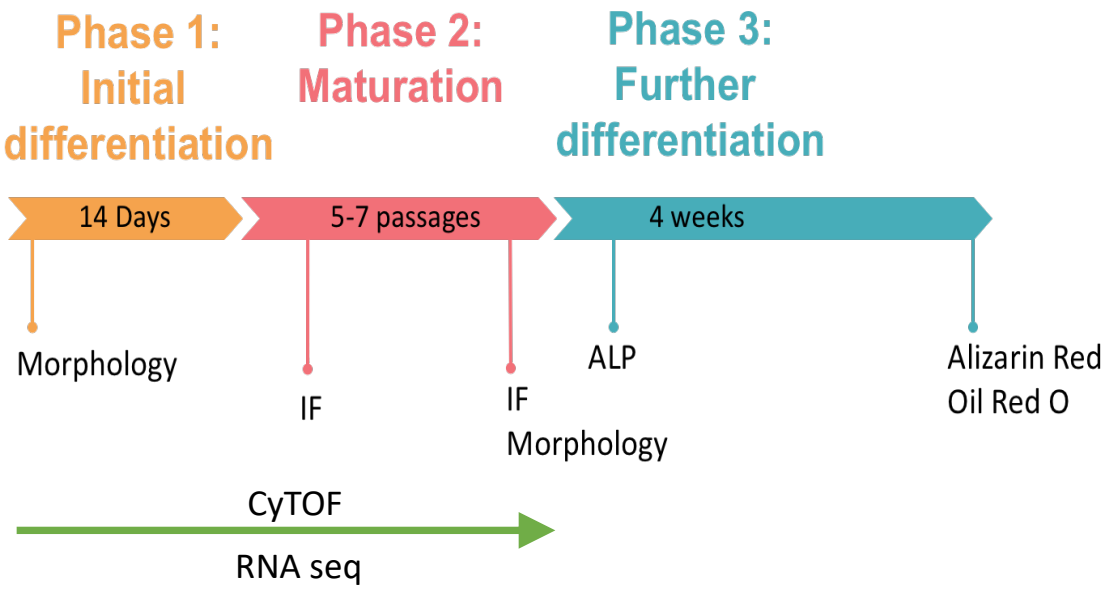


Figure 2.1 Schematic overview of the three phases and experiments executed per phase.

2.3 Immunofluorescence

For the immunofluorescence experiments either round glass coverslips in 12-well plates (Greiner CELLSTAR® multiwell culture plates; Sigma-Aldrich; M9187 SIGMA) or chamber slides (LabTek II; Thermofisher; 154534) were used. Both the glass coverslips and chamber slides were covered with Geltrex®.

Samples were fixed in ice cold methanol for 10 minutes and were subsequently stored in PBS at 4°C wrapped in parafilm. Staining was performed at room temperature in a humid environment to prevent samples from drying out.

First, samples were blocked with 5% normal goat serum (NGS) for 30 minutes at room temperature (RT) in PBS containing saponin at a ratio of 0.059 grams per 100 ml. The solution was made up fresh every time as its stability decreases after 1-2 days. The saponin was added in order to permeabilize the cell membrane for the intracellular protein targets to be made available for antibody detection. No further washing was needed after removing the solution. Thereafter, the primary antibodies were added, made up in 5% NGS in PBS with saponin, and incubated for 2 hours at RT or overnight at 4°C. Antibodies for pluripotency markers used were Nanog (Sigma-Aldrich; SaB1405280), Oct4 (Abcam; ab18976) and Sox2 (Abcam; ab79351). Markers used related to mesenchymal stem cells were CD44 (Abcam; ab6124), CD90 (Abcam; ab133350) and CD105 (Abcam; ab11414). All dilutions used were per the manufacturer's instructions and detailed information regarding these can be found in table 2.4. Following the primary antibody incubation time, samples were washed three times with PBST (PBS Tween20) with a ratio of 1 ml Tween 20 per 500 ml PBS - each wash lasting 10 minutes adding up to a total of 30 minutes. A secondary antibody cocktail, all diluted 1:200, was made up in 5% equine serum in PBS with saponin and incubated at RT for 2 hours. Information about primary-secondary antibody combinations can be found in table

2.4. From this step onwards, the samples were shielded with foil to avoid bleaching of the fluorophores. After staining with secondary antibodies, samples were again washed three times with PBST, each wash lasting 10 minutes. Nuclear stain POPO-1 diluted 1:500 in PBS with saponin was then applied to the cells and incubated for 20 minutes at RT followed by the same washing protocol as mentioned before - 3 washes with PBST each lasting 10 minutes. From this point onwards, the humid chamber was not necessary anymore. A drop of Vectashield Mountant H1000 (Vector laboratories; H-1000 (without DAPI)) was applied to each well or to the chamber slides from which the plastic walls had been removed. The round glass coverslips were placed and sealed on a glass slide. Chamber slides were sealed with a rectangle-shaped coverslip. Sealing was done with nail varnish and slides were kept in a dark place at 4°C left to dry overnight. Slides were subsequently stored in histology-slide boxes in the cold room at 4°C. Plates could be stored for up to 2 weeks before being imaged on a confocal microscope (Zeiss).

Images of the samples were obtained in conjunction with the Zeiss Software used for analysis. Settings vary for different samples as was needed to get a clear image. All samples were accompanied by a control to adjust for background noise.

Pluripotency markers

Antibody	Host	Clonality	Epitope target	Concentration	In combination with (secondary antibody)	Concentration sec. antibody
Nanog	Mouse	Monoclonal	IgG2bκ	1:100	AF568	1:200
Oct4	Rabbit	Polyclonal	IgG	1:100	AF633	1:200
Sox2	Mouse	Monoclonal	IgG1	1:100	FITC	1:200

Mesenchymal stem cell markers

Antibody	Host	Clonality	Epitope target	Concentration	In combination with (secondary antibody)	Concentration sec. antibody
CD44	Mouse	Monoclonal	IgG2a	1:100	AF568	1:200
CD90	Rabbit	Monoclonal	IgG	1:100	AF633	1:200
CD105	Mouse	Monoclonal	IgG1	1:250	FITC	1:200

Table 2.4. Pluripotency and mesenchymal stem cell-related antibodies for immunofluorescence. Detailed information on concentrations and secondary antibody combinations.

2.4 Fluorescence-activated cell sorting (FACS)

Pluripotency markers:

Antibody	Host	Clonality	Epitope target	Concentration	In combination with (secondary antibody)	Concentration sec. antibody	Live/dead stain
TRA-1-81	Mouse	Monoclonal	IgM	1:200	FITC	1:200	Zombie Dye NIR
SSEA-4	Mouse	Monoclonal	IgG3	1:200	FITC	1:200	Zombie Dye NIR
ALP	Mouse	Monoclonal	IgM	1:200	FITC	1:200	Zombie Dye NIR

Mesenchymal stem cell markers:

Antibody	Host	Clonality	Epitope target	Concentration	In combination with (secondary antibody)	Concentration sec. antibody	Live/dead stain
CD106	Mouse	Monoclonal	IgG1	1:100	FITC	1:200	Zombie Dye NIR
Stro-1	Mouse	Monoclonal	IgM	1:200	FITC	1:200	Zombie Dye NIR

Table 2.5 Pluripotency and mesenchymal stem cell-related antibodies for FACS. Detailed information on concentrations and secondary antibody combinations.

FACS was used for validation of antibodies to be used eventually for CyTOF after metal conjugation. Cells were washed twice with PBS after which Accutase (Thermo Fisher; 00-4555-56) was used for 10 minutes to release cells from the plastic culture plates. The cells were subsequently transferred to FACS tubes and spun at 400 x g for 5 minutes. Zombie Dye NIR was used to determine populations of live and dead cells in the sample. Zombie Dye attaches irreversibly to primary amines on proteins, which on live cells are only available on the cell surface. Dead cells have lost their membrane integrity, meaning the dye can now freely access intramembranous proteins as well, yielding a much higher fluorescence. Zombie Dye solution was made as follows: 1ul of Zombie Dye in 100ul PBS. Samples in each FACS tube were resuspended in 200ul of Zombie Dye solution and incubated for 15 minutes at

room temperature. Thereafter, cells were washed twice in PBS by resuspending and sedimentation in a centrifuge (conditions). Fixation was done by adding 200 ul Maxpar Fix1 Buffer (5x) diluted 1:5 in PBS for 20 minutes at room temperature. Samples were washed again twice, this time in MaxPar Perm-S buffer. The primary antibodies were added to the samples and incubated for 30 minutes on ice, in concentrations as per the manufacturer's instructions (see table) - diluted in MaxPar Perm-S buffer. After incubation, cells were washed twice after which the secondary antibodies were added (1:200 in MaxPar Perm-S Buffer) for 30 minutes (on ice). Cells were subsequently washed with PBS and resuspended in 200ul PBS. Samples were stored (up to 2 weeks) in the cold room (4°C) wrapped in aluminium foil.

2.5 Colorimetric assays

2.5.1 Alizarin Red Staining

Alizarin Red Staining (ARS) was used to determine calcium deposition in the extracellular matrix of osteoblasts differentiated from BM-MSCs and iMSCs. ARS was performed after 4 weeks to allow sufficient time for the formation of mineralized nodules. 1% ARS solution was made using Alizarin Red S (Merck; A5533) dissolved in MilliQ (MQ) Water (0.5 grams powder per 50 ml MQ) by thorough mixing. Potential of hydrogen (pH) adjustments are needed to acquire complete dissolution - using a pH between 4.1 and 4.3. Ammonium hydroxide was used to increase the pH, whereas acetic acid was used to lower the pH. For the staining itself, cells were fixed using 4% formaldehyde for 10 minutes followed by a wash with 70% ethanol (EtOH). After washing, samples were air dried. Cells were then stained with ARS for 5-10 minutes and subsequently washed three times with 50% EtOH. Thereafter, plates were ready for imaging.

2.5.2 Oil Red O

Oil Red O (ORO) was used to stain for lipid droplets in adipocytes differentiated from BM-MSCs and iMSCs. This experiment was performed at week 4. 1% saturated ORO was made up of ORO (Merck; O0625) powder dissolved in 99% isopropanol. Cells were fixed in 4% formaldehyde for 10 minutes, subsequently rinsed with 60% isopropanol and were left to dry. Samples were then stained with ORO for 15 minutes after which they were gently washed three times with PBS. Plates were then ready for imaging.

2.6 Alkaline phosphatase (ALP) assay

Alkaline Phosphatase (ALP) protein expression was measured at day 7 after osteogenic induction. Volumes mentioned all refer to 96-well plate experiment setups. First, PrestoBlue (ThermoFisher, A13261) was added (1:10) to the medium to estimate cell numbers as per their metabolic rate. PrestoBlue contains a non-fluorescent cell-permeable blue compound named resazurin that will be transformed into resorufin - a highly fluorescent red compound - due to the reducing power of living cells. Cells with PrestoBlue were incubated for 1.5 hours (37°C, 5% CO2) after which the fluorescence was measured using a fluorescence plate reader (FLUOstar OPTIMA, BMG Labtechnologies; Excitation: 535 nm, Emission: 580 nm, Gain: 1008). Cells were washed three times with PBS. Cells were lysed using 20 ul CelLytic M (Sigma-Aldrich, C2978) combined with 2% protease inhibitor and incubated for 15 minutes at room temperature. The plate was subsequently shaken at 600 rpm for 30 seconds. To determine the ALP protein concentration, 4-Methylumbelliferyl phosphate (4-MUP) (Sigma-Aldrich; M3168-100ML) was added to the wells in a mixture of 60 ul 4-MUP combined with 20 ul tromethamine (TRIS; 50 mM; pH 8). Fluorescence was measured directly after adding the 4-MUP to avoid a skewed timepoint T0 as cells start reducing the non-fluorescent 4-MUP to the highly fluorescent methylumbelliferone immediately. The same fluorescence plate reader was used (Excitation: 340 nm, Emission: 520 nm, Gain: 1008). Cells were left in the incubator (37°C, 5% CO2) for 60 minutes followed by measuring the fluorescence (T60) with the same settings as T0.

2.7 Mass cytometry (CyTOF)

Cells were washed twice with PBS before Accutase was added to detach the cells from the plate/flask. After cells had detached, an equal amount of cell culture medium was added to inactivate the cell detachment enzymes. Cells were then centrifuged at 400 x g for 5 minutes and stained with the Maxpar Cell-ID Intercalator-103Rh (1:2000) in PBS, which is used as a live/dead stain, for 15 minutes at RT. Cells were washed twice with Maxpar Cell Staining Buffer (CSB). The Cell-ID™ 20-Plex Pd Barcoding Kit (Fluidigm) enabled barcoding of the different cell types and subsequent multiplexing of samples, as they were cultured separately and needed to be distinguishable during analysis. Each sample was resuspended in 1 ml of 1x Fix I Buffer and incubated for 10 minutes at RT. Thereafter, these samples were centrifuged at 400 x g for 5 minutes and washed twice with 1 ml of 1x Barcode Perm Buffer. Each sample to be barcoded was resuspended in 800 ul of 1x Barcode Perm Buffer. Each barcode was resuspended in 100 ul 1x Barcode Perm Buffer and transferred to the corresponding sample. The mixture had to be mixed immediately by pipetting thoroughly, followed by a 30-minute incubation at RT. Sample was centrifuged (400 x g, 5 min) and washed twice with Maxpar CSB. Then, the barcoded samples were resuspended in 100 ul Maxpar CSB and combined. First, cell surface antibodies were stained, diluted in CSB in concentrations as mentioned in table 2.6. 100ul was added to the sample, followed by thorough mixing and an incubation time of 30 minutes on ice. Thereafter, cells were washed twice with CSB. A second round of staining was performed, this time including both cytoplasmic and nuclear markers. A fixation and permeabilization step was required this time prior to the actual staining. 1 ml of eBioScience FoxP3 (1ml FoxP3 in 3 ml diluent) was added to each sample followed by a gentle vortex and an incubation time of 60 minutes at 4°C (ice). Samples were washed twice with 1x Perm buffer (stock = 10x, dilute in MiliQ Water to obtain 1x). Then, the antibody mastermix, this time made up in 1x Perm buffer, including cytoplasmic and

nuclear markers could be added (100ul per sample) to each sample. Again, samples had to be incubated for 30 minutes on ice, followed by 2x washing. Last step on the first day included another fixation step. Cell-ID Intercalator Ir-125 was diluted in Fix perm (1:1000) together with 1.6% paraformaldehyde (PFA). A total of 1 ml of this mixture was added to each sample and incubated overnight at 4°C in the fridge. The following day cells were centrifuged at 700 x g for 5 minutes and washed twice in Maxpar CSB. Thereafter, cells were washed twice in MilliQ water. Before the last wash, cells were counted. The final resuspension volume of water was adjusted accordingly, including 10% calibration beads. This solution of polystyrene beads contain known concentrations of metal ions (151Eu and 153Eu) and are used to normalize data for signal variation that may occur in the CyTOF instrument over time.

Marker	**Metal tag**	**Purchased from**	**Concentrations used**
Nanog	169Tm	Fluidigm	0.5ul
Oct4	165Ho	Fluidigm	0.5ul
Sox2	150Nd	Fluidigm	0.13ul
ALP	153Eu	R&D Systems	2ug/ml
TRA-1-60	148Nd	Fluidigm	0.13ul
SSEA-4	156Gd	R&D Systems	0.5ug/ml

Marker	**Metal tag**	**Purchased from**	**Concentrations used**
CD45	154Sm	Fluidigm	0.5ul
CD44	171Yb	Fluidigm	0.06ul
CD73	168Er	Fluidigm	0.5ul
CD90	159Tb	Fluidigm	0.5ul
CD105	163Dy	Fluidigm	0.5ul
CD106	147Sm	Origene	0.5ug/ml
CD146	155Gd	Fluidigm	0.5ul
CD166	164Dy	Fluidigm	0.5ul
CD271	149Sm	Fluidigm	0.5ul
CD14	160Gd	Fluidigm	0.5ul

Table 2.6 Antibody list for mass cytometry (CyTOF). Includes pluripotency markers (top) and mesenchymal stem cell + and – markers (bottom). These concentrations were based on previous validation experiments.

2.7.1 Metal conjugation of FACS antibodies

Antibodies validated through FACS intended for CyTOF use had to be labeled with a stable metal ion. This was established through a protocol provided on the Fluidigm website (PRD002 Version 10) for which the Maxpar Antibody Labeling Kit was used. Metal conjugation was performed for antibodies TRA-1-81, SSEA-4, ALP, CD106 and Stro-1 (table 2.6). TRA-1-81 and Stro-1 conjugation did not result in proper metal conjugated antibodies and are therefore left out of table 2.6.

2.8 RNA sequencing (RNA seq)

RNA sequencing was employed to analyze the gene expression profiles in a time course-based manner. Samples from multiple time points were collected during the differentiation of iPSCs into iMSCs. Figure 2.2 shows a schematic overview of the RNA seq setup. Day 0 (D0) was used as control, followed by collection of samples on D1, D4, D7, D14, passage 1 (P1), P2, every subsequent passage until P9. P9 iMSCs were eventually compared to BM-MSCs of P9 (figure 2.2).

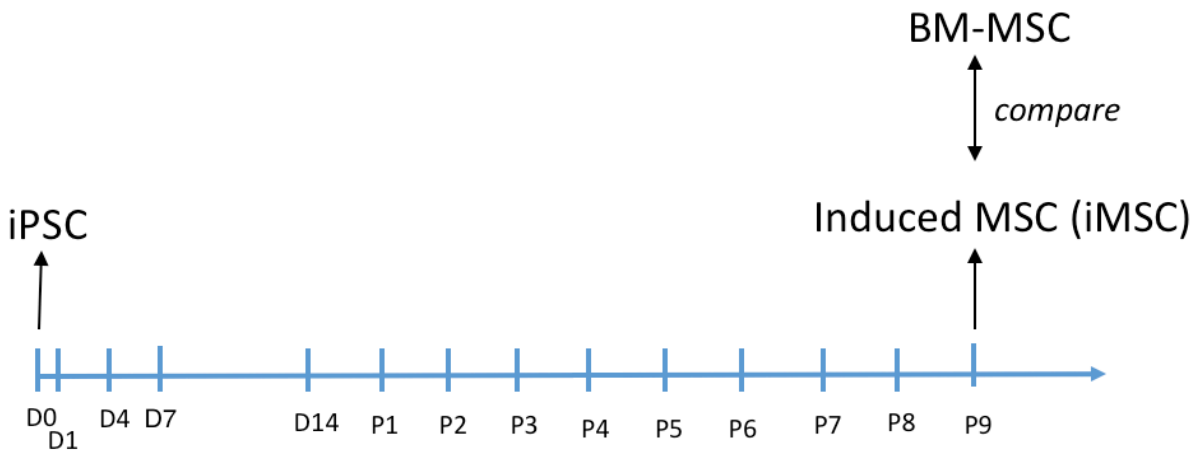


Figure 2.2 Schematic overview of the RNA sequencing experiment. Phase 1 (up to 14 days) and the subsequent passaging phase are included. P9 iMSCs are compared to BM-MSCs.

For this experiment, RNA was extracted as mentioned in section 2.8.1 below. mRNA was isolated from the total RNA through poly-A selection using magnetic beads. RNA was fragmented (200-300bp) and converted into cDNA. Sequencing adapters including indexes were added to the DNA fragments (a unique index per sample), forming the sequencing library on a flow cell (Illumina). Bridge amplification was used to amplify the fragments (with adapters/indexes). Library concentration and library fragment lengths were verified using the Agilent 2200 TapeStation in conjunction with the High Sensitivity D1000

screentape and reagents. The library was sequenced using the sequencing by synthesis technique. Sequencing depth was set to 16 million reads, divided over two separate runs. Samples were de-multiplexed according to their indexes and reads were aligned to a reference genome.

2.8.1 RNA extraction

TRIzol (Thermo Fisher; 15596026) was used to disrupt the cells upon which they were stored in the -80°C freezer awaiting further RNA extraction. RNA extraction was carried out with the Direct-Zol RNA MiniPrep Kit (Zymo; R2052) according to the accompanying protocol. RNA was stored in the -80°C freezer.

Chapter 3. Results

3.1 Comparison of iMSC differentiation protocols

The first set of differentiation experiments included a range of differentiation protocols with varying media conditions as suggested in the current literature (Hynes et al., 2014; Kang et al., 2015; Sheyn et al., 2014; Chen et al., 2012; Liu et al., 2012). The different conditions have been assigned numbers together with a short description, further details including their precise contents can be found in the Materials and Methods section 2.2. These protocols specifically focused on the differentiation strategy based on replacing the iPSC medium to MSC medium, rather than using EBs, co-culture or spontaneous differentiation. Two donors were used for the initial experiments, of which donor 840 supplied two clones (840-03-01 and 840-03-03) and donor 841 supplied one clone (841-03-02). To identify the potential of these protocols to indeed transform iPSCs into iMSCs, their cell viability, morphology, upregulation of MSC markers and downregulation of pluripotency markers were analysed for all three clones.

3.1.1 Cell viability

Cell viability presented in table 3.1 could refer to cells dying at any stage in phase 2 (passaging phase) of the differentiation process, as none of the cells died during phase 1. This table does not, however, go into further detail regarding the exact time the cells failed to survive passaging.

	Condition 1 (DMEM)	Condition 2 (αMEM)	Condition 3 (αMEM + Dex)	Condition 4 (TGF-β pathway inhibitor)	Condition 5 (TGF-β)
Donor 840-03-01	+	+	+	-	-
Donor 840-03-03	+	+	+/-	-	+
Donor 841-03-02	-	+	+	-	-

Table 3.1. Cell viability of differentiating iPSCs induced through various protocols. Three iPSC clones were used; 840-03-01, 840-03-03 and 841-03-02. + = good cell survivability, - = poor to no cell survivability.

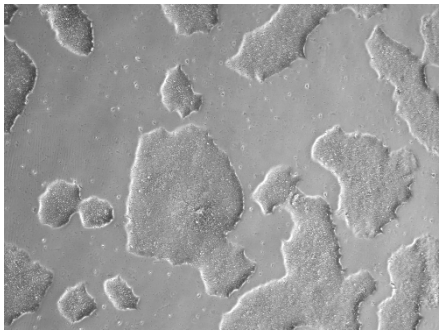
3.1.2 Cell morphology

To determine morphological similarities between iMSCs and BM-MSCs, photos were taken using a bright field microscope at various points throughout the differentiation process. Several of these snapshots can be seen in figure 3.1. Seeding density was around 20%, allowing the cells to form large colonies before the differentiation process started, as was suggested per most protocols. This consequently resulted in a confluent cell culture after a few days. Cell seeding densities were similar for all clones and conditions. Moreover, no morphological difference could be identified between the different clones and conditions at the end of phase 1. For this reason only one photo is shown for Day 0 (D0) and the end of phase 1. Passage 1 (P1) is the first passage upon splitting, meaning a change in phase going from the first (initial) phase to the second (maturation/passaging) phase. Geltrex-coated plates were still used for the first two passages (P1, P2) upon the start of phase 2. Cell culture was subsequently resumed on non-coated plates.

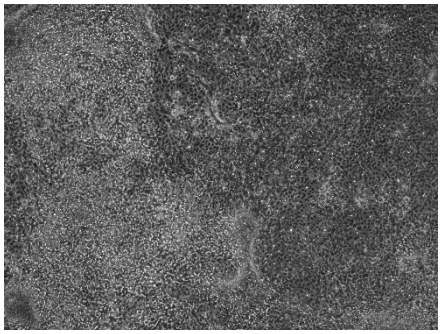
Cells from donor 841-03-02 performed well for conditions 2 and 3 as these iMSCs looked viable when inspected under the microscope. Condition 1 only failed later at P3, with a visible reduction of cells and an unusual morphology. Cells in conditions 4 and 5 both did

survive the phase switch, however upon splitting once more to P2 cells in both conditions failed to continue proliferating. Donor 840-03-01 showed a similar trend in cell survivability and equally in morphology. Conditions 1, 2 and 3 all displayed a similar morphology, closely resembling that of BM-MSCs. Contrary to other donors, condition 5 in donor 840-03-03 did yield viable cells that looked MSC-like. Moreover, conditions 1, 2 and to a lesser degree condition 3 all seemed to produce MSC-like cells that survived through the initial passaging. However, once stable iMSC lines had been created, upon passaging the cells from a Geltrex-coated plate to a non-Geltrex-coated plate, they all showed a decrease in proliferation. A senescence-like phenomenon seemed to occur after their transfer, making them unusable for further experimentation.

D0

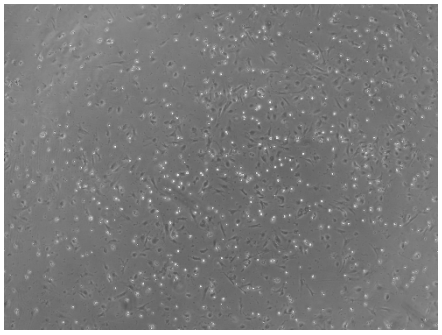


End of phase 1 – 14D

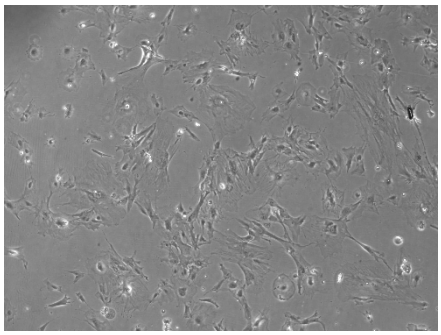


Donor 841-03-02

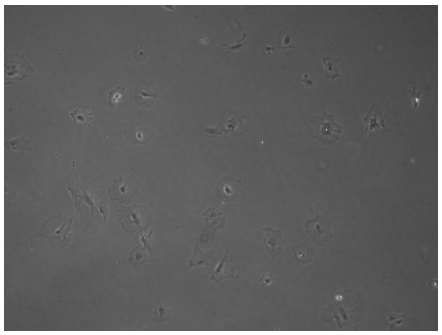
P1 – condition 1



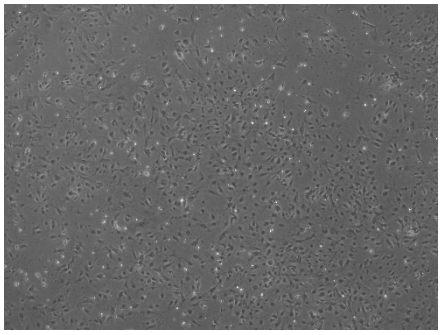
P2 – condition 1



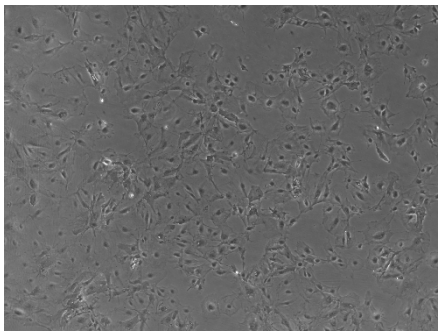
P3 – condition 1



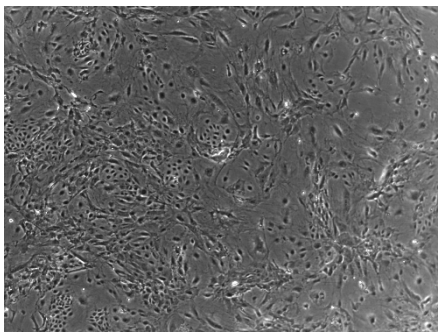
P1 – condition 2



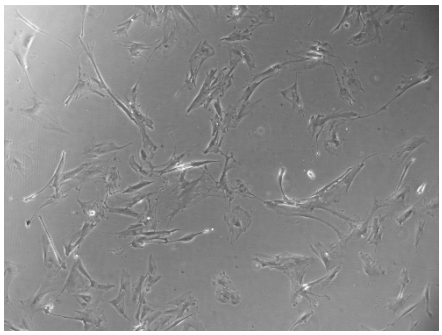
P2 – condition 2



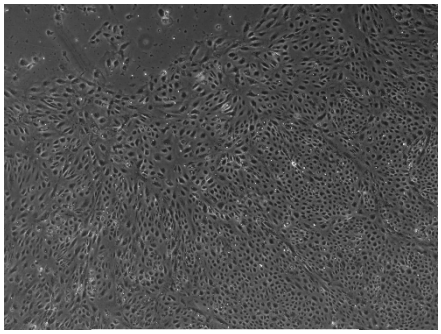
P1 – condition 3



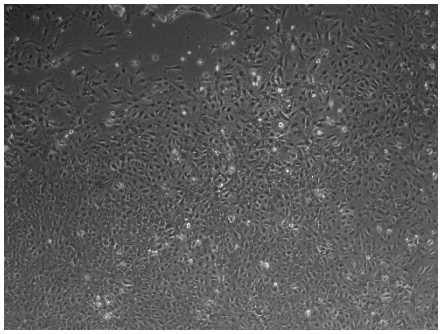
P2 – condition 3



P1 – condition 4

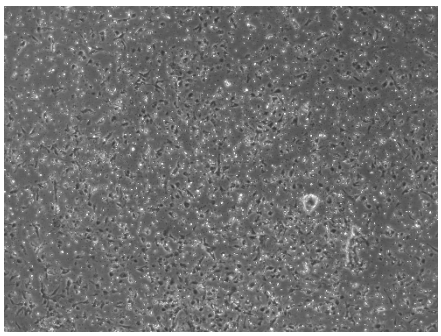


P1 – condition 5

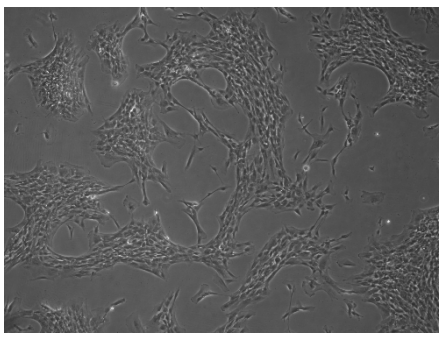


Donor 840-03-01

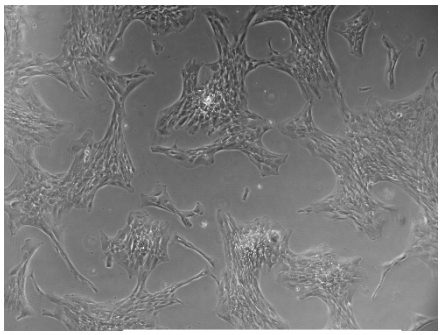
P1 – condition 1



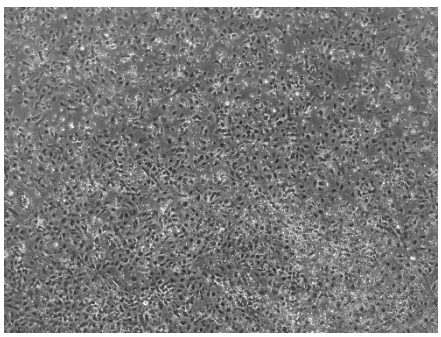
P2 – condition 1



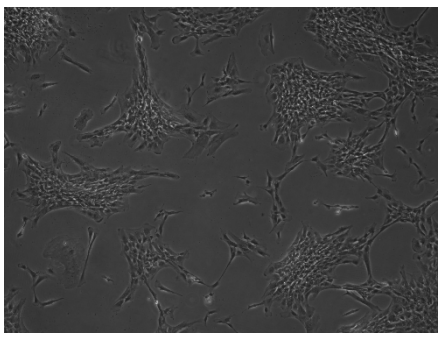
P3 – condition 1



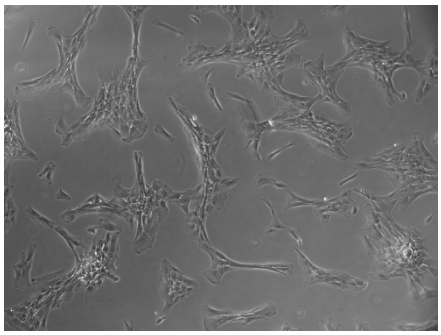
P1 – condition 2



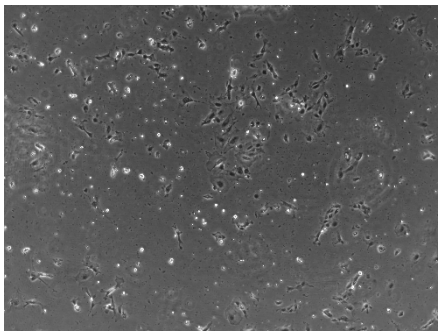
P2 – condition 2



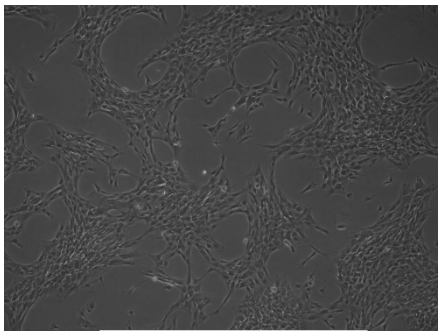
P3 – condition 2



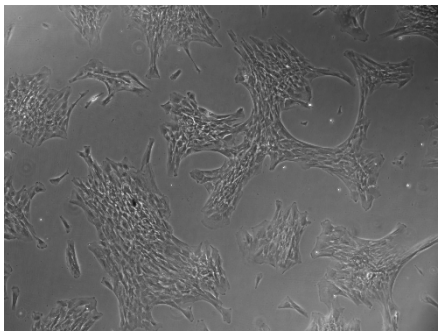
P1 – condition 3



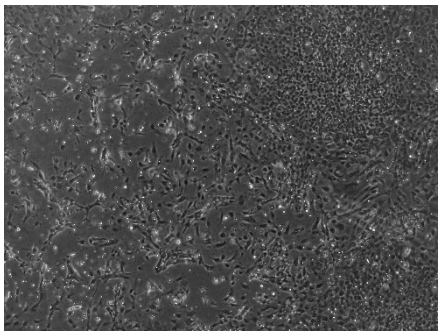
P2 – condition 3



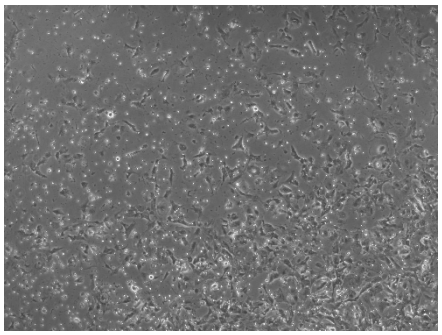
P3 – condition 3



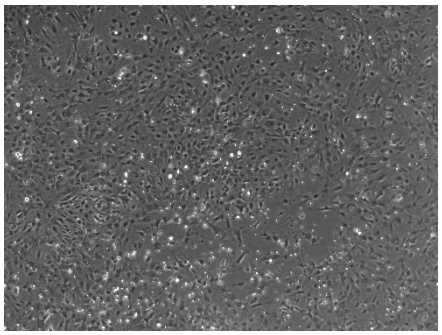
P1 – condition 4



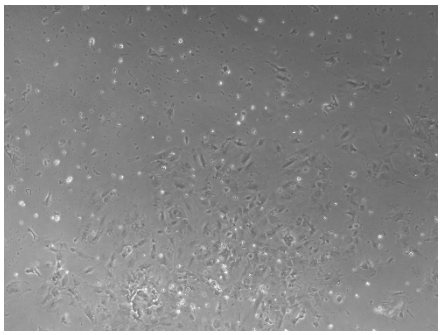
P2 – condition 4



P1 – condition 5

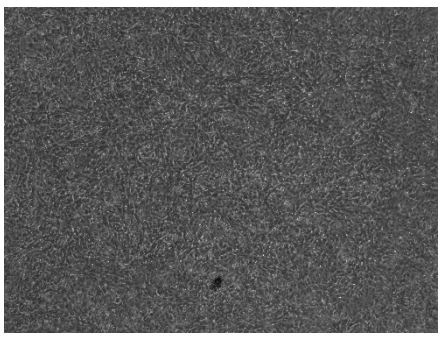


P2 – condition 5

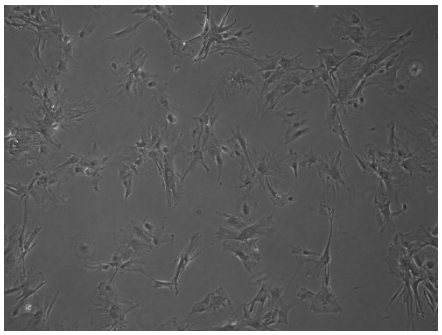


<u>Donor 840-03-03</u>

P1 – condition 1



P3 – condition 1



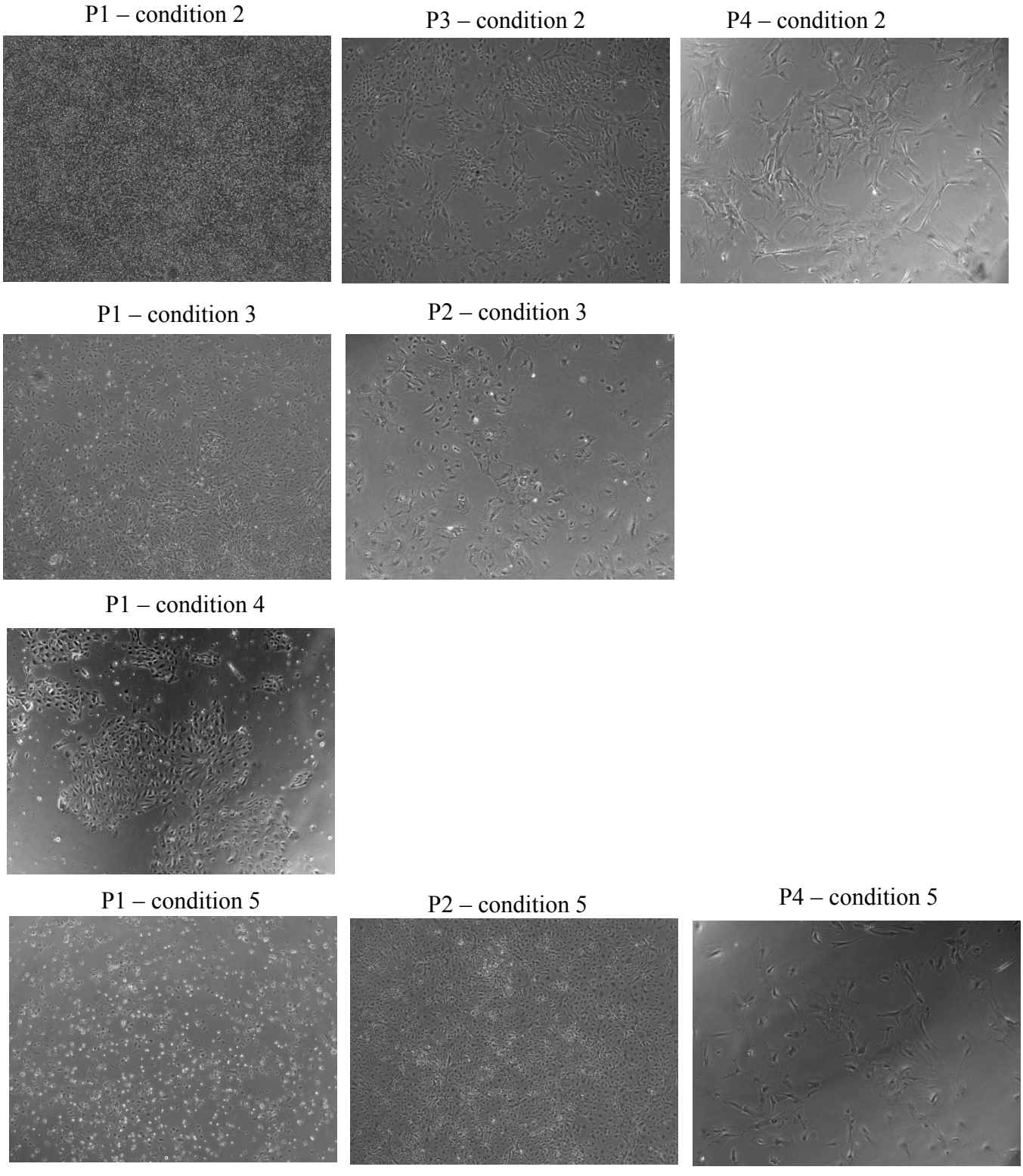


Figure 3.1. Cell morphology of various donor-condition combinations I. P = passage number after switching from phase 1 (initial phase) to phase 2 (passaging protocol). More detailed information on the exact conditions can be found in the Materials and Methods section. Donors: 840-03-01, 840-03-03, 841-03-02.

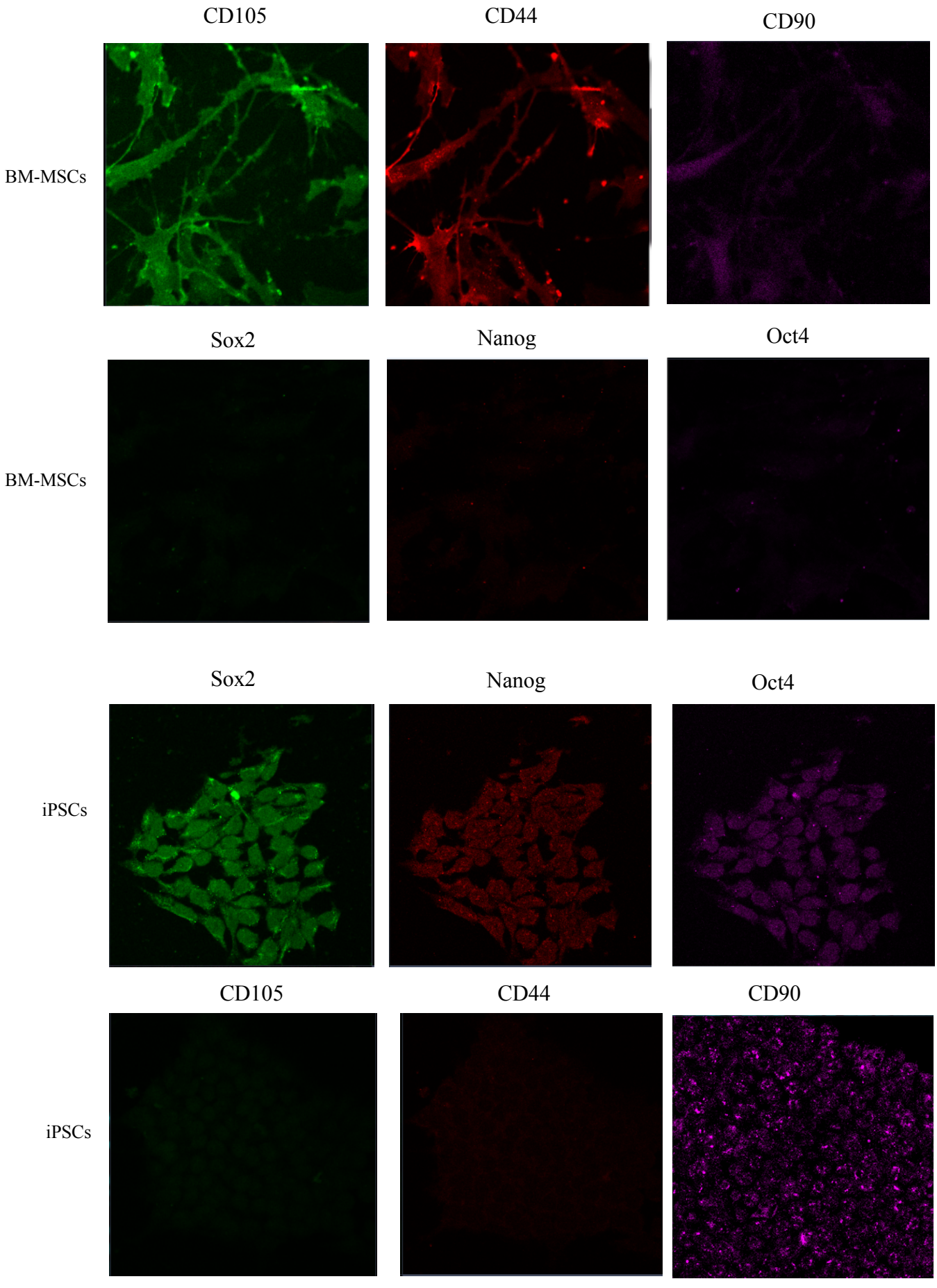
3.1.3 Immunofluorescence

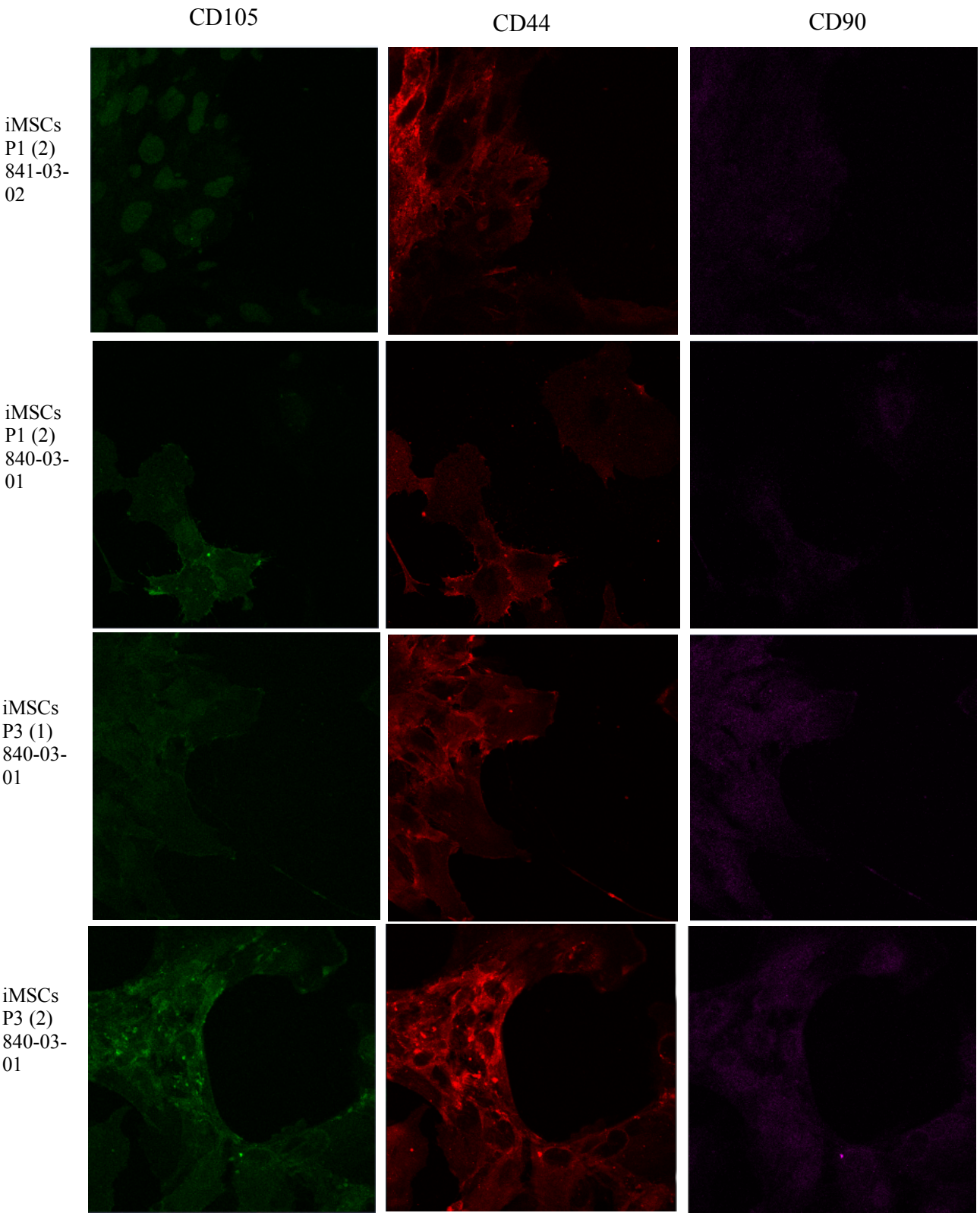
Immunofluorescence was employed to stain for three known pluripotency transcription factors and three known mesenchymal stem cell markers. Pluripotency markers included Nanog, Oct4 and Sox2, all of which are required to be upregulated for the cells to remain in a pluripotent state. MSC markers CD44, CD73 and CD90 were stained for as all of these are components of the minimal requirements for cells to be termed MSC-like as set by the ISCT. As mentioned before, not all protocols yielded viable cells and thus only a selection of condition-donor combinations could be stained and analysed. It is also important to note that not all the gain settings are the same between samples, as this was highly dependent on the control used for that round of staining. Gain is a relative measure of the amplification of a photon detection system. An increase in gain settings results in a brighter image, but consequently leads to an increase in background noise. For this reason, the results should not be interpreted in a quantitative way, but rather in a binary way of the respective marker proteins being present or not.

First, pluripotency and MSC markers were stained for in both iPSCs and BM-MSCs. CD105, CD44 and CD90 were all upregulated in BM-MSCs, albeit CD90 did not yield a strong signal after background correction. All three pluripotency markers were not detected in BM-MSCs. iPSCs showed upregulation of Sox2, Nanog and Oct4, without any expression of CD105 or CD44. CD90, however, was also upregulated as pluripotent cells are known to express this cell surface marker (figure 3.2).

Condition 2 for donor 841-03-02 displayed clear upregulation of CD44 and some minor upregulation of CD105, although it is difficult to tell whether this was residual background fluorescence. CD90 was not expressed. A similar pattern continues for most conditions in donor 840-03-01. CD44 is often the most highly expressed protein among all donors with a

clear cell surface marker pattern for each distinct cell. Comparing the CD44 expression levels in the iMSCs - irrespective of their induction medium - to levels in iPSCs, gives the impression that this specific marker is one of the first MSC markers to be highly expressed in these differentiating cells. The expression of CD105 across the different conditions and donors seems to be dependent on their current phase in the passaging protocol, as later passages demonstrate a stronger fluorescent signal. Donor 840-03-01 in particular shows distinct upregulation of CD105 for conditions 2 and 3, whereas donor 840-03-03 shows minimal staining at P1 with an increase in fluorescence at P4, condition 2. Results can be seen in figure 3.2.


CD105
CD44
CD90
BM-MSCs
Sox2
Nanog
Oct4
BM-MSCs
Sox2
Nanog
Oct4
iPSCs
CD105
CD44
CD90
iPSCs


CD105
CD44
CD90
iMSCs P1 (2) 841-03-02
iMSCs P1 (2) 840-03-01
iMSCs P3 (1) 840-03-01
iMSCs P3 (2) 840-03-01

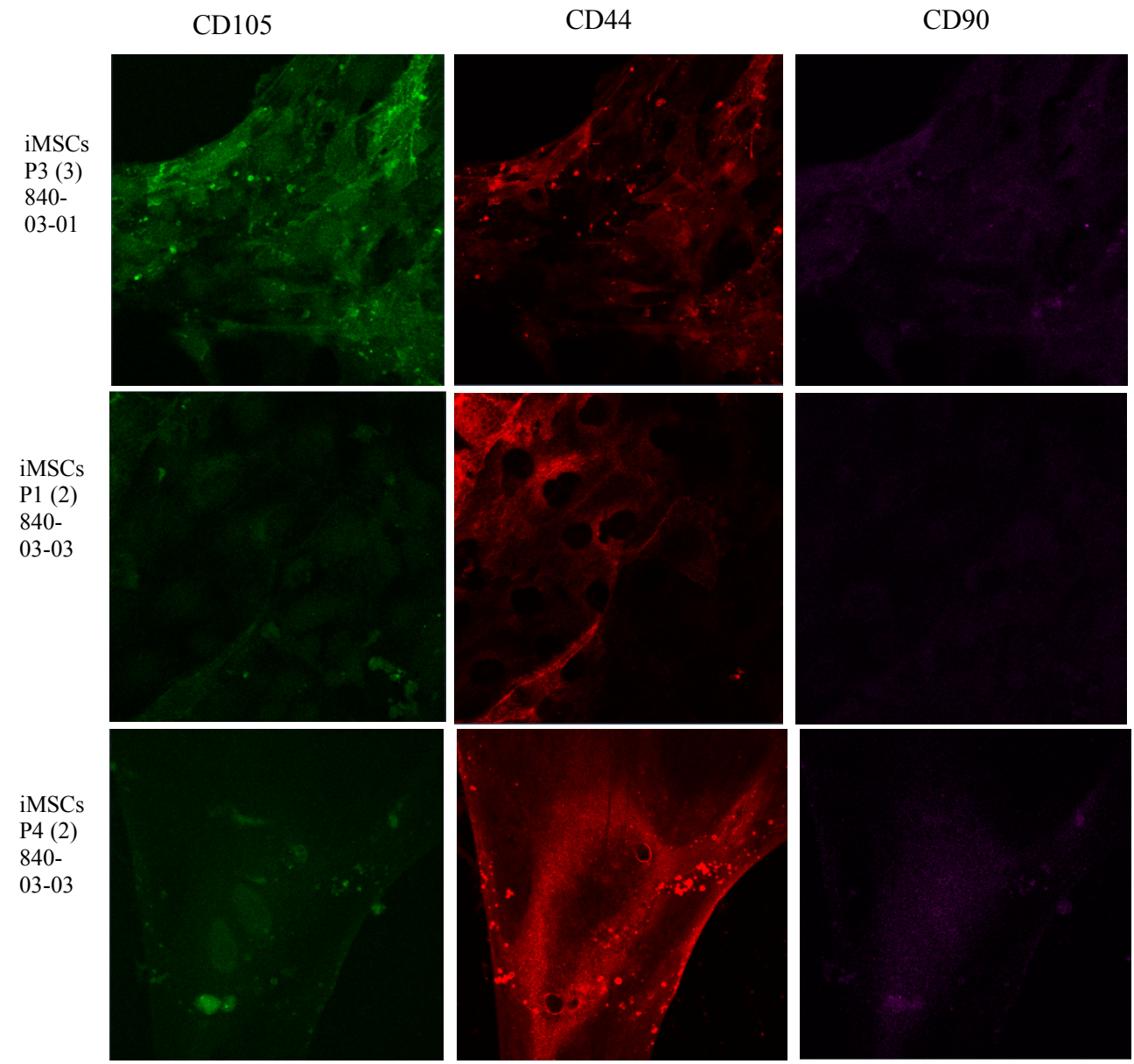


Figure 3.2. Immunofluorescence staining I. iMSCs that were used for this staining were made through protocols using 5 different medium conditions. P = passage number after switching from phase 1 (initial phase) to phase 2 (passaging protocol). Detailed information on the exact composition of the medium conditions can be found in the Materials and Methods section. Donors: 840-03-01, 840-03-03, 841-03-02. P = passage number. Number in brackets is condition number. MSC markers CD44, CD90 and CD105 were stained for using a red, purple and green secondary antibody, respectively. Pluripotency markers Sox2, Nanog and Oct4 were stained for using a green, red and purple secondary antibody, respectively.

3.1.4 Summary

The objective of the first set of differentiation experiments was to directly compare various protocols from the literature in different donors and thereupon decide the most suitable protocol for further in-depth analysis. This comparison was based on results from a cell morphology and protein expression perspective. However, during these experiments it became clear that not all protocols yielded viable cells for unknown reasons and thus a cell viability observation was added to the results section. Specifically conditions 1, 2 and 3 seemed to do well across all donors regarding viability, morphology and MSC marker upregulation. Notwithstanding, after switching to a non-Geltrex-coated plate after P2, cells appeared to undergo a senescent state, slowly decreasing proliferation. Therefore, a new approach had to be taken to circumvent this issue. For cell types such as MSCs, it is known that upon resting in an over-confluent state, their proliferation capacities might attenuate without altering their morphology or viability. For this reason, it was decided that the initial 10 to 14 day phase 1 of the protocol – leaving the cells in an over-confluent state for over a week – might have to be shortened. Moreover, the overall best performing condition (2) was used for further experiments to triage the experimental efforts. Also, a new condition, a commercial MSC medium (MesenPro), was added.

3.2 Continuation of protocol comparison - Focus on two conditions: αMEM and MesenPro

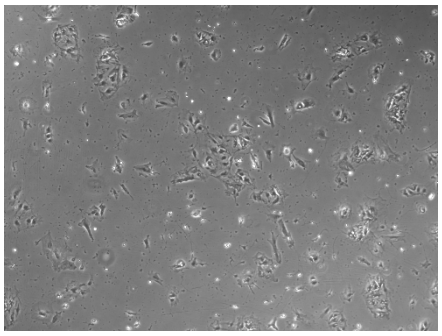
Upon selecting two conditions – αMEM medium from the previous experiments (2) and a commercial MSC medium (MesenPro) - a re-analysis of both phase 1 and 2 of the differentiation process was initiated. Phase 1 was shortened - for sample III this lasted 7 days and sample IV was passaged upon reaching confluency, usually taking 2 to 3 days. Cell seeding densities were similar to before, allowing large colonies to form prior to the induction. Upon the phase switch from phase 1 to 2, cells were previously cultured on Geltrex for the first 2 passages followed by culturing without a Geltrex base. This resulted in cell senescence for unknown reasons and it was therefore, as mentioned before, decided to shorten phase 1. However, even though the first phase was shortened the cell senescence still occurred. Hence, it was decided to keep the cells cultured on Geltrex-based plates which resulted in continued proliferation. All images shown are iMSCs cultured on Geltrex. This phenomenon suggested the length of phase 1 had less of an effect on cell senescence than did the Geltrex coating.

3.2.1 Assessment of morphology and viability

Cell morphology was analysed, again using the bright field microscope (figure 3.3). A brief overview is given this time of all the condition-donor combinations, showing images of one of their latest passages. For replicate III – 7 day phase 1 - the MesenPro medium performed worse overall regarding the cell survival and morphology of the iMSCs, especially for donors 840-03-01 and 841-03-02. The only donor that seemed to create viable MSC-like cells with this medium was 840-03-03. αMEM, on the other hand, showed more potential as cells

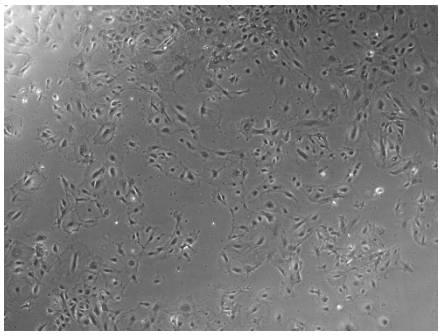
survived the phase switch from phase 1 to 2 in all donors, one of the more critical moments. Donor 840-03-01 and 841-03-02 iMSCs did survive but presented a typical MSC-like morphology to a lesser degree than did donor 840-03-03. iMSCs from donor 840-03-03 performed best as they continued to grow through several passages without senescence and with an MSC-like morphology. The last image for this donor was taken on day 38, but cells continued to grow for many more passages. For replicate IV – splitting upon reaching confluence – both MesenPro and αMEM did not produce viable cells in donors 841-03-02 and 840-03-01 during the course of phase 2. Cells showed unusual morphology instead of forming robust cells with MSC-like morphological features. However, even though this protocol was not helping cells to transform into solid iMSCs for the above mentioned donors, iPSCs from donor 840-03-03 did not seem to be affected by the shortened phase 1 and thus allowed the creation of healthy iMSCs with typical MSC morphology.

iMSC III MP
Donor 840-03-01



D14 (P2)
On Geltrex

iMSC III αMEM
Donor 840-03-01

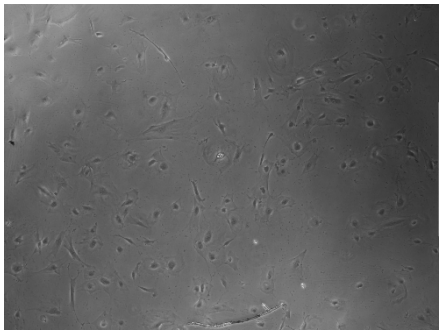


D14 (P2)
On Geltrex

iMSC III MP
Donor 841-03-02

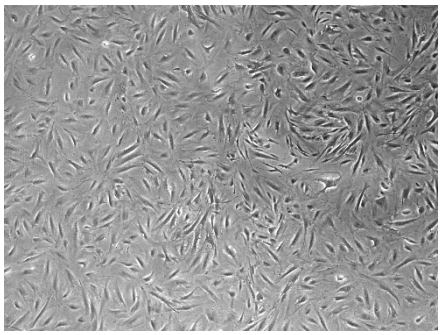
No survival

iMSC III αMEM
Donor 841-03-02



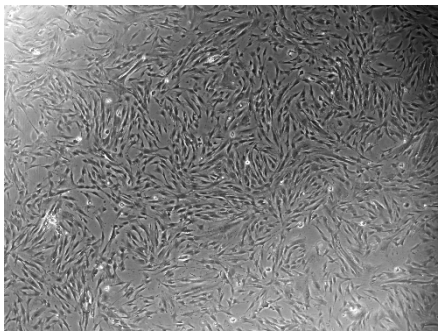
D17 (P5)
On Geltrex

iMSC III MP
Donor 840-03-03



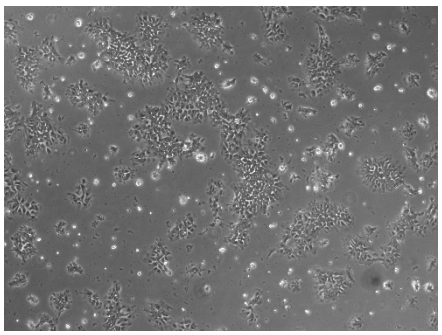
D38 (P7)
On Geltrex

iMSC III αMEM
Donor 840-03-03



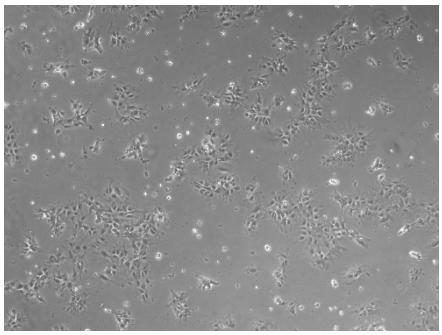
D38 (P10)
On Geltrex

iMSC IV MP
Donor 840-03-01



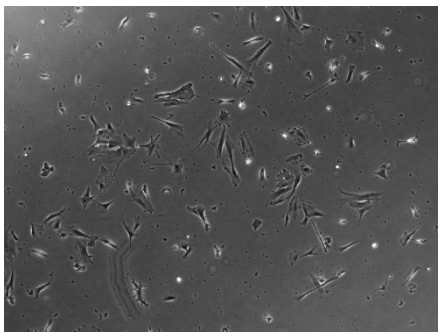
D3 (P1)
On
Geltrex

iMSC IV αMEM
Donor 840-03-01



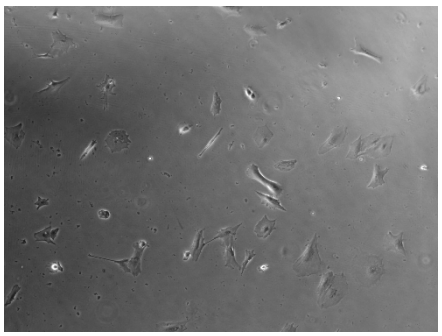
D3 (P1)
On Geltrex

iMSC IV MP
Donor 841-03-02



D12 (P3)
On
Geltrex

iMSC IV αMEM
Donor 841-03-02

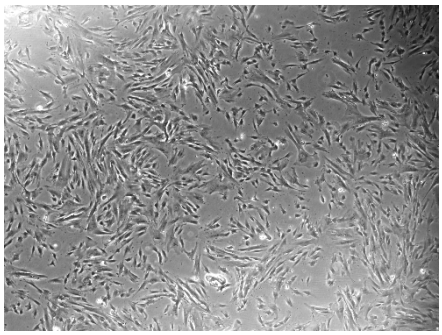


D12 (P3)
On
Geltrex

iMSC IV MP
Donor 840-03-03

No survival

iMSC IV αMEM
Donor 840-03-03



D38 (P9)
On
Geltrex

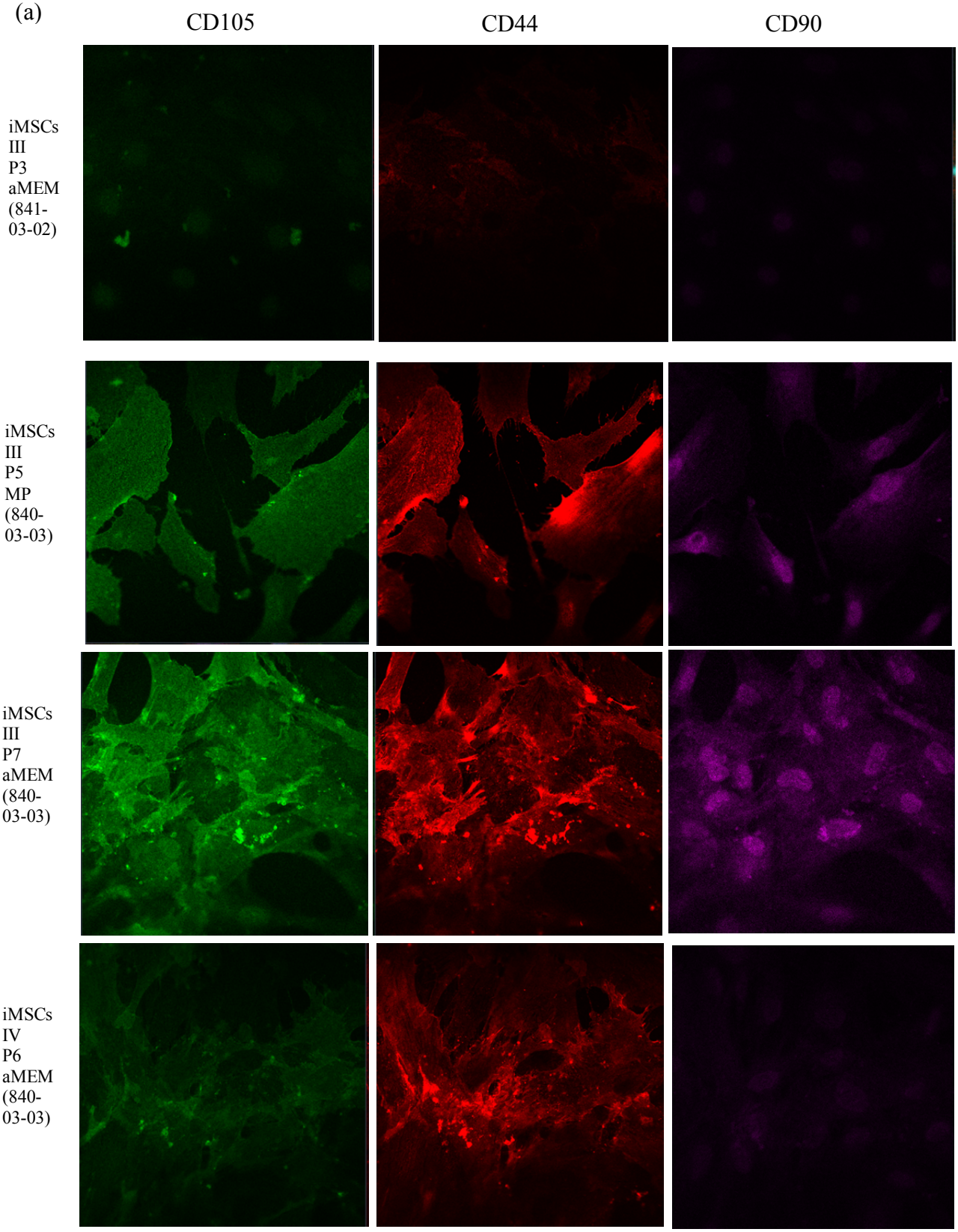
Figure 3.3. Cell morphology of various donor-condition combinations II. P = passage number after switching from phase 1 (initial phase) to phase 2 (passaging protocol). MP = MesenPro medium, αMEM = condition 2 from previous experiments. Sample III = phase 1 of 7 days, sample IV = split-upon-confluency protocol, usually taking around 2-3 days. Donors: 840-03-01, 840-03-03, 841-03-02.

3.2.2 Immunofluorescence

Immunofluorescence was employed for this second set of experiments to determine the expression of MSC and pluripotency markers. A brief overview is given in figure 3.4, displaying the difference in expression of the before mentioned markers for both conditions. Treatment of donor 840-03-02 upregulates the designated MSC markers. However, this is not to the same extent as in donor 840-03-03, where both MesenPro and αMEM induced iMSCs display strong fluorescence and upregulate the MSC markers in replicate III. In replicate IV of the same donor, staining resulted in clear upregulation of CD105 and CD44, but not of CD90. None of the iMSCs from donor 840-03-01 survived whilst passaging onto a plate for immunofluorescence analysis.

Some of the pluripotency proteins were still upregulated even after the phase switch, mainly for donor 841-03-02 and for the MesenPro induced iMSCs from donor 840-03-03. From the same donor (840-03-03) from both replicate III (αMEM) and IV (αMEM) cells did not show upregulation of pluripotency genes, which is an important step in becoming more MSC-like. It must be noted, however, that the iMSCs from 841-03-02 III αMEM and 840-03-03 III MP were of a lower passage when employed for IF experiments compared to the further developed 840-03-03 III αMEM and IV αMEM at P7 and P6, respectively. Thus, these results do not take into account the passage-related effects of phase 2.

(a)


CD105
CD44
CD90
iMSCs III P3 aMEM (841-03-02)
iMSCs III P5 MP (840-03-03)
iMSCs III P7 aMEM (840-03-03)
iMSCs IV P6 aMEM (840-03-03)

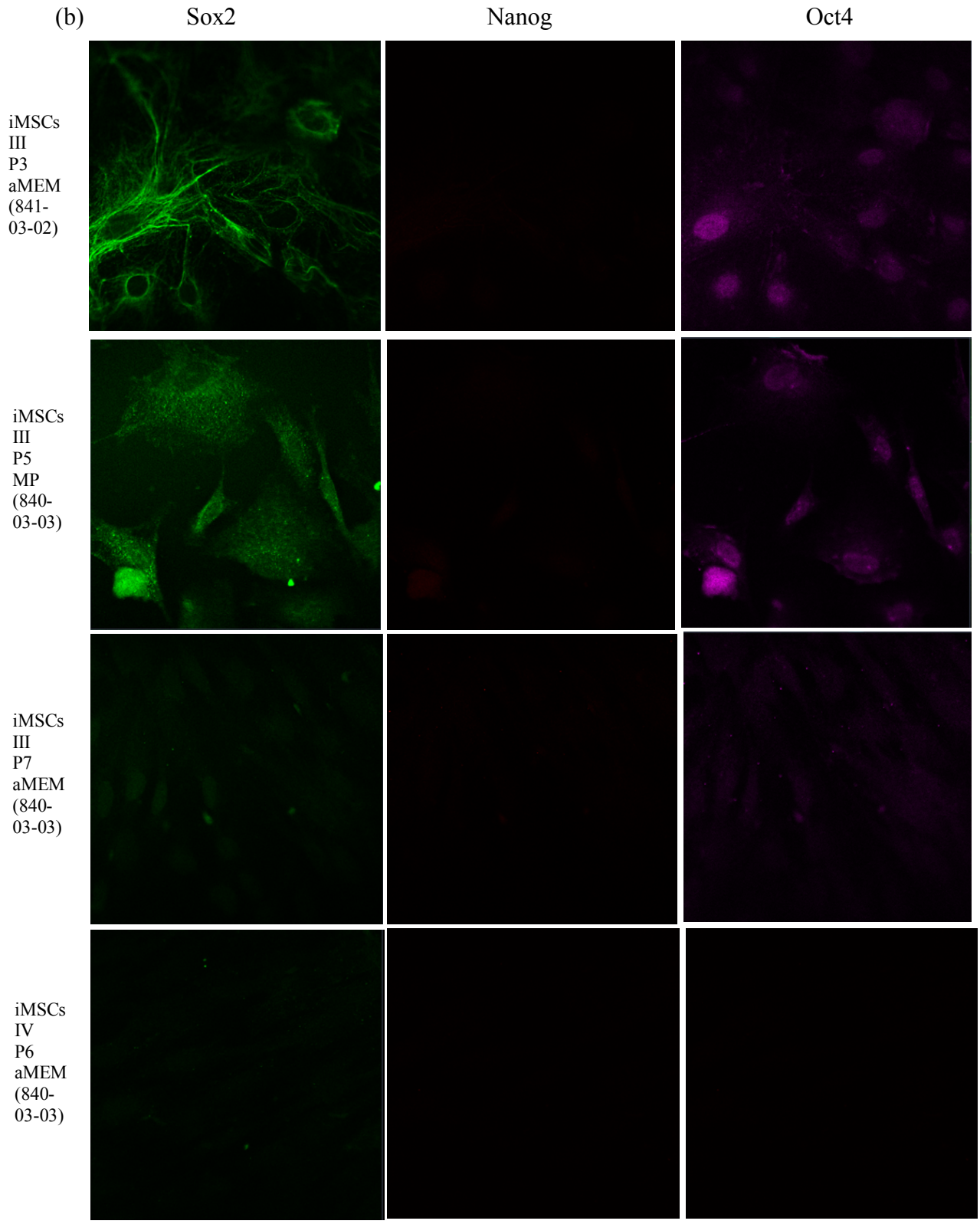


Figure 3.4. Immunofluorescence staining II. iMSCs that were used for this staining were made through protocols using MesenPro (MP) and αMEM. Sample III = 7-day phase 1 protocol, sample IV = split-upon-confluency protocol. P = passage number. Donors 841-03-02 and 840-03-03 were stained as 840-03-01 did not survive for this particular experiment. (a) MSC markers CD44, CD90 and CD105 were stained for using a red, purple and green secondary antibody, respectively. (b) Pluripotency markers Sox2, Nanog and Oct4 were stained for using a green, red and purple secondary antibody, respectively.

3.2.3 Alkaline phosphatase (ALP) assays

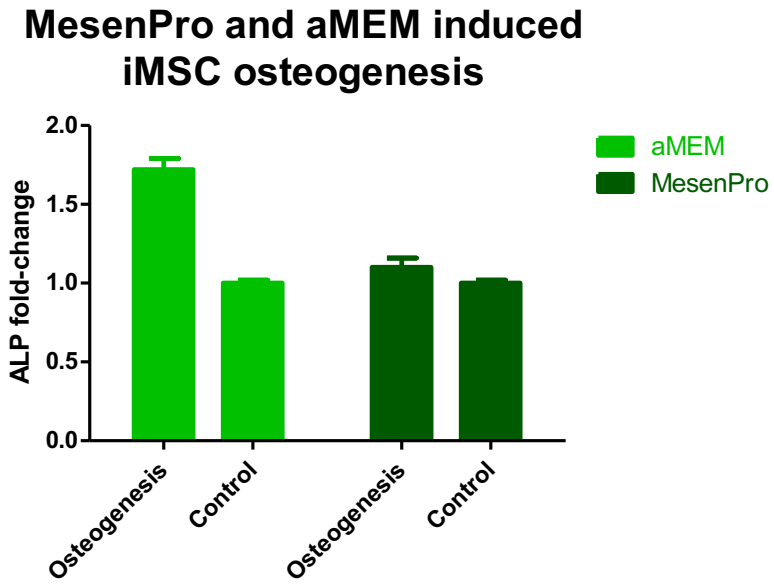
The enzyme alkaline phosphatase (ALP) is used as a determinant of osteogenesis, normally measured relative to its control on day 7. A dexamethasone-based osteogenic medium was used to initiate the differentiation process. Controls in this instance are non-osteogenic induced iMSCs and/or BM-MSCs. Only donor 840-03-03 iMSCs were used for these experiments.

Firstly, ALP activity was measured in iMSCs induced with αMEM and MesenPro, and compared to their non-osteogenic induced counterparts which were used as controls. The aim for this experiment was to check whether iMSCs upregulate ALP to a similar extent as do BM-MSCs – on average a 2 to 3 times fold-change as known from prior experiments performed in this lab and in the literature (Chen et al., 2013). Figure 3.5(a) shows the combined measurements of both replicate III and IV for αMEM compared to MesenPro III iMSCs. Beforehand, the intention was to combine MesenPro III and IV, however due to cells not surviving the phase-switch, the ALP assay with MesenPro could only be done with III. Clearly, a highly significant upregulation of ALP is present in osteogenic induced αMEM-iMSCs. On the other hand, the MesenPro-iMSCs did not show any sign of an increased ALP enzyme presence compared to their control thus suggesting these cells did not undergo the proper transformation into MSC-like cells based on their osteogenic capacities.

Thereafter, ALP was measured specifically in iMSCs induced with αMEM both for replicate III and IV, and in BM-MSCs. Additionally, this ALP assay analysed the relative difference in ALP protein present during osteogenesis in Geltrex-coated (g) and non-Geltrex coated (ng) plates, for both iMSCs and BM-MSCs. Figure 3.5(b) shows results from the above mentioned experiment. The overall graph clearly displays a difference in ALP between the g and ng plates, with the Geltrex yielding a higher base-level ALP (figure 3.5(b), graph on the right). The same graph on the right shows a significant difference between BM-MSC (g) and all of

the ng plates. Specifically, $P<0.05$ for BM-MSC (ng) and αMEM IV (ng), and $P<0.01$ for αMEM III (ng). On the left, the relative ALP fold-change on day 7 is plotted for all the different combinations of BM-MSCs and αMEM iMSCs. They have all been plotted against their respective control. Both BM-MSC (ng and g) and αMEM III (ng and g) show a similar highly significant ($P<0.001$) upregulation pattern. This suggests a comparable ALP regulation mechanism for osteogenesis in BM-MSCs and αMEM III. αMEM IV, on the other hand, also displays a significant relative upregulation compared to its own control, albeit to a lesser extent than does αMEM III.

(a)



(b)

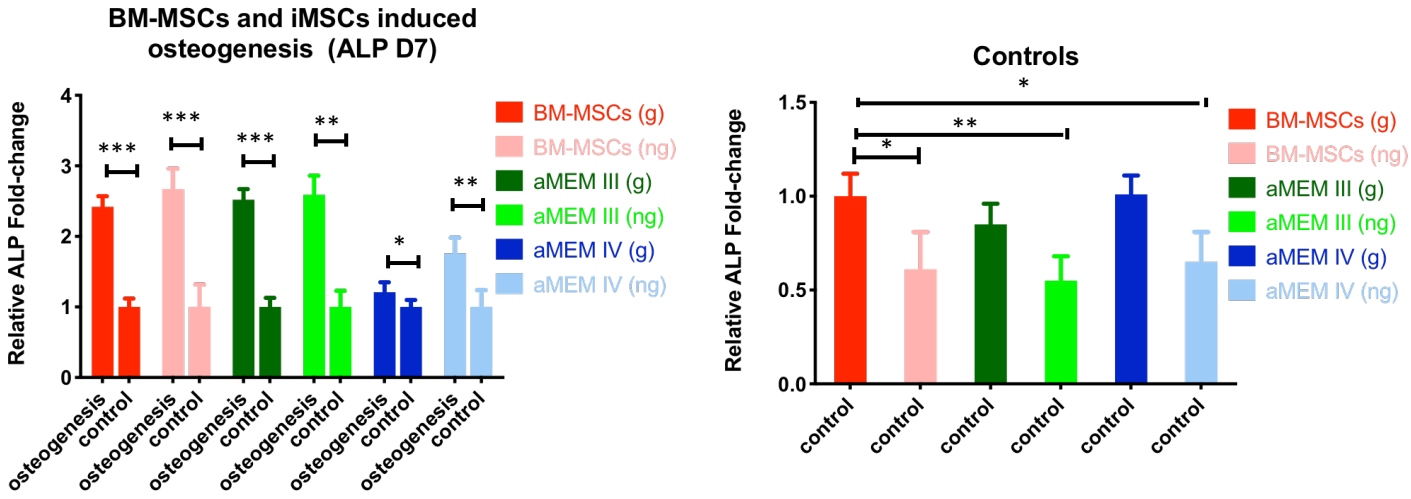


*Figure 3.5 Alkaline phosphatase (ALP) assay performed at day 7 after the start of differentiation into osteoblasts using a dexamethasone-based medium. (a) Comparison of iMSCs differentiated through αMEM or MesenPro (MP) and their subsequent differentiation along the osteoblast lineage. αMEM includes both iMSCs from replicates III (7-day phase 1 protocol) and IV (split-upon-confluency in phase 1 protocol). MesenPro includes only iMSCs from replicate III. N=4, donor = 840-03-03. P5-P7 iMSCs were used for this assay. (b) On the left: ALP assay comparing BM-MSCs, αMEM iMSCs III and IV with their respective control. Moreover, the effect of a Geltrex base (g) versus a non-Geltrex base (ng) on ALP expression levels were tested. On the right: all the controls compared to the BM-MSC (g) control, reflecting their relative base ALP levels. N=4. BM-MSCs P=9, iMSCs III P=10, iMSCs IV P=9. *=p<0.05, **=p<0.01, ***=p<0.001.*

3.2.4 Alizarin Red Staining (ARS) and Oil Red O (ORO)

Alizarin Red Staining (ARS) was employed for identification of mineralized nodules in osteoblasts, whereas Oil Red O (ORO) was used for identification of lipid fat droplets in adipocytes.

Firstly, a set of mineralization and lipid droplet staining experiments was conducted in both MesenPro and αMEM iMSCs. Moreover, these stainings were performed both on Geltrex-coated (g) and non-Geltrex-coated (ng) plates. Figure 3.6 displays these results. Specifically, ARS in αMEM-iMSCs for both replicates III and IV on Geltrex plates, displayed the potential to form mineralized nodules with dexamethasone-based osteogenic medium (figure 3.6(a)). iMSCs MP III did not show any major sign of mineralization. Interestingly, none of the iMSCs cultured on plates without Geltrex presented staining of mineralized nodules (figure 3.6(b)).

At first sight, the adipocyte (AD) staining ORO seemed to have worked for all conditions, regardless of their coating. However, upon further inspection by use of microscopy, this red background was deemed unspecific staining. No lipid droplets could be seen in the microscope.

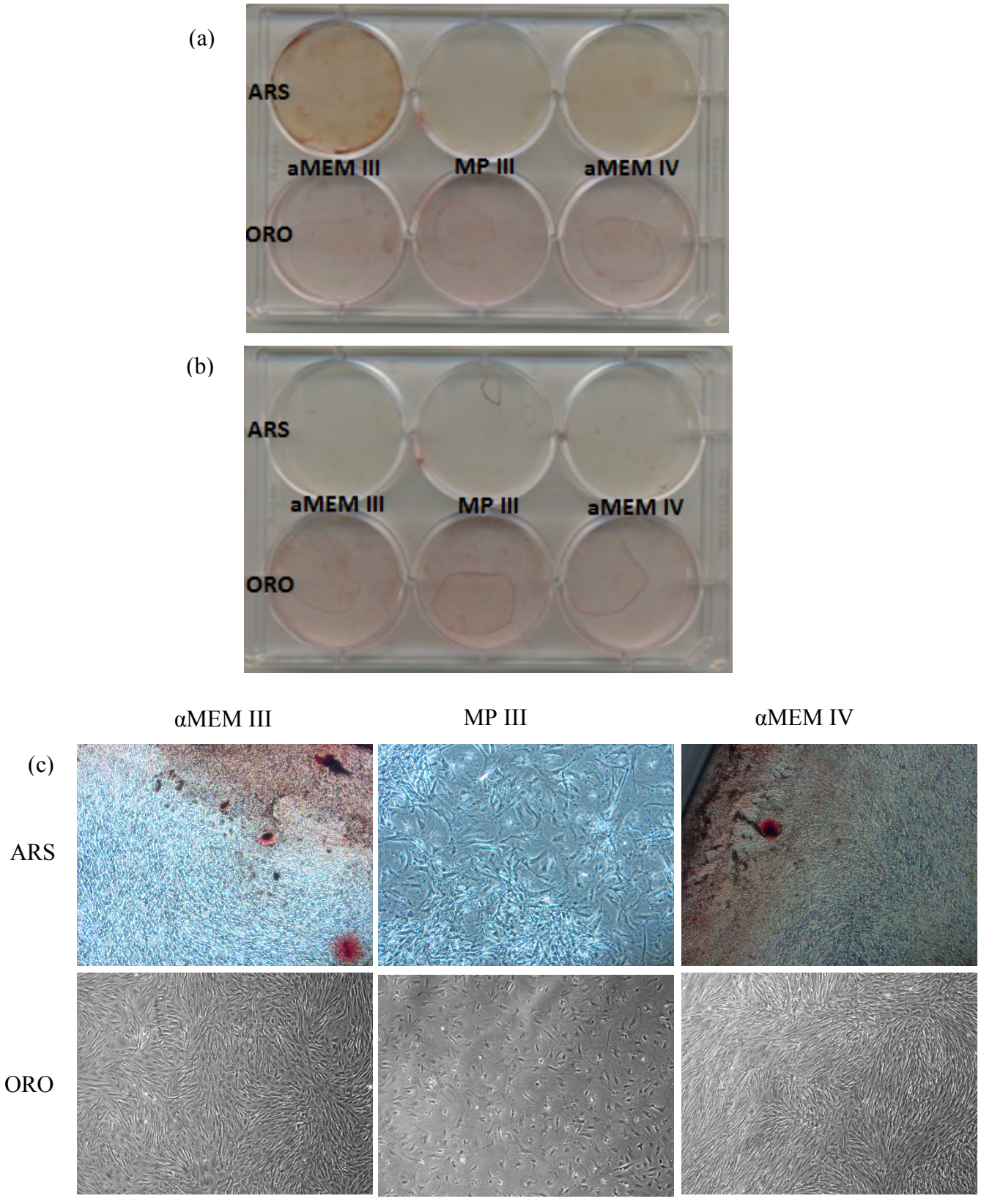


Figure 3.6. Alizarin Red Staining (ARS) and Oil Red O (ORO) Staining for detection of mineralized nodules and lipid fat droplets, respectively I. (a) Scan of ARS and ORO stained plate with iMSCs induced via either αMEM (III + IV) or MesenPro (MP - III), grown on a Geltrex base. (b) shows similar scans with the same conditions, except without the Geltrex base. (c) Microscopic images from scan (a). Here, both for conditions αMEM III and IV mineralized nodules were stained through ARS. ORO did not yield any visible staining in the iMSCs induced with adipogenic medium.

Further colorimetric staining experiments were conducted whereby only αMEM-iMSCs were employed, and BM-MSCs were included for similarity measurements, displayed in Figure 3.7. A newly synthesized iMSC replicate (V) was also included, transformed using the now standardized protocol using αMEM and a phase 1 of 14 days, followed by a passaging protocol on Geltrex-coated plates. Different passages were used, from early P5 to late P23 iMSCs and late P15 BM-MSCs. For these, osteoblast lineage differentiation potential was tested using dexamethasone (Dex) and Oncostatin M (OSM)-based conditions. Adipocyte lineage differentiation potential was tested using a standardized adipogenic medium, as described in the Materials and Methods section. The cells referred to as controls were continuously grown in their respective maintenance medium, αMEM for iMSCs and MesenPro for BM-MSCs.

All the controls appeared similar, with absent mineralized nodules and lipid fat droplets. However, a light yellow-red background tone was visible in the iMSCs V controls. The same iMSCs V stained for ARS, indicating a strong osteogenic potential. iMSCs III and IV were tested at a much later passage (P23, P22 resp.) which resulted in close to no calcified nodules for the Dex-based condition. OSM showed more potential for these two replicates, as both produced a yellow-red staining with accompanying calcified nodules. BM-MSCs did not mineralize nor stained for lipid fat droplets. This, however, could be due to the late passage of these cells, which is a phenomenon known to occur whilst sub-culturing, as they slowly halt proliferation, going into a senescent state. A microscopic image from an earlier adipogenesis experiment in BM-MSCs P8 is presented to show the adipogenic capacities of BM-MSCs at an earlier passage. Also, colleague Chao Jiang was kind enough to provide an extra adipogenesis image from P5 BM-MSCs.

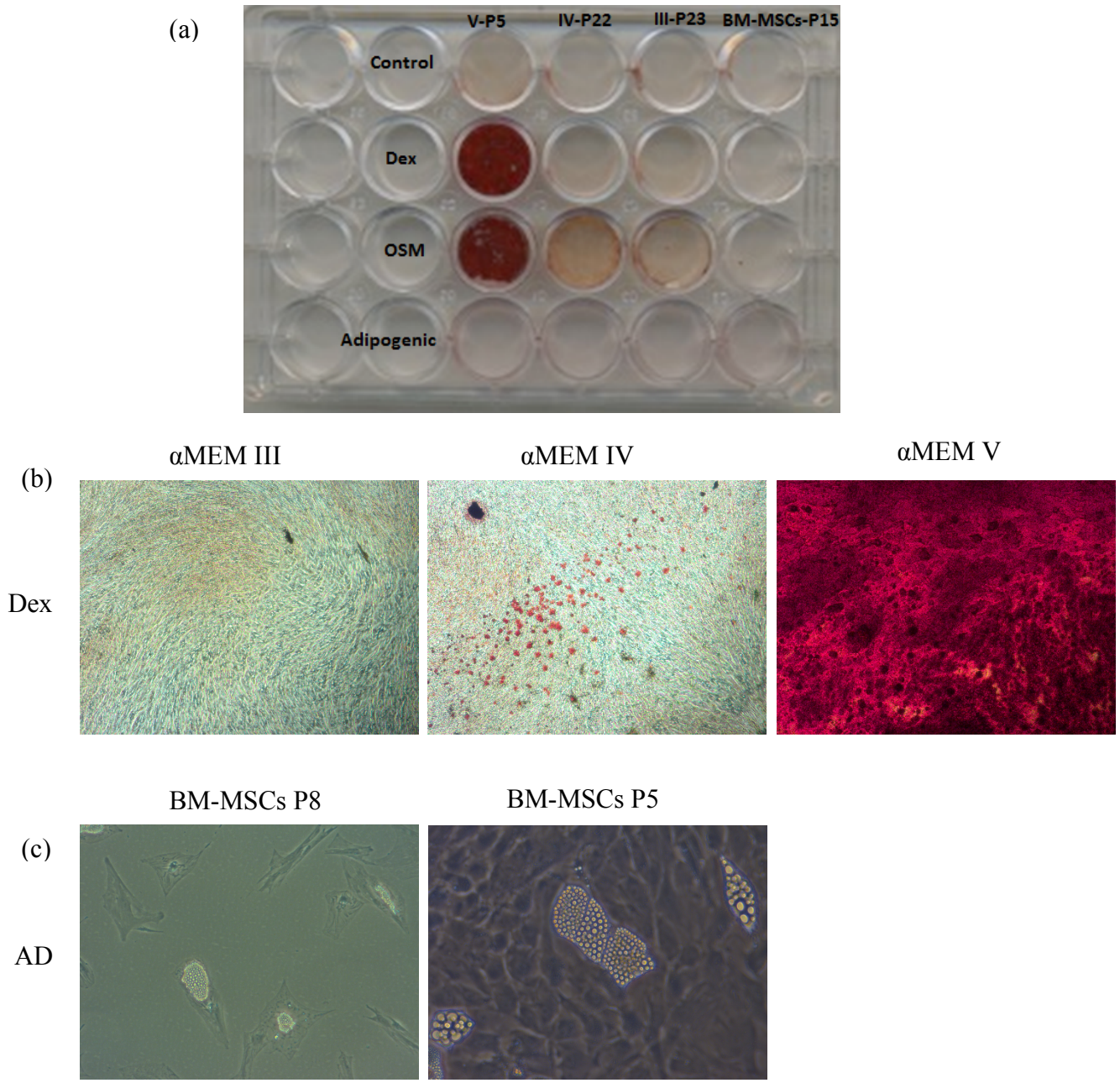


Figure 3.7. Alizarin Red Staining (ARS) and Oil Red O (ORO) staining for detection of mineralized nodules and lipid fat droplets, respectively II. iMSCs of different passages and late passage BM-MSCs (P15) were employed. Osteogenesis was induced through both a dexamethasone-based medium (Dex) and an Oncostatin M (OSM)-based medium. Adipogenic induction was done using a standard adipocyte medium, as mentioned the Materials and Methods. (a) A scan of both ARS and ORO staining. (b) Microscopy images of the same plate. (c) On the left, an image showing earlier P8 BM-MSCs and their ability to form lipid fat droplets during adipocyte differentiation. On the right, P5 BM-MSCs, an image received from colleague Chao Jiang.

3.2.5 Summary

The main objective of the second set of experiments was to ascertain a protocol that could provide a constant supply of iMSCs. Two conditions were tested - MesenPro and αMEM – as well as an adjusted length of phase 1, both 7-day (replicate III) and split-upon-confluency (replicate IV). Moreover, the dependence and effects of Geltrex-coated plates were also analysed. Results indicated that the growth of iMSCs on Geltrex-coated plates, and not per se the phase 1 length, was the determining factor of cells undergoing senescence. Therefore, iMSCs were continuously cultured on Geltrex-coated plates.

MesenPro did not transform iPSCs into usable iMSCs. Even though all MSC markers were expressed above background level, Sox2 and Oct4 remained upregulated as well, indicating an incomplete transition. The best performing condition was αMEM, which in donor 840-03-03 yielded iMSCs that upregulated all MSC markers, albeit CD90 in replicate IV only minimally, and downregulated all pluripotency markers.

Taking the morphology, viability and immunofluorescence results into account it was decided to continue further experiments with donor 840-03-03 in combination with the αMEM protocol. An ALP assay was employed to determine osteogenic capacities of iMSCs compared to BM-MSCs. Both αMEM replicates III and IV were capable of differentiating along the osteogenic lineage, based on the significance of their relative ALP fold-change. However, replicate III displayed a better potential to do so, demonstrating a similar pattern to BM-MSC ALP upregulation, with an approximate 2 to 2.5 fold increase compared to their respective controls. The osteogenic capacity of iMSCs was verified using ARS to stain for calcified nodules. BM-MSCs P8 produced lipid fat droplets, whereas none of the iMSCs showed the potential for differentiation along the adipogenic lineage as measured by these fat droplets.

3.3 In-depth analysis using CyTOF and RNA sequencing

CyTOF is a form of mass cytometry, combining both mass spectrometry and flow cytometry elements for analysis on a single cell level. Here, CyTOF was employed to determine the relative protein expression of MSC and pluripotency markers, as well as hematopoietic markers which were used as controls. Protein expression was measured and compared between 4 cell types: iPSCs, end of phase 1 cells, iMSCs (of different passages) and BM-MSCs (of different donors and passages). RNA sequencing is a tool used to measure the mRNA content present in cells. Here, this tool was employed to compare gene expression profiles between the above mentioned 4 cell types in a time course-based manner. Timepoints included day 0 (D0, iPSCs), D1, D4, D7, D14 (end of phase 1), P1, P2, …, P9. P8 iMSCs and P9 BM-MSCs were used for comparison of gene expression profiles.

3.3.1 Protein expression measurements using CyTOF

Figures 3.8 (a) and (b) display viSNE plots and graphs visualizing the CyTOF data. In the top left viSNE plot in figure 3.8(a), all the cell populations have been labelled with different colours – brown-red being iPSCs, light blue being cells at the end of phase 1 during the differentiation, orange-yellow being iMSCs of different passages and dark blue representing BM-MSCs of two different passages. These viSNE plots are based on barcoding of the different cell types prior to them being added to one sample. viSNE plots aim to display a more general overview of how protein expression levels change, whereas the graphs aim to display the same data in a more quantitative manner, also allowing to visualize the homogeneity between different passages in both iMSCs and BM-MSCs.

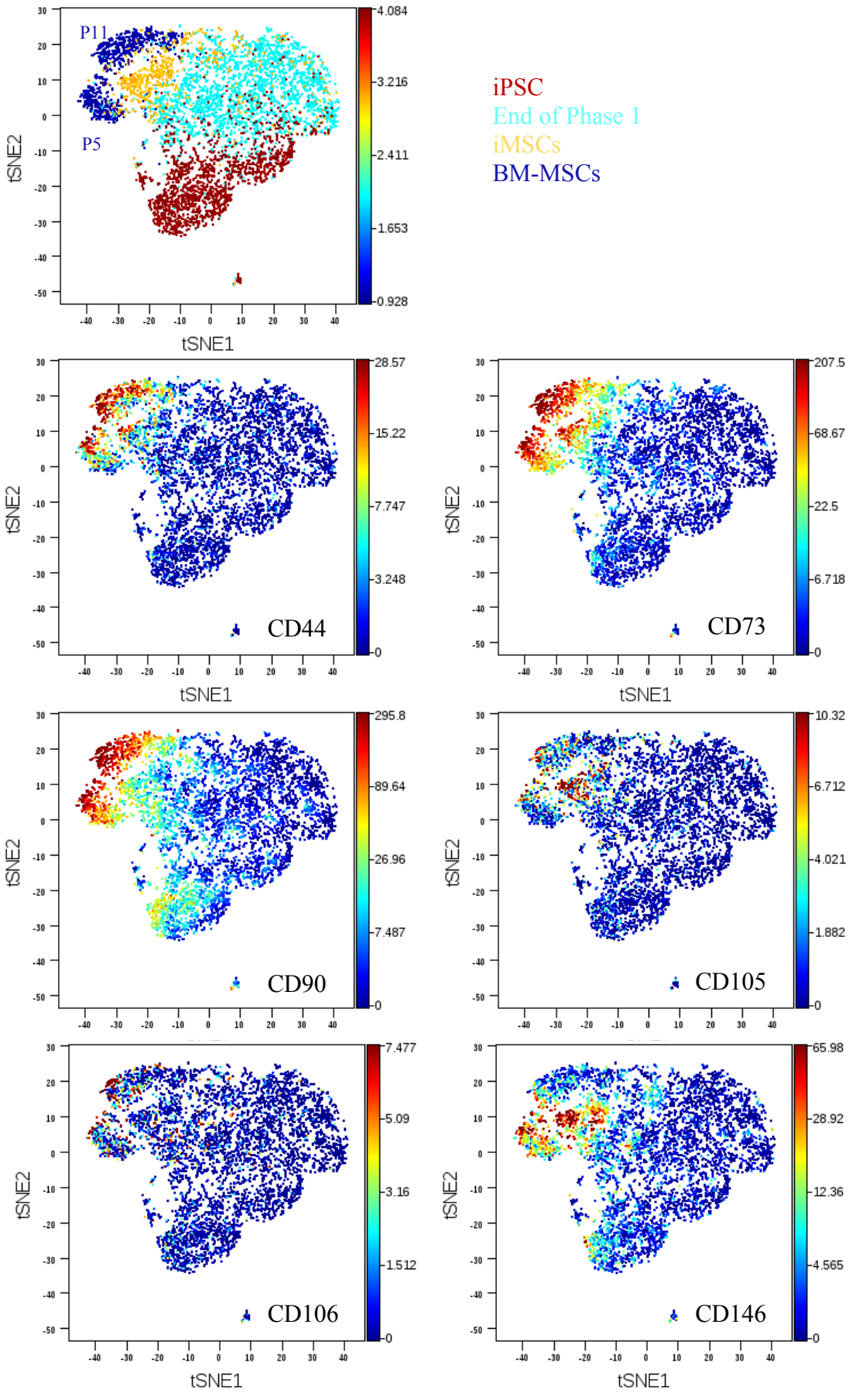
An initial change in protein expression can be seen between iPSCs and cells at the end of phase 1 (day 14). This is followed by the phase switch of the protocol. The switching of phases is a selection procedure whereby only cells (iMSCs) survive with the correct features. Consequently, marker protein expression patterns of iMSCs are similar to those of BM-MSCs and are thus presented in closer proximity to BM-MSCs in the viSNE plots as compared to their iPSC predecessor.

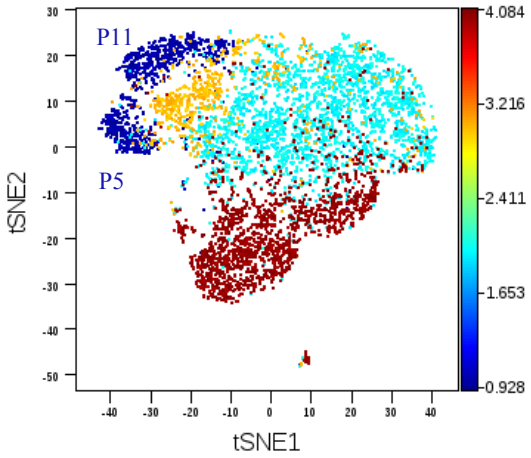
Protein expression trends for the MSC markers CD44, CD73, CD90, CD105 and CD166 are similar between iMSCs and BM-MSCs. CD44 in particular, was dependent on the passage number of the iMSC, the expression increasing following continued sub-culturing. The other MSC markers did not seem to rely on passaging for an increase in protein expression to take place. Expression levels remained similar in iMSCs even after thorough passaging for over 3 months. Markers CD106 and CD271 did, however, not show a similar pattern between iMSCs and BM-MSCs. CD106 specifically, seems only to be upregulated in BM-MSCs and not to a visible extent in any of the other cell types. CD271 was, interestingly, most strongly upregulated in iPSCs and BM-MSCs, with a decrease in expression upon the start of the differentiation process as presented by the end of phase 1 cells, which did not recover in iMSCs thereafter. The effect passage number has on certain cell surface markers was most apparent in CD146 – as suggested by the literature -, as well as in CD271. BM-MSCs of an earlier passage had these two markers expressed to a higher degree. Expression dropped significantly in later passage BM-MSCs. Hematopoietic markers CD14 and CD45 were not or barely expressed in any of the cell types.

For pluripotency markers Oct4, Sox2, Nanog and Tra-1-60, trends were similar in that all markers were declining as the differentiation process continued. A different viSNE plot is displayed for Sox2 and Nanog. Sox2 showed a clear difference in expression between iPSCs and the other cell types, starting with a high expression level and dropping to sub-threshold in

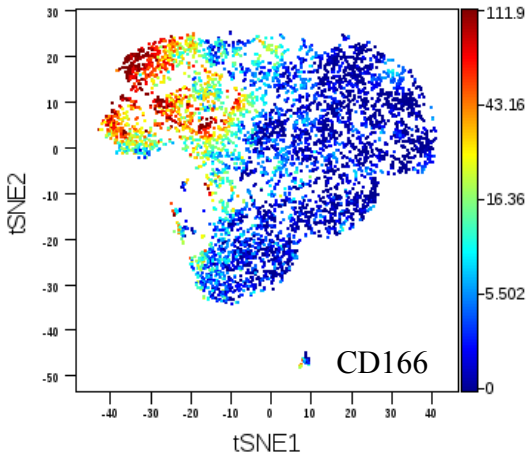
iMSCs, comparable to BM-MSCs. In iPSCs, Oct4 and TRA-1-60 both did not present a strong (>90%) expression, as they displayed a score between 40-50% upregulation within the population. However, relative to other cell types this was still considered highly significant. This might be related to the antibody concentration or quality rather than them not expressing the protein. The same, but to a more severe extent, is true for Nanog. Normally, iPSCs should upregulate all these pluripotency markers at least 90-95%. However, results in this experiment were not conform literature standards, probably due to the wrong antibody concentration or human error during the preparation of the samples. ALP was highly expressed in iPSCs and expressed to a varying degree in BM-MSCs, mostly dependent on their respective passage number. Both end of phase 1 cells and iMSCs did express ALP, although much less so than did iPSCs. However, the expression levels in iMSCs were comparable to late P11 BM-MSCs.

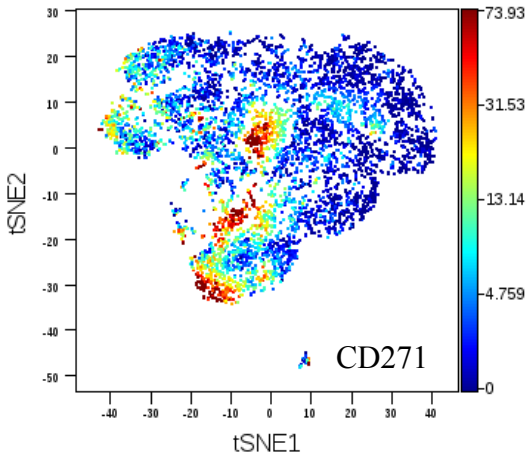
(a)

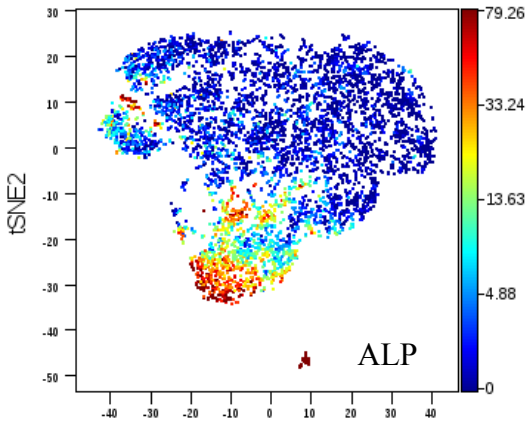

P11
P5
iPSC
End of Phase 1
iMSCs
BM-MSCs
tSNE1
tSNE2
CD44
CD73
CD90
CD105
CD106
CD146

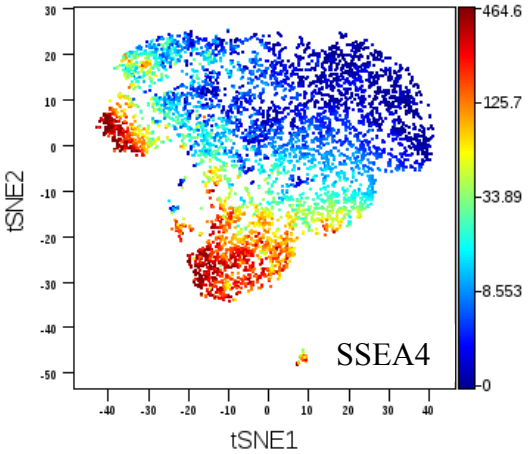


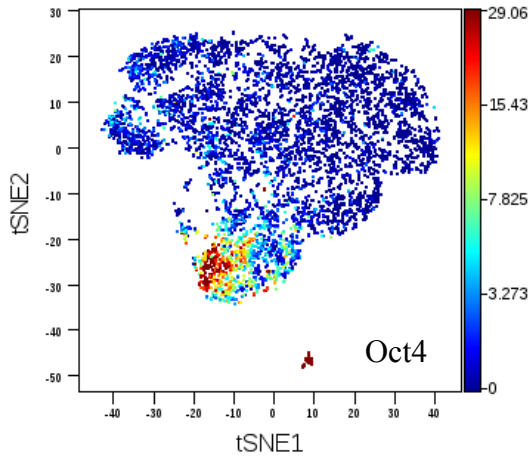
iPSC
End of Phase 1
iMSCs
BM-MSCs

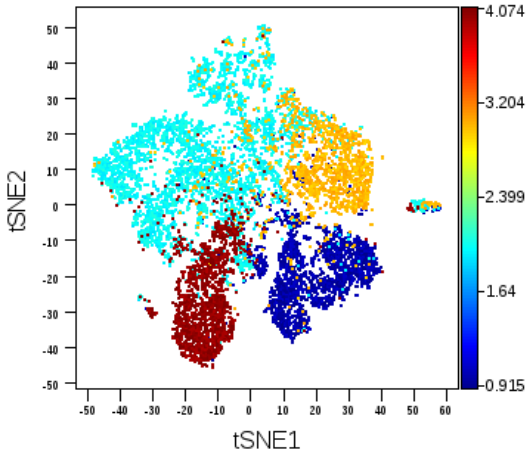




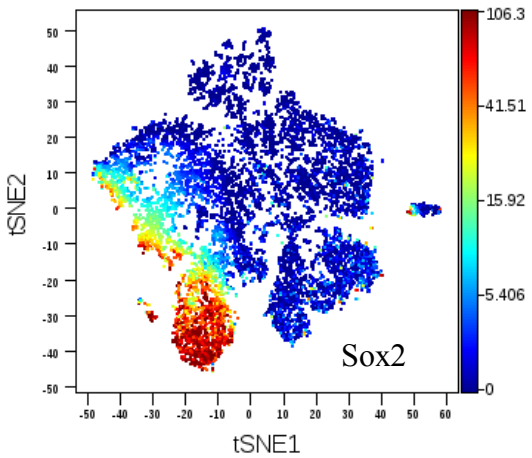


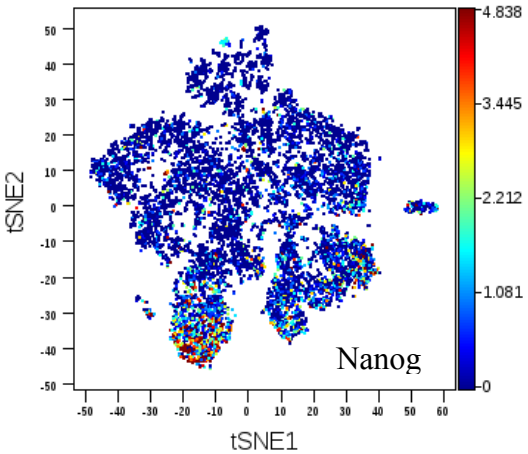




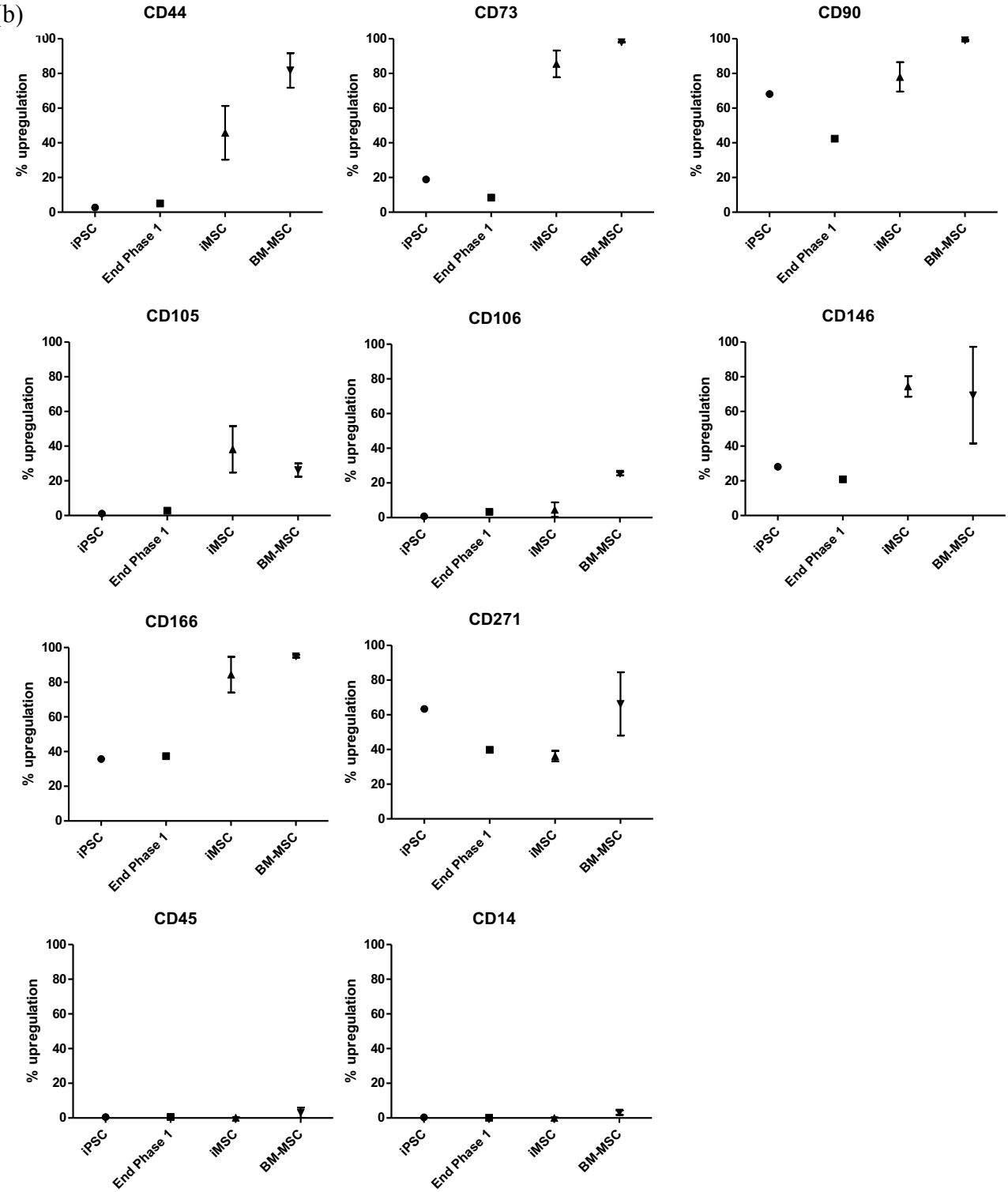


iPSC
End of Phase 1
iMSCs
BM-MSCs





(b)


CD44
CD73
CD90
CD105
CD106
CD146
CD166
CD271
CD45
CD14
% upregulation
0
20
40
60
80
100
iPSC
End Phase 1
iMSC
BM-MSC

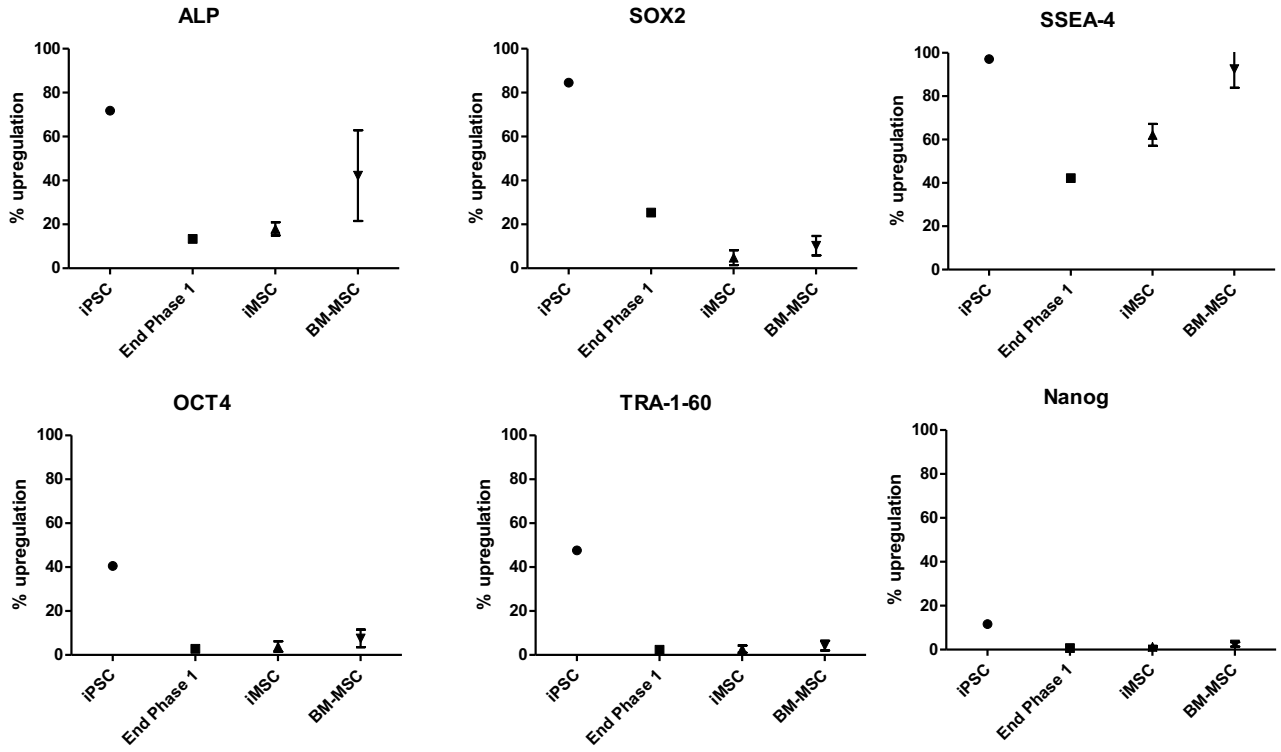


Figure 3.8 Protein expression levels during the iPSC into iMSC differentiation process. (a) ViSNE plots representing protein expression levels gathered through CyTOF. These plots are based on (dis)similarities between cell types, based on neighbouring distance between dots using T-distributed Stochastic Neighbor Embedding (t-SNE) on both the y-axis and x-axis. Each cell type is assigned a different colour in the viSNE plot in the top left corner of each page. Brown-red = iPSCs (N=1), light blue = end of phase 1 cells (N=1), yellow-orange = iMSCs (N=5), dark blue = BM-MSCs (N=2). All other viSNE plots describing protein expression of a single marker are coloured in such a way that the colour ascribed to a dot represents the expression level of that protein. Dark red meaning high expression and dark blue meaning no expression, as indicated in the coloured bar to the right of each viSNE plot. All the iPSCs and the iMSCs differentiated from them are of the same donor 840-03-03. BM-MSCs used originated from 2 different donors, both at different passages: Black P11 and Millipore P5. Mesenchymal stem cell (MSC) markers used: CD44, CD73, CD90, CD105, CD106, CD146, CD166, CD271. Negative (hematopoietic) MSC markers used: CD14, CD45. Pluripotency markers used: ALP, SSEA-4, Oct4, TRA-1-60, Nanog. (b) Results from the same CyTOF experiment as (a), with protein expression levels represented in a more quantitative manner. % upregulation on the y-axis and the different cell types (iPSC, end of phase 1, iMSC, BM-MSC) on the x-axis.

3.3.2 Gene expression profiling using RNA sequencing

Results for RNA seq experiments are displayed in figures 3.9, 3.10, 3.11 and 3.12. These include heatmaps and PCA plots. Heatmaps describe the relative gene expression over time compared to other timepoints. Expression levels are visualised in colour, dark blue describing minimum expression and dark red correlating to high levels of gene expression. The below mentioned epithelial-mesenchymal transition (EMT), MSC and pluripotency markers are all extracted from the current literature. In this thesis, these markers are the main focus within the RNA seq data analysis. RNA seq is, however, also able to identify new unknown important factors that play a role in molecular processes. This form of *de novo* gene identification was performed on the available data, yielding over 5000 differentially expressed genes (DEGs), including 547 transcription factors (TFs) and 28 epigenetic factors (EFs) in iPSC into iMSC differentiation. A complete list of differentially expressed TFs and EFs (per cluster) are presented in the supplemental data. For iMSC comparison to BM-MSC this yielded 1814 DEGs (data not shown). This thesis does not, however, go into detail regarding the individual *de novo* found DEGs. The supplemental data include a cluster heatmap for the differentiation of iMSCs into iPSCs with the accompanying Gene Ontology (GO) analysis.

3.3.2.1 Gene expression changes during iPSC to iMSC differentiation

Figure 3.9 shows a time course-based heatmap of gene expression changes, specifically mRNA, related to pluripotency, mesenchymal stem cells and EMT. A top 20 EMT gene list is included (table 3.2), ranked by their importance in EMT-related pathways (Zhao et al., 2015). *SMAD3, TGFB1, HIF1A, ZEB2, EGFR, ILK, ZEB1, TWIST1, SNAI2, EPAS1, SNAI1, MET* and *AKT1* display a similar gene expression pattern. Gene expression of these genes in iPSCs

is low and increases as the differentiation process into iMSCs continues. Most EMT-related genes show a gradual increase in their expression, the most profound effect being after the phase switch. Some genes, including *TWIST1, MET* and *EGFR*, present a direct expression increase compared to iPSCs. This increase is, however, followed by a fast decrease in expression, suggesting this effect might in part be due to stress-related events such as a change of medium. Interestingly, *ERBB2 (HER2)* is downregulated upon mesenchymal stem cell induction of iPSCs. ERBB2 is part of the EGF family of receptors and enhances kinase-mediated activation through binding with other members of the receptor family. In the literature, an increase in ERBB2 is linked to the EMT process (Ingthorsson et al., 2016). *CDH1 (Cadherin 1),* also known as E-cadherin (epithelial cadherin), is highly expressed in iPSCs. iPSCs and their pluripotency status depend on cell-cell connections. E-cadherin is a crucial cell-cell adhesion protein and hence part of the pluripotency maintenance mechanism (Soncin and Ward, 2011). Upon induction with mesenchymal condition medium, E-cadherin expression gradually declines throughout the first phase. However, a major decrease in gene expression is present upon switching to the second phase. This effect persists as passaging continues and upon reaching P4 the iMSCs have reached a stable state with low E-cadherin expression. EMT genes *CTNNB1, SMAD2, SMAD4, IGFR1* and *SMAD7* seem to be unaffected by the differentiation process.

Pluripotency marker genes *Sox2, Nanog, Oct4 (POU5F1), PODXL (TRA-1-60* and *TRA-1-81)* and *ALPL* display strong mRNA expression in iPSCs. Expression gradually decreases upon initiation of the differentiation process. The most profound effect in reduction of mRNA expression shows after the phase-switch. Upon reaching passage 3 (P3), expression of all pluripotency markers seemed to be stably and significantly decreased.

Mesenchymal stem cell marker genes *CD44, CD73 (NT5E), CD105 (ENG), CD106 (VCAM1), CD146 (MCAM)* and *CD166 (ALCAM)* displayed a slight increase in mRNA expression during phase 1 of the differentiation protocol. This was followed by a distinct increase in expression levels upon sub-culturing during phase 2. *CD271 (NGFR)* expression increased mainly in phase 1, followed by a decrease upon the switching of phases. *CD90 (THY1)* is a cell surface marker known to be upregulated in both pluripotent and mesenchymal stem cells. The heatmap displays *CD90* upregulated in iPSCs, followed by a decrease upon the initial mesenchymal induction and at the end of phase 1. However, after the phase-switch, *CD90* regains its initial expression value. Negative (hematopoietic) marker (*CD14* and *CD45 (PTPRC))* expression remained similar during the iPSC to iMSC differentiation process, both presenting low levels.

Gene	Name	Function
CTNNB1	Catenin-β1	Maintenance of epithelial cell layers through cell growth and adhesion
SMAD3	SMAD family member 3	TGF-β mediates formation of SMAD2/3/4 complex leading to transcriptional activation followed by EMT
HIF1A	Hypoxia Inducible Factor 1A	Master regulator of cellular and systemic homeostatic response to hypoxia by activating transcription of genes, together with HIF2A
TFGB1	Transforming Growth Factor β1	Multifunctional protein that controls proliferation, differentiation and other functions through activation of SMAD elements
ZEB2	Zinc Finger E-Box Binding Homeobox 2	Transcriptional inhibitor, repressing E-cadherin transcription together with ZEB1
EGFR	Epidermal Growth Factor Receptor	Induces cell differentiation and proliferation through binding of a ligand and activation, as well as EMT upon gene amplification
CDH1	E-cadherin (epithelial cadherin)	Tumor suppressor gene and cell-cell adhesion molecule keeping cells in an epithelial state
ILK	Integrin Linked Kinase	Part of the focal adhesion complex, transmitting extracellular matrix (ECM) signals into the cell
ZEB1	Zinc Finger E-Box Binding Homeobox 1	Transcriptional inhibitor, repressing E-cadherin transcription together with ZEB2
TWIST1	Twist-related protein 1	Transcriptional regulator important during embryonic development, and for EMT-like processes by sequestering E-cad
SNAI2	Snail Family Transcriptional Repressor 2	Transcriptional repressor downstream effector of the TGF-β and ILK pathways
EPAS1/HIF2A	Hypoxia Inducible Factor 2α	Master regulator of cellular and systemic homeostatic response to hypoxia by activating transcription of genes, together with HIF1A
SMAD2	SMAD family member 2	TGF-β mediates formation of SMAD2/3/4 complex leading to transcriptional activation followed by EMT
SNAI1	Snail Family Transcriptional Repressor 1	Transcriptional repressor, downstream effector of the TGF-β and ILK pathways
SMAD4	SMAD family member 4	TGF-β mediates formation of SMAD2/3/4 complex leading to transcriptional activation followed by EMT
IGF1R	Insulin-like Growth Factor Receptor 1	Binding of a ligand to this receptor initiates an intracellular cascade upregulating ZEB, TWIST and SNAIs
ERBB2/HER2	Proto-Oncogene Tyrosine Kinase 2	Member of the EGF receptor family, this subunit combines with other subunits to be able to bind a ligand, subsequently inducing differentiation and proliferation
MET	MET Proto-Oncogene, Receptor Tyrosine Kinase	This receptor binds hepatocyte growth factor (HGF) and initiates intracellular signalling upregulating EMT-related regulators including SNAI
AKT1	Protein Kinase B	Downstream regulator in the TGF-β pathway
SMAD7	SMAD family member 7	Context dependent regulatory protein occupying a dual role in the effects of the TGF-β pathway on EMT

Table 3.2 List of genes related to epithelial-mesenchymal transition (EMT) and their function.

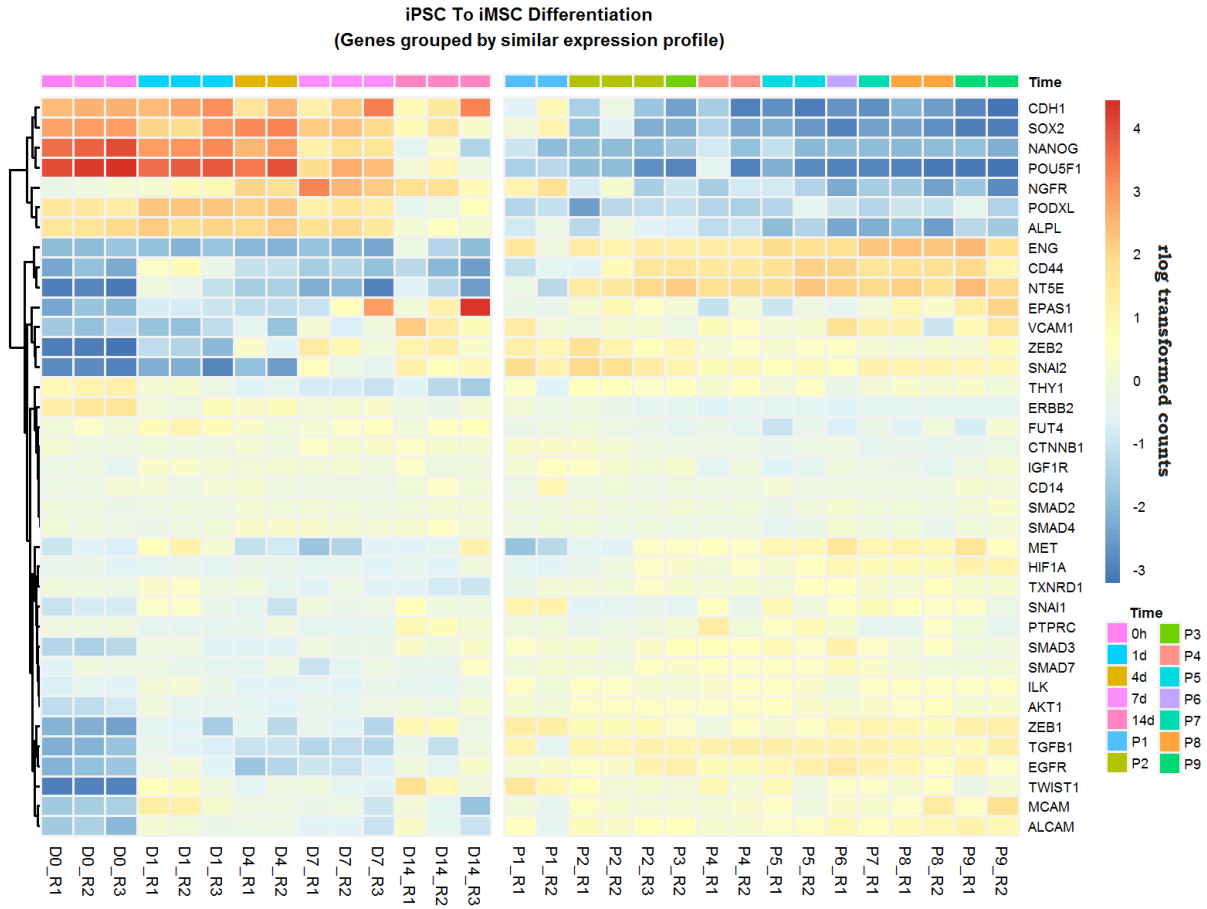


Figure 3.9 Heatmap representing gene expression changes during the iPSC into iMSC differentiation process. MSC^{+} markers include CD44, CD73 (NT5E), CD90 (THY1), CD105 (ENG), CD106 (VCAM1), CD146 (MCAM), CD166 (ALCAM), CD271 (NGFR). MSC^{-} markers include CD14 and CD45 (PTPRC). Pluripotency markers include Nanog, Oct4 (POU5F1), Sox2, SSEA-4 (FUT4), PODXL (TRA-1-60, TRA-1-81), ALPL. This heatmap is represented in a time course-based manner, phase 1 (14 days) on the left y-axis and phase 2 (passaging) on the right y-axis. Difference in gene expression levels is based on a colour-scheme, dark red representing high expression and dark blue representing low expression level. These expression levels are in rlog format, similar to log2 scale except with a minimised difference between samples for rows with small counts, and normalised with respect to library size.

Figure 3.10 displays a PCA (Principal Component Analysis) plot, often used to produce a new, easily readable set of dimensions, such that these dimensions are orthogonal (linearly independent) and ranked according to the variance of data along them. Thus, data with a smaller variance are less spread out than data with a big variance. In the PCA plot, both the x and y-axis have a variance measurement, PC1 (x-axis) being 68% and PC2 (y-axis) 12%. Upon induction of the differentiation process from iPSCs into iMSCs with a switch of medium, cells change their mRNA expression levels which is visualised as an upward movement on the y-axis (PC2). However, after the phase-switch, the same cells undergo a more significant change. They move towards the BM-MSCs, to the left on the x-axis and down on the y-axis. This plot aims to create a general gene expression profile overview during iPSC to iMSC differentiation and compared to BM-MSCs. Differentiating cells undergo gene expression changes in two phases, with the second phase resulting in the most profound change.

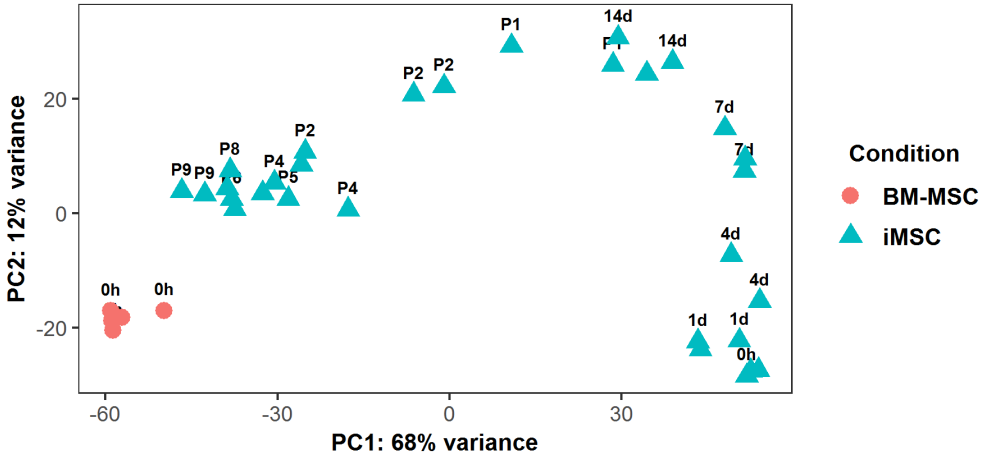


Figure 3.10 Principal Component Analysis (PCA) plot representing iPSC into iMSC differentiation. This plot restructures data to fit an orthogonal format based on the variance between cells during the iPSC to iMSC differentiation. Moreover, it compares the iMSCs to BM-MSCs in a similar manner based on differential gene expression profiles. This plot describes an x-axis (PC1) of 68% variance and a y-axis (PC2) of 12%. BM-MSCs include a variety of donors and passages of different experiments. BM-MSCs are represented by the dots, iMSCs by triangles in a time course-based manner.

3.3.2.2 Gene expression comparison of iMSCs and BM-MSCs

Gene expression profiles of iMSCs and BM-MSCs were compared. The analysis resulted in a DEG profile of 1814 genes with significant results. The PCA plot in figure 3.11 includes a comparison between the complete DEG profiles of iMSCs and BM-MSCs. Herein, PC1 (x-axis) shows a larger variance of 72%, compared to PC2 (y-axis) of 10%. BM-MSCs include a variety of donors and passages from different experiments. Within this range of BM-MSCs, a difference in variance can be seen in the plot on the y-axis (PC2). However, their variance on the x-axis (PC1) is minimal. iMSCs are displayed on the far right of the x-axis, thus indicating that the difference between iMSCs and BM-MSCs is much larger than between a wide variety of BM-MSCs.

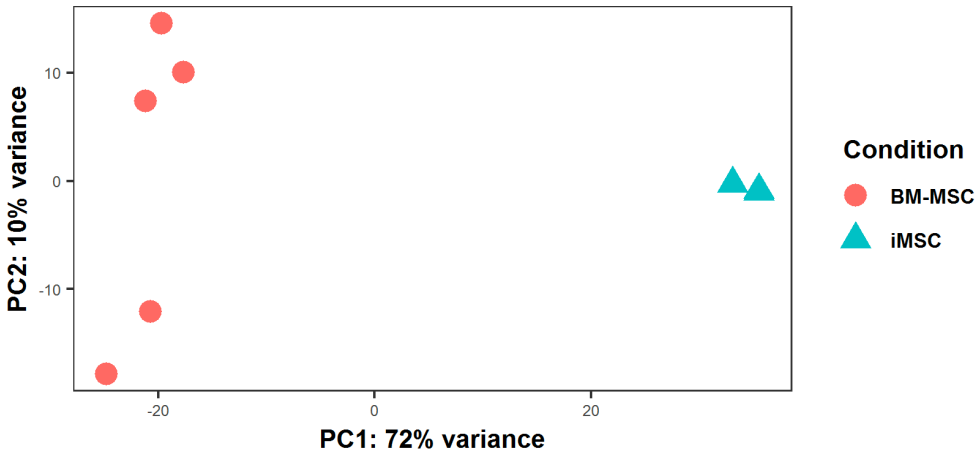


Figure 3.11 Principal Component Analysis (PCA) plot comparing iMSCs with BM-MSCs. This plot restructures data to fit an orthogonal format based on the variance between cell populations. Here, it compares the iMSCs to BM-MSCs based on differential gene expression profiles. This plot describes an x-axis (PC1) of 72% variance and a y-axis (PC2) of 10%. BM-MSCs include a variety of donors and passages of different experiments, hence the variation between those cell populations. iMSCs samples used were of P9. BM-MSCs are represented by the dots, iMSCs by triangles in a time course-based manner.

iMSCs and BM-MSCs were directly compared in terms of differentially expressed genes (DEGs), to determine (dis)similarities in known MSC and pluripotency markers (raw data not included). Between these two cell types, *CD90 (THY1)*, *CD105 (ENG)*, *CD106 (VCAM1)* and *CD146 (MCAM)* were differentially expressed. Of the negative MSC markers, *CD14* was also significant. Other MSC markers did not show significant differentially expressed genes. Of the pluripotency genes, *PODXL (TRA-1-60* and *TRA-1-81)* was the only gene differentially expressed. Figure 3.12 presents these results in heatmap form. *CD90 (THY1)*, *CD105 (ENG)*, *CD106 (VCAM1)* and *CD14* are downregulated in iMSCs compared to BM-MSCs. *CD146 (MCAM)* and *PODXL* are upregulated in iMSCs compared to BM-MSCs.

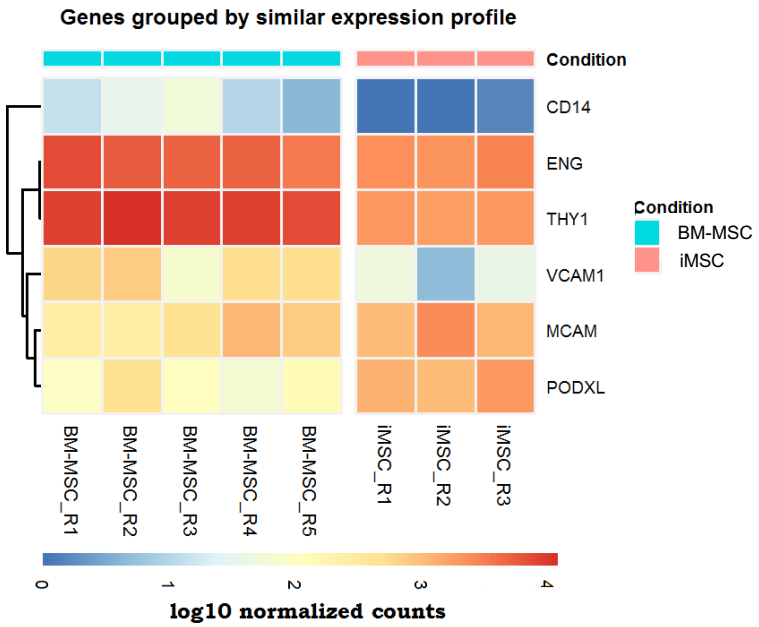


Figure 3.12 Heatmap of differentially expressed genes (DEGs) between iMSCs and BM-MSCs. It shows 5 BM-MSC replicates of various passages and donors, and 3 iMSC replicates of P8-9 of the same donor (840-03-03). Difference in gene expression levels is based on a color-scheme, dark red representing high expression and dark blue representing low expression level. These expression levels are in rlog format, similar to log2 scale except with a minimised difference between samples for rows with small counts, and normalised with respect to library size.

Furthermore, a Gene Ontology (GO) Enrichment Analysis was performed. GO is a categorical framework to define gene function. These categories include molecular functions, cellular components and biological processes. Differentially expressed genes between iMSCs and BM-MSCs were analysed using this tool. A complete list of the GO Enrichment Analysis can be found in the supplementary data. Within this list a few gene pathways and processes are of interest related to this thesis' purpose and aim. However, the general results are only briefly mentioned. A detailed pathway analysis using GO is beyond the scope of this work. The process network "ossification and bone remodelling", including related genes such as *BSP (bone sialoprotein), OPG (osteoprotegerin)* and certain *BMPs (bone morphogenetic proteins)* displayed a significant DEG profile. Osteogenesis is an important feature in BM-MSCs, as they are responsible for the production of new bone through their differentiation into osteoblasts. A complete list of pathways/processes and related genes can be found in the supplementary data.

3.3.3 Summary

The aim of subsection 3.3 was to provide a detailed analysis of the differentiation process of iPSCs into iMSCs using CyTOF and RNA seq. Protein expression levels were measured throughout this process using CyTOF, specifically comparing 4 subsets of cells: iPSCs, end of phase 1 cells, iMSCs and BM-MSCs. Pluripotency markers as well as MSC^+ and MSC^- markers were included in the panel. Protein expression trends started changing immediately upon the initiation of the differentiation process. Results are visualised using both viSNE plots and graphs (figure 3.8). The general trend among this data set shows a decrease in pluripotency markers, an increase in MSC^+ markers and stable MSC^- markers. The biggest change in protein expression occurs after the phase-switch, indicating that this event has a significant impact on the cell's transcriptional machinery. Moreover, it suggests survival of those cells that have been primed correctly towards a mesodermal lineage. Most MSC^+ marker and pluripotency marker expression levels in iMSCs compare to those of BM-MSCs, including CD44, CD73, CD90, CD105, CD146, CD166, ALP, Sox2, Oct4, Tra-1-60 and Nanog. However, CD106, CD271 and SSEA-4 are exceptions. These three markers were less upregulated in iMSCs compared to BM-MSCs. Interestingly, both CD271 and SSEA-4 marker expressions were similar between iPSCs and BM-MSCs.

Gene expression levels were also analysed during the differentiation process using RNA seq. This time course-based experiment included timepoints from both phase 1 and 2, specifically D0, D1, D4, D7, D14, P1, P2, P3……, P9. The data was visualised using heatmaps and PCA plots (figures 3.9, 3.10, 3.11 and 3.12). Moreover, the last paragraph includes a brief Gene Ontology (GO) analysis for the comparison between iMSCs and BM-MSCs.

The same pluripotency and MSC markers were included, as well as EMT markers. This analysis yielded over 5000 DEGs for the iPSC into iMSC differentiation and 1814 DEGs for the comparison between iMSCs and BM-MSCs. However, this thesis does not go into further detail regarding the *de novo* identified DEGs.

A list of 20 EMT-related genes (table 3.2) were included. Of these 20 genes *SMAD3, TGFB1, HIF1A, ZEB2, EGFR, ILK, ZEB1, TWIST1, SNAI2, CDH1, EPAS1, SNAI1, MET* and *AKT1* display similar gene expression patterns. This means that their expression levels increased as the differentiation process continued, with the most profound effect taking place after the phase switch event. However, some of the EMT genes did not follow this pattern. *ERBB2* is such an exception, whose expression decreased during this process rather than increased. *CTNNB1, SMAD2, SMAD4, IGFR1* and *SMAD7* seemed to be unaffected by the differentiation process. Pluripotency markers *Sox2, Nanog, Oct4, TRA-1-60, TRA-1-81* and *ALPL* all display a similar pattern; their expression decreased as the differentiation process proceeded. MSC markers *CD44, CD73, CD105, CD106, CD146* and *CD166* demonstrated a similar trend. A slight increase upon the start of the differentiation process, followed by an abrupt expression increase after switching to phase 2. As phase 2 progressed, a continuation of increased mRNA expression levels was notable. An exception to the trend in downregulation of pluripotency markers and upregulation in MSC markers was *CD271*, whose expression decreased upon the phase switch. The PCA plot (figure 3.10) – which includes all gene expression information – gives a general overview of the differentiation process and compares cells at different stages with BM-MSCs. It shows an initial conversion to a cell type less similar to BM-MSCs, but upon the phase switch this process is reversed. With each passage the cells are moving towards a more MSC-like transcriptomic profile.

Combining the findings of gene expression and protein expression levels throughout the differentiation process of iPSCs into iMSCs, it is notable that the trend between the two is similar. That is, pluripotency markers were downregulated, mainly in phase 1, whereas MSC^{+} markers were slowly upregulated, primarily in phase 2.

The RNA seq experiment also compared gene expression profiles between iMSCs and BM-MSCs. A DEG analysis was performed and resulted in a significant differential gene expression of *CD90, CD105, CD106*, *CD146, CD14* and *PODXL (TRA-1-60* and *TRA-1-81)*, as displayed in the heatmap (figure 3.12). Furthermore, in the GO Enrichment Analysis the pathway "ossification and bone remodelling" also displayed a significant DEG profile, suggesting a possible stronger osteogenic potential in iMSCs compared to BM-MSCs.

Chapter 4. Discussion

Mesenchymal stem cells (MSCs) are popular tools for a variety of applications due to their multitude of capabilities including self-renewal, multi-potential differentiation and their immunomodulatory role (Horwitz et al., 2005). However, use of MSCs is still limited due to *in vitro* and *in vivo* (clinical) related reasons. Clinical limitations refer to invasive harvesting of MSCs and the impaired self-renewal capacities of MSCs from older patients, making them undesirable for stem cell transplantation (Liu et al., 2017; Hynes et al., 2014). Furthermore, MSCs are popular *in vitro* tools used in a variety of experiments due to their multifunctional nature. The main limitation in using them for *in vitro* purposes is senescence, whereby MSCs undergo an artificial aging process and consequently stop proliferating. This in turn affects their usability as high cell numbers are difficult to attain, hindering use in specific experiments and creating reproducibility issues. For example, gene modification using the CRISPR/Cas9 system would be extremely difficult due to the low efficiency and subsequent need for colony selection. Therefore, it is highly desirable to develop and use an alternative MSC source. This is where induced MSCs (iMSCs) may offer a solution. Synthesized via iPSC differentiation, these iMSCs show greater proliferation and self-renewal capacities whilst preserving their tri-lineage differentiation abilities.

This thesis aimed to develop a standardized and reproducible protocol to establish viable iMSCs, to be used as a substitute tool for BM-MSCs. In order to establish this, protocols from the literature describing the differentiation of iPSCs into iMSCs were compared. Protocols used in this thesis are all based on the simple method of switching from iPSC to MSC medium, as described by Diederichs and Tuan (2014). This is currently the most popular method for producing iMSCs due to its practical nature. Within this overarching method of iMSC creation, there are slight variations. These variations are related to the type

of MSC medium. As such, different protocols, and thus different MSC medium conditions, were compared between each other to see which of these would create the 'best' iMSCs, based on their morphology and expression of the MSC markers CD44, CD90 and CD105 (Dominici et al., 2006). The protocol that resulted in viable and MSC-like cells was subsequently selected for more in-depth experimentation. Differentiation of iPSCs into iMSCs comprised two phases, of which the first 'initial' phase lasted for 14 days, followed by the second 'maturation' phase, also known as a passaging protocol.

Results for the first set of experiments, in which 5 protocols were compared, were surprising as many of the donor-condition combinations did not survive the phase-switch or shortly thereafter. Chapter 2.2 (table 2.1) recapitulates the various medium conditions used in these experiments. The cell death was an interesting and unexpected observation as all protocols were directly taken from the literature (Hynes et al., 2014; Kang et al., 2015; Chen et al., 2012; Sheyn et al., 2014; Liu et al., 2012), implying they should in principle all work. Protocols 4 and 5 performed worst, whereas protocol 2 seemed to be doing well across all three clones, purely regarding cell survival. The cell death issues could be related to immaturity of the cells, meaning they might not have had enough time to upregulate certain genes necessary to survive passaging without ROCK inhibitor (Boyd et al., 2009). iPSC reprogramming methods could also be of influence, affecting suitability of the cells for differentiation along the mesodermal lineage. The Sendai virus used for the reprogramming of these iPSCs, however, is widely used without any problems occurring in these iPSCs (Nakanishi and Otsu, 2012), making it highly unlikely that this is having a negative effect on their survival during the differentiation process. Cell seeding density is a factor known to be important for cell survivability and differentiation processes of iPSCs and other stem cells (Wilson et al., 2015; Zhou et al., 2011; Du et al., 2015; Nagasaka et al., 2017). Although cell seeding densities were monitored before the start of differentiation, iPSCs in conditions with

low cell survival could have had an undesirable cell seeding density to start with or colonies might not have had sufficient time to develop appropriately. Immunofluorescence for the surviving conditions (phase 2) generally resulted in a recurring pattern with upregulation of CD44 and CD105, with varying degrees of CD90 upregulation. However, upon reaching passage (P) 2 or 3, newly produced iMSCs turned senescent, halting their proliferation. Senescence is an aging related issue, known to occur in BM-MSCs directly upon the start of *in vitro* culturing (Bonab et al., 2006; Legzdina et al., 2016; Yu et al., 2018). The idea of creating iMSCs, however, was to circumvent this senescence issue, which meant the induction protocol had to be adjusted accordingly.

Confluency of endogenous MSC culture is known to correlate to senescence. Leaving MSCs at high confluency for too long causes them to acquire a more fibroblastic phenotype, resulting in the aforementioned cell senescence (Turinetto et al., 2016). Thus, phase 1 was shortened to decrease the time spent by iPSCs in an overly confluent state. However, this, again, resulted in cell senescence and thus the decision was made to leave the iMSCs growing on a Geltrex base, as the senescence phenomenon at P2 coincided with a transfer from the original Geltrex-coated plates to a non-coated plate. This indeed resulted in continued proliferation of iMSCs, which meant the loss of Geltrex coating, and not length of phase 1, was the senescence initiator.

This led to the second set of experiments, comparing the αMEM (previously known as condition 2) medium with a commercial MSC medium (MesenPro). Results for MSC marker expression in the αMEM condition showed upregulation of all three markers and downregulation of all three pluripotency markers. Similar to Hynes et al (2014), the upregulation of this set of MSC markers was part of the initial minimal requirements for these cells to be considered iMSC, as set by the ISCT (Dominici et al., 2006). Alkaline

Phosphatase (ALP) assays comparing αMEM -iMSCs and BM-MSCs during osteogenesis both with and without Geltrex-coatings, resulted in similar upregulation patterns, especially for replicate III. Kang et al (2015) found similar results, comparing ALP expression levels through qPCR between iMSCs and BM-MSCs, albeit their findings showed a more robust ALP presence in BM-MSCs. The tri-lineage differentiation potential, as mentioned before, is an essential criterion for MSCs. Therefore, iMSCs should in theory present the same differentiation abilities compared to (BM-)MSCs. In the literature, chondrogenic and osteogenic potential was found to be similar between iMSCs and BM-MSCs (Kang et al., 2015; Hynes et al., 2014; Liu et al., 2012; Sheyn et al., 2014; Chen et al., 2012; Diederichs et al., 2014; Frobel et al., 2014). Taking together the results of the ALP assay and Alizarin Red Staining for identification of osteogenic potential, it appears iMSCs and BM-MSCs show similar patterns. Early passage (P5) iMSCs exhibit abundant osteogenic potential, albeit this potential is slowly reduced during sub-culturing. This decrease in osteogenic potential also occurs in BM-MSCs via the same artificial aging process causing them to senesce (Turinetto et al., 2016). However, the decline of osteogenic potential in BM-MSCs is much quicker. iMSCs differentiating along the osteogenic lineage remained capable of mineralization even at P24, although, as mentioned before, to a much lesser degree than at P5. BM-MSCs typically completely loose osteogenic potential anywhere between P6 and P14, depending on the donor. Chondrogenic potential was not analysed in this thesis. Adipogenic potential in this thesis was determined by staining for lipid fat droplets using Oil Red O (ORO). None of the iMSCs formed lipid droplets, whereas BM-MSCs did result in formation of fat droplets. In the literature, adipogenic potential is uniformly found to be less pronounced in iMSCs, or not present at all (Hynes et al., 2014; Kaltz et al., 2008; Zhao et al., 2009; Diederichs et al., 2014; Frobel et al., 2014), which is in line with the current results of this thesis. The opposite happens in many pathological mechanisms, as well as during aging. Here, a shift of

differentiation propensity towards the adipogenic lineage occurs. The potential of MSCs to differentiate into chondrocytes and osteoblasts decreases, whereas their adipogenic potential significantly increases, resulting in an overall higher fat ratio and thus weakening the bones (Marędziak et al., 2016). Therefore it is tempting to speculate that a type of MSC with less adipogenic potential could actually be beneficial for certain therapeutic implications and be useful in *in vitro* research to understand MSC-related adipogenesis.

Results for the in-depth single cell protein expression analysis using CyTOF clearly presented the different profiles (using viSNE plots) of the four distinct cell populations: iPSCs, end of phase 1 cells, iMSCs and BM-MSCs. This data can be compared to the time course-based RNA seq data, specifically by using the heatmaps and PCA plots. Indeed, this data shows a similar change in initial gene expression upon the start of the differentiation process. This is subsequently followed by a more profound gene expression profile change after the phase-switch, acquiring a profile more similar to BM-MSCs as passaging continues.
In theory, all pluripotency marker expression should be decreased in iMSCs and MSC marker expression should increase, compared to their iPSC predecessor. Moreover, these values should in theory be similar to BM-MSCs. In practice, most of the MSC markers including CD44, CD73, CD90, CD105, CD146 and CD166 showed similar protein expression patterns between iMSCs and BM-MSCs, with CD106 and CD271 being two exceptions. CD106 was hardly expressed in iMSCs. This marker is known to vary in regular MSCs from different sources and even within BM-MSCs of different passage numbers and donors (Halfon et al., 2011; Yang et al., 2013). CD271 is a marker used in the detection of MSC (sub)-populations (Álvarez-Viejo et al., 2015; Rojewski et al., 2008). Results for BM-MSC CD271 expression in the current experiments were variable, highly dependent on the passage number, whereas iMSCs expressed this marker to a lesser extent. Interestingly, iPSCs expressed CD271 similar

to BM-MSCs, something not mentioned before in the literature. To confirm CyTOF protein expression, the results were compared to those from the time course-based RNA seq experiments. As the heatmap indicates, MSC gene marker expressions correlate to patterns in protein expression for all but CD271. *CD271* in iPSCs shows lower gene expression levels compared to iMSCs, whereas protein expression suggests a higher base level in iPSCs compared to iMSCs. On the other hand, pluripotency markers should ideally be highly expressed in iPSCs and modestly (to none) expressed in MSCs, and thus iMSCs. CyTOF results displayed this pattern for the markers Sox2, Tra-1-60, Oct4 and Nanog. Sox2 expression perfectly represented the ideal course of change in protein expression level, starting with high expression levels that decline towards the end of phase 1, followed by close to no expression in both iMSCs and BM-MSCs. Even though TRA-1-60, Oct4 and Nanog presented a similar pattern, it appeared that expression levels in iPSCs were not as high as expected. However, this is likely to be a result of an antibody concentration that was too low for this specific sample rather than the iPSCs not properly expressing these proteins. As mentioned before, the most important factor is the comparison of expression levels between iMSCs and BM-MSCs, not the purely quantitative protein expression level results. Comparing these results to those of the RNA seq experiments show similar expression patterns. All pluripotency marker genes are highly upregulated in iPSCs as shown in the heatmap, followed by a decrease mainly upon entering phase 2.

As mentioned in the introduction, current literature hypothesises an EMT-like process to occur during the differentiation of iPSCs into iMSCs (Boyd et al., 2009; Chen et al., 2012). Besides characterising the iPSC into iMSC differentiation process on the basis of MSC and pluripotency markers, this thesis aims to detail the mechanisms underlying this process a bit further. Thus, using the RNA seq data, this process was screened for gene expression changes

in 20 EMT-related genes (Zhao et al., 2015). Most of the EMT genes including *SMAD3, TGFB1, ZEB2, EGFR, ILK, ZEB1, TWIST1, SNAI2, EPAS1, SNAI1, MET* and *AKT1* have upregulated expression levels. TGFB1 comprises a large pathway and within the context of EMT includes regulatory proteins ZEB1, ZEB2, SNAI2, SNAI1, SMAD3, TWIST and consequently causes downregulation of CDH1 (E-cadherin) upon activation (Hanrahan et al., 2017; Xu et al., 2009). Other pathways include those related to hypoxia (through HIF1A) (Biddlestone et al., 2015), EGF (through EGFR) and MET receptor-activated pathways (Morgillo et al., 2016). AKT1 acts downstream in the EGF pathway and ILK initiates downregulation of CDH1 through activation of SNAI (Tan et al., 2001). These results link to the migratory feature of MSCs, independent of cell-cell contact for survival, as implied by the name of the above process: epithelial-to-mesenchymal transition.

To conclude, the iMSCs obtained from iPSCs using the αMEM medium method display similarities in their osteogenic potential, and protein and gene expression profiles. Adipogenic potential was found to be non-existent in iMSCs, whereas BM-MSCs formed lipid droplets, indicative of adipocyte formation. However, it should not be forgotten that BM-MSCs are a heterogeneous cell population and thus within this population there are proteomic and phenotypic differences to be found (Jones and Schäfer, 2015; Ullat et al., 2015). This heterogeneity inevitably means a wide variety of cells (BM-MSCs) all considered to be the same without necessarily being alike in phenotypic features and function, which makes employment of bulk methods directly comparing them with iMSCs challenging. Moreover, the process by which the iPSC differentiation into iMSCs takes place seems to rely on an EMT-like mechanism. However, these results should be viewed as a starting point and thus more research needs to be done in order to elucidate the differentiation mechanism.

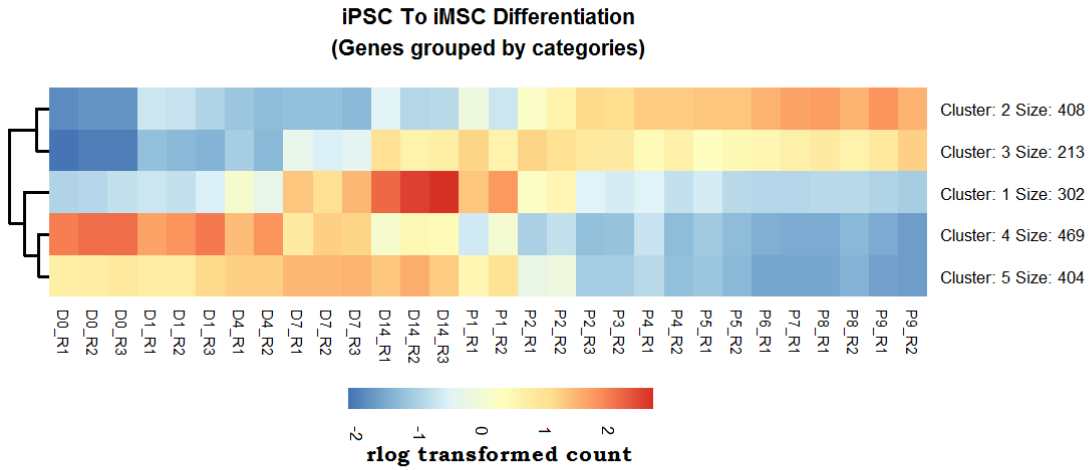
The aim for this thesis was to establish a standardized protocol based on results from multiple initial and in-depth experiments. The chosen protocol uses αMEM medium with a 14-day first phase followed by a passaging protocol. By comparison through several techniques it becomes evident that iMSCs are a distinct, yet similar cell population compared to BM-MSCs. They do present similar expression patterns both on a protein and gene expression level, with significant proliferative and osteogenic capabilities. The iMSCs therefore do seem like a plausible alternative to BM-MSCs. However, even though the initial results are promising, more repeats need to be done and different donors need to be included before definitive conclusions can be made.

4.1 Future work

If the project were to continue, several experiments could be included to further explore the mechanisms underlying the differentiation process and to compare between the iMSCs and BM-MSCs. Since the final in-depth experiments have used only one donor, it would be key to include more donors, and possibly iPSCs from different tissues of origin. A significant addition to the results would be to include the differentiation into the chondrogenic lineage, comparing the chondrogenic potential between iMSCs and BM-MSCs. Also, because the adipogenic differentiation did not work for iMSCs, different adipogenic protocols could be tested to see if any of these do induce differentiation along this lineage. Furthermore, osteoblast, adipocyte and chondrocyte markers could be included in the CyTOF panel, analysing the protein expression levels during differentiation from iPSCs into iMSCs and eventually differentiation into osteoblasts, adipocytes and chondrocytes. This same experiment could subsequently be performed using RNA seq to analyse the gene expression profiles of iMSC trilineage differentiation. A more advanced experiment could include an *in vivo* mouse model to test the bone regeneration capacity of these iMSCs and to compare those results to that of BM-MSCs.

Supplemental Data

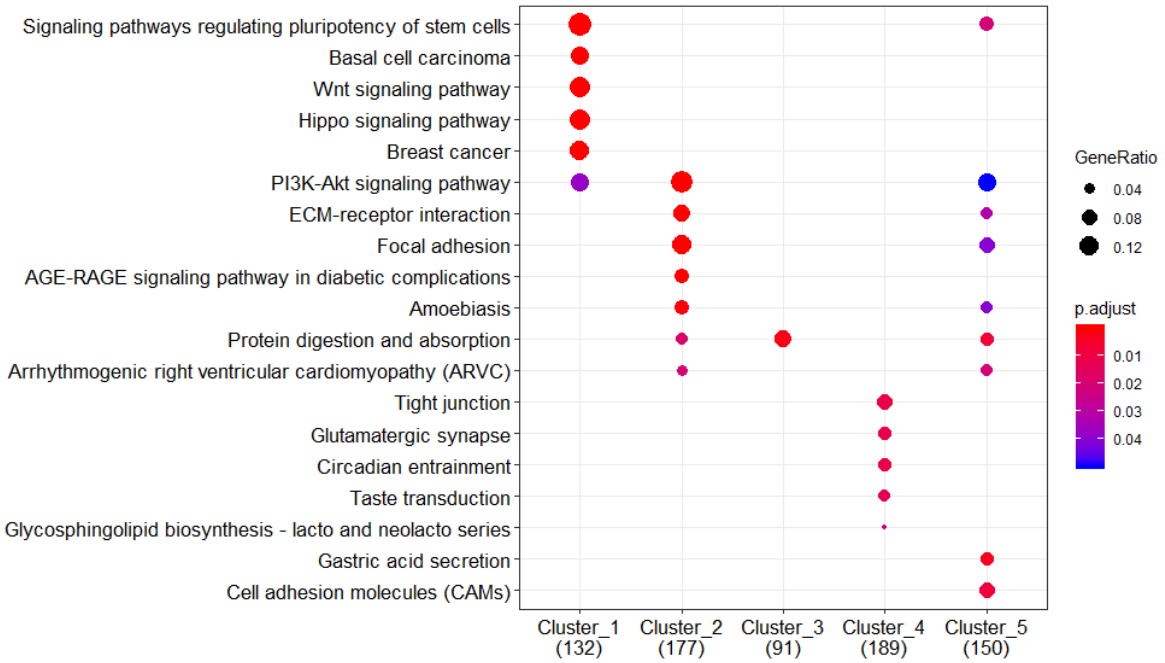
Clustered Gene Expression Profiles – iPSC differentiation into iMSCs



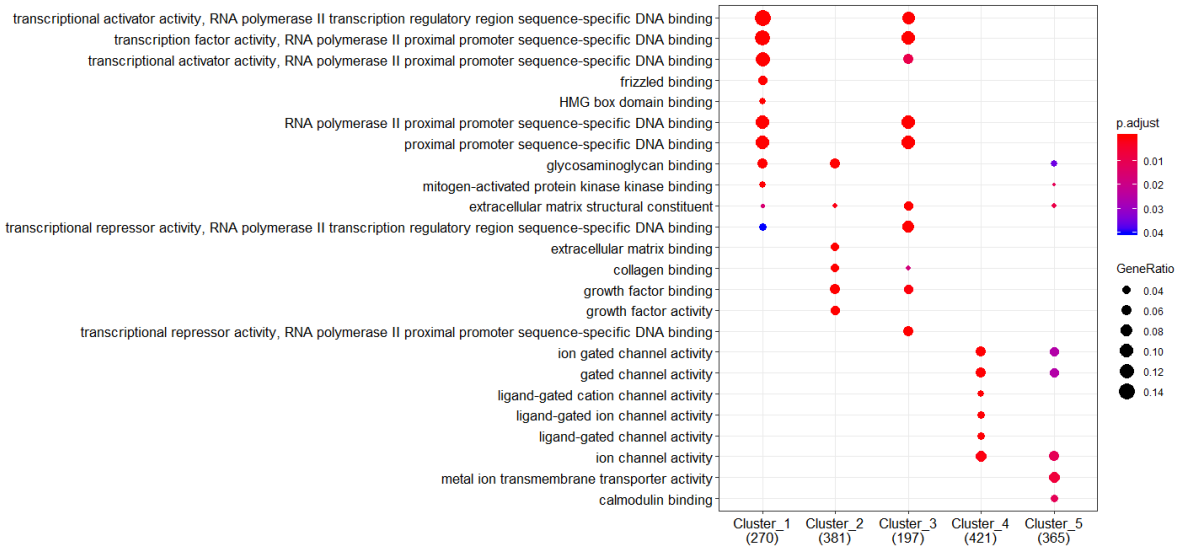
S1 Clustered heatmap of gene expression changes during iPSC into iMSC differentiation. Genes are clustered according the time of up- or downregulation. Within this heatmap, dark blue represents low to no expression, whereas dark red represents a high expression level.



S2 Clustered Gene Ontology (GO) Enrichment Analysis for the iPSC into iMSC differentiation process I. The categories include molecular functions, cellular components and biological processes. The clusters depicted on the x-axis represent the same clusters as those in figure S1. The epigenetic factors (EFs) and transcription factors (TFs) of these clusters are extracted and can be viewed in figures S5 and S6, respectively. In this graph, dots with a bright red colour represent a higher significance than dots with a blue colour.



S3 Clustered Gene Ontology (GO) Enrichment Analysis for the iPSC into iMSC differentiation process II. The categories include molecular functions, cellular components and biological processes. The clusters depicted on the x-axis represent the same clusters as those in figure S1. The epigenetic factors (EFs) and transcription factors (TFs) of these clusters are extracted and can be viewed in figures S5 and S6, respectively. In this graph, dots with a bright red colour represent a higher significance than dots with a blue colour.



S4 Clustered Gene Ontology (GO) Enrichment Analysis for the iPSC into iMSC differentiation process III. The categories include molecular functions, cellular components and biological processes. The clusters depicted on the x-axis represent the same clusters as those in figure S1. The epigenetic factors (EFs) and transcription factors (TFs) of these clusters are extracted and can be viewed in figures S5 and S6, respectively. In this graph, dots with a bright red colour represent a higher significance than dots with a blue colour.

Differentially expressed transcription factors and epigenetic factors – iPSC differentiation into iMSCs

Epigenetic Factors (EFs) – Per cluster

Gene	Gene description	Cluster
ASXL3	additional sex combs like 3, transcriptional	1
CRB2	crumbs 2, cell polarity complex component	1
ERBB4	erb-b2 receptor tyrosine kinase 4	1
EYA1	EYA transcriptional coactivator and phosphatase 1	1
EYA2	EYA transcriptional coactivator and phosphatase 2	1
EYA4	EYA transcriptional coactivator and phosphatase 4	1
ZBTB16	zinc finger and BTB domain containing 16	1
DPF3	double PHD fingers 3	2
PRDM8	PR/SET domain 8	2
SP100	SP100 nuclear antigen	2
SP140L	SP140 nuclear body protein like	2
NPAS2	neuronal PAS domain protein 2	2
PADI2	peptidyl arginine deiminase 2	2
VDR	vitamin D receptor	2
SMARCD3	SWI/SNF related, matrix associated, actin dependent	3
FOXP2	forkhead box P2	3
GADD45B	growth arrest and DNA damage inducible beta	3
SNAI2	snail family transcriptional repressor 2	3
CECR2	CECR2, histone acetyl-lysine reader	4
DNMT3B	DNA methyltransferase 3 beta	4
JARID2	jumonji and AT-rich interaction domain containing 2	4
NAP1L2	nucleosome assembly protein 1 like 2	4
PRDM14	PR/SET domain 14	4
PHC1	polyhomeotic homolog 1	4
PRKCB	protein kinase C beta	4
USP44	ubiquitin specific peptidase 44	4
CHD7	chromodomain helicase DNA binding protein 7	5
PHF21B	PHD finger protein 21B	5

S5 Epigenetic Factors (EFs) differentially expressed per cluster during the iPSC into iMSC differentiation process.

Transcription Factors (TFs) – Per Cluster

Gene	Gene description	Cluster
HAND1	heart and neural crest derivatives expressed 1	1
SP5	Sp5 transcription factor	1
TFAP2B	transcription factor AP-2 beta	1
HOXB2	homeobox B2	1
LMX1A	LIM homeobox transcription factor 1 alpha	1
ALX4	ALX homeobox 4	1
MSX1	msh homeobox 1	1
HOXB3	homeobox B3	1
CDX2	caudal type homeobox 2	1
HOXB1	homeobox B1	1
NEUROD1	neuronal differentiation 1	1
PAX7	paired box 7	1
DACH1	dachshund family transcription factor 1	1
LMX1B	LIM homeobox transcription factor 1 beta	1
LEF1	lymphoid enhancer binding factor 1	1
POU4F1	POU class 4 homeobox 1	1
ZIC1	Zic family member 1	1
SOX1	SRY-box 1	1
SOX10	SRY-box 10	1
HOXB4	homeobox B4	1
ATOH1	atonal bHLH transcription factor 1	1
PAX3	paired box 3	1
DLX5	distal-less homeobox 5	1
POU3F2	POU class 3 homeobox 2	1
HOXB9	homeobox B9	1
RFX4	regulatory factor X4	1
HOXA2	homeobox A2	1
HOXA1	homeobox A1	1
DLX3	distal-less homeobox 3	1
NEUROG1	neurogenin 1	1
PAX6	paired box 6	1
HOXB6	homeobox B6	1
GATA3	GATA binding protein 3	1
MEIS1	Meis homeobox 1	1
EOMES	eomesodermin	1
HOXB8	homeobox B8	1
ISL1	ISL LIM homeobox 1	1
NHLH1	nescient helix-loop-helix 1	1
GATA4	GATA binding protein 4	1
DACH2	dachshund family transcription factor 2	1
HOXC8	homeobox C8	1
ZBTB16	zinc finger and BTB domain containing 16	1
TSHZ2	teashirt zinc finger homeobox 2	1
TP63	tumor protein p63	1
NKX2-6	NK2 homeobox 6	1
SOX5	SRY-box 5	1
NEUROD4	neuronal differentiation 4	1
SOX17	SRY-box 17	1
HOXC6	homeobox C6	1
SOX6	SRY-box 6	1
EMX2	empty spiracles homeobox 2	1
HAND2	heart and neural crest derivatives expressed 2	1
ONECUT2	one cut homeobox 2	1
HEYL	hes related family bHLH transcription factor with YRPW motif-like	1
ZNF467	zinc finger protein 467	1

TBX4	T-box 4	1
DLX6	distal-less homeobox 6	1
EBF3	early B cell factor 3	1
EGR2	early growth response 2	1
PROX1	prospero homeobox 1	1
ELF3	E74 like ETS transcription factor 3	1
BARHL1	BarH like homeobox 1	1
MAFB	MAF bZIP transcription factor B	1
MIXL1	Mix paired-like homeobox	1
SP6	Sp6 transcription factor	1
IRX3	iroquois homeobox 3	1
HOXA3	homeobox A3	1
MEOX1	mesenchyme homeobox 1	1
PITX2	paired like homeodomain 2	1
FOXA2	forkhead box A2	1
SIX1	SIX homeobox 1	2
SP100	SP100 nuclear antigen	2
NFIX	nuclear factor I X	2
TBX18	T-box 18	2
FOXC2	forkhead box C2	2
DPF3	double PHD fingers 3	2
AHRR	aryl-hydrocarbon receptor repressor	2
SP140L	SP140 nuclear body protein like	2
KLF2	Kruppel like factor 2	2
DLX1	distal-less homeobox 1	2
MSC	musculin	2
HNF1B	HNF1 homeobox B	2
FOXS1	forkhead box S1	2
GLIS1	GLIS family zinc finger 1	2
SIM2	single-minded family bHLH transcription factor 2	2
FOXD1	forkhead box D1	2
FOSL1	FOS like 1, AP-1 transcription factor subunit	2
MYBL1	MYB proto-oncogene like 1	2
FOXL1	forkhead box L1	2
FLI1	Fli-1 proto-oncogene, ETS transcription factor	2
RUNX2	runt related transcription factor 2	2
HIC1	HIC ZBTB transcriptional repressor 1	2
AHR	aryl hydrocarbon receptor	2
NFIC	nuclear factor I C	2
CREB3L1	cAMP responsive element binding protein 3 like 1	2
NPAS2	neuronal PAS domain protein 2	2
VDR	vitamin D receptor	2
MKX	mohawk homeobox	2
ELF4	E74 like ETS transcription factor 4	2
PRDM8	PR/SET domain 8	2
FOSL2	FOS like 2, AP-1 transcription factor subunit	2
HLX	H2.0 like homeobox	2
PRRX1	paired related homeobox 1	3
NR2F2	nuclear receptor subfamily 2 group F member 2	3
NR2F1	nuclear receptor subfamily 2 group F member 1	3
ZNF503	zinc finger protein 503	3
MEIS2	Meis homeobox 2	3
SNAI2	snail family transcriptional repressor 2	3
PITX1	paired like homeodomain 1	3
MSX2	msh homeobox 2	3
TFAP2A	transcription factor AP-2 alpha	3

DLX2	distal-less homeobox 2	3
GATA6	GATA binding protein 6	3
ATOH8	atonal bHLH transcription factor 8	3
ARID5B	AT-rich interaction domain 5B	3
NKX6-1	NK6 homeobox 1	3
EPAS1	endothelial PAS domain protein 1	3
PLAGL1	PLAG1 like zinc finger 1	3
MBNL2	muscleblind like splicing regulator 2	3
FOXC1	forkhead box C1	3
TBX3	T-box 3	3
ZIC4	Zic family member 4	3
GLIS3	GLIS family zinc finger 3	3
ZNF703	zinc finger protein 703	3
ZEB2	zinc finger E-box binding homeobox 2	3
ZNF469	zinc finger protein 469	3
PKNOX2	PBX/knotted 1 homeobox 2	3
OSR1	odd-skipped related transciption factor 1	3
TBX2	T-box 2	3
FOXF2	forkhead box F2	3
EBF2	early B cell factor 2	3
EBF1	early B cell factor 1	3
TBX15	T-box 15	3
FOXP2	forkhead box P2	3
ZFHX4	zinc finger homeobox 4	3
FOSB	FosB proto-oncogene, AP-1 transcription factor subunit	3
RARB	retinoic acid receptor beta	3
RUNX1	runt related transcription factor 1	3
ZNF25	zinc finger protein 25	3
TSHZ1	teashirt zinc finger homeobox 1	3
TWIST1	twist family bHLH transcription factor 1	3
TCF21	transcription factor 21	3
ZEB1	zinc finger E-box binding homeobox 1	3
JUNB	JunB proto-oncogene, AP-1 transcription factor subunit	3
MEF2C	myocyte enhancer factor 2C	3
NFATC2	nuclear factor of activated T cells 2	3
TAL1	TAL bHLH transcription factor 1, erythroid differentiation factor	3
POU5F1	POU class 5 homeobox 1	4
LIN28A	lin-28 homolog A	4
ZSCAN10	zinc finger and SCAN domain containing 10	4
PRDM14	PR/SET domain 14	4
SOX2	SRY-box 2	4
ZFP42	ZFP42 zinc finger protein	4
NANOG	Nanog homeobox	4
SALL4	spalt like transcription factor 4	4
NR6A1	nuclear receptor subfamily 6 group A member 1	4
NKX1-2	NK1 homeobox 2	4
ZIC3	Zic family member 3	4
FOXH1G	forkhead box H1	4
RHL2	grainyhead like transcription factor 2	4
SOX3	SRY-box 3	4
POU5F1B	POU class 5 homeobox 1B	4
SALL3	spalt like transcription factor 3	4
SOX14	SRY-box 14	4
HES3	hes family bHLH transcription factor 3	4
SIX6	SIX homeobox 6	4
FOXA3	forkhead box A3	4

NANOGP8	Nanog homeobox retrogene P8	4
YBX2	Y-box binding protein 2	4
HMX2	H6 family homeobox 2	4
SPIB	Spi-B transcription factor	4
SALL1	spalt like transcription factor 1	4
TFCP2L1	transcription factor CP2 like 1	4
NR5A2	nuclear receptor subfamily 5 group A member 2	4
VENTX	VENT homeobox	4
ZNF483	zinc finger protein 483	4
OVOL2	ovo like zinc finger 2	4
SOX15	SRY-box 15	4
HESX1	HESX homeobox 1	4
ETV4	ETS variant 4	4
EMX1	empty spiracles homeobox 1	4
TCF15	transcription factor 15	4
TERF1	telomeric repeat binding factor 1	4
ZNF850	zinc finger protein 850	4
RORB	RAR related orphan receptor B	4
ETV1	ETS variant 1	4
SALL2	spalt like transcription factor 2	4
MYCN	orthodenticle homeobox 2	5
OTX2	LIM homeobox 5	5
LHX5	forkhead box D3	5
FOXD3	SRY-box 21	5
SOX21	FEZ family zinc finger 1	5
FEZF1	forkhead box I3	5
FOXI3	oligodendrocyte transcription factor 3	5
OLIG3	Sp8 transcription factor	5
SP8	grainyhead like transcription factor 3	5
GRHL3	INSM transcriptional repressor 1	5
INSM1	diencephalon/mesencephalon homeobox 1	5
DMBX1	iroquois homeobox 1	5
IRX1	forkhead box B1	5
FOXB1	zinc finger protein 423	5
ZNF423	cut like homeobox 2	5
CUX2	lin-28 homolog B	5
LIN28B	MYCL proto-oncogene, bHLH transcription factor	5
MYCL	BARX homeobox 1	5
BARX1	orthodenticle homeobox 1	5
OTX1	SIX homeobox 3	5
SIX3	AT-rich interaction domain 3B	5
ARID3B	BTB domain and CNC homolog 2	5
BACH2	SRY-box 8	5
SOX8	Kruppel like factor 15	5
KLF15	iroquois homeobox 2	5
IRX2	zinc finger protein 704	5
ZNF704	Zic family member 5	5
ZIC5	forkhead box J1	5
FOXJ1	LIM homeobox 8	5
LHX8	forkhead box I2	5
FOXI2	zinc finger and BTB domain containing 8B	5
ZBTB8B	thyroid hormone receptor beta	5
THRB	ERG, ETS transcription factor	5
ERG	Zic family member 2	5
ZIC2	interferon regulatory factor 6	5
IRF6	SRY-box 13	5
SOX13	zinc finger protein 385C	5

ZNF385C	grainyhead like transcription factor 1	5
GRHL1	hes family bHLH transcription factor 6	5
HES6	orthodenticle homeobox 2	5

S6 Transcription Factors (TFs) differentially expressed per cluster during the iPSC into iMSC differentiation process.

Gene Ontology Enrichment Analysis – iMSCs vs BM-MSCs

Pathway maps:

Protein folding and maturation_POMC processing	
Stromal-epithelial interaction in Prostate Cancer	
Bone metastases in Prostate Cancer	
Main genetic and epigenetic alterations in lung cancer	
Role of DNA methylation in progression of multiple myeloma	
IL-1 beta- and Endothelin-1-induced fibroblast/ myofibroblast migration and extracellular matrix production in asthmatic airways	
TGF-beta signaling via SMADs in breast cancer	
Cell adhesion_ECM remodeling	
Angiogenesis in HCC	
Transcription_HIF-1 targets	

S7 Gene Ontology (GO) Enrichment Analysis "pathway maps" comparing iMSCs with BM-MSCs. Genes related to these pathway maps are significantly higher expressed in iMSCs compared to BM-MSCs.

Process Networks:

Cell adhesion_Platelet-endothelium-leucocyte interactions	
Cell adhesion_Attractive and repulsive receptors	
Development_Regulation of angiogenesis	
Cell adhesion_Cell-matrix interactions	
Development_Ossification and bone remodeling	**SFRP4, PGE2R4, MSX-2, HOXA13, Galpha(s)-specific prostanoid GPCRs, HNF1, HOXC8, FGFR2, Tetranectin, BMP6, ENPP1, ETS, WNT, Bone sialoprotein, BMP4, IGF-2, BMPR1B, Activin, ActRIIB, Follistatin, ActRIIA, ANKH, ETS2, HOXA9, TGF-beta, Collagen X, Collagen II, Osteoprotegerin, CSF1, IBP4, OSF-2, DLX5, IGF-1, TBX3, p90Rsk, IBP, Frizzled, RANK(TNFRSF11A), GHR, C/EBPdelta**
Proteolysis_ECM remodeling	
Development_Neurogenesis_Synaptogenesis	

Reproduction_Progesterone signaling	
Development_Neurogenesis_Axonal guidance	
Development_Neurogenesis in general	

S8 Gene Ontology (GO) Enrichment Analysis "process networks" comparing iMSCs with BM-MSCs. Genes related to these process networks are significantly higher expressed in iMSCs compared to BM-MSCs. A complete list of genes within the "development_ossification and bone remodelling" process network is given due to its importance related to osteogenesis in iMSCs and BM-MSCs.

GO Processes:

system development	
multicellular organism development	
anatomical structure development	
developmental process	
anatomical structure morphogenesis	
nervous system development	
regulation of multicellular organismal process	
cell differentiation	
cellular developmental process	
animal organ development	

S9 Gene Ontology (GO) Enrichment Analysis "GO processes" comparing iMSCs with BM-MSCs. Genes related to these processes are significantly higher expressed in iMSCs compared to BM-MSCs.

References

Abdi R, Fiorina P, Adra CN, Atkinson M, Sayegh MH. Immunomodulation by mesenchymal stem cells: a potential therapeutic strategy for type 1 diabetes. *Diabetes*. 2008;57(7):1759–67

Altun G, Loring JF, Laurent LC. DNA methylation in embryonic stem cells. *Journal of Cellular Biochemistry*. 2010;109(1):1-6.

Álvarez-Viejo M, Menéndez-Menéndez Y, Otero-Hernández J. CD271 as a marker to identify mesenchymal stem cells from diverse sources before culture. *World Journal of Stem Cells*. 2015;7(2):470-476.

Bar-Nur O, HA Russ, S Efrat and N Benvenisty. Epigenetic memory and preferential lineage-specific dif- ferentiation in induced pluripotent stem cells derived from human pancreatic islet beta cells. *Cell Stem Cell.* 2011;9:17–23.

Barberi T, LM Willis, ND Socci and L Studer. Derivation of multipotent mesenchymal precursors from human embryonic stem cells. 2005.

Beevers J.E., Lai M.C., Collins E., Booth H.D.E., Zambon F., Parkkinen L., Vowles J., Cowley S.A., Wade-Martins R., Caffrey T.M. MAPT genetic variation and neuronal maturity alter isoform expression affecting axonal transport in iPSC-derived dopamine neurons. Stem Cell Reports. 2017;9:587–599.

Bendall SC, Simonds EF, Qiu P, Amir el- AD, Krutzik PO, Finck R, et al. Single-cell mass cytometry of differential immune and drug responses across a human hematopoietic continuum. *Science*. 2011.

Bennett, C. N., S. E. Ross, K. A. Longo, L. Bajnok, N. Hemati, K. W. Johnson, S. D. Harrison, and O. A. MacDougald. Regulation of Wnt signaling during adipogenesis. *J. Biol. Chem.* 2002;277:30998–31004.

Bentley DR, et al. Accurate whole human genome sequencing using reversible terminator chemistry. *Nature*. 2008;456:53–59.

Benvenuti S, Cellai I, Luciani P, Deledda C, Baglioni S, Giuliani C, et al. Rosiglitazone stimulates adipogenesis and decreases osteoblastogenesis in human mesenchymal stem cells. *J Endocrinol Invest.* 2007;30(9).

Biddlestone J, Bandarra D, Rocha S. The role of hypoxia in inflammatory disease (review). *Int J Mol Med*. 2015;35(4):859–69.

Bieback K, S Kern, A Kocaomer, K Ferlik and P Bugert. Comparing mesenchymal stromal cells from dif- ferent human tissues: bone marrow, adipose tissue and umbilical cord blood. *Biomed Mater Eng.* 2008; 18:S71–S76.

Bonab MM, Alimoghaddam K, Talebian F, et al. Aging of mesenchymal stem cell in vitro. *BMC Cell Biol.* 2006;7:14.

Bonab MM, et al. Aging of mesenchymal stem cell in vitro. *BMC Cell. Biol*. 2006;7:14.
Boyd N. L., Robbins K. R., Dhara S. K., West F. D., Stice S. L. Human embryonic stem cell-derived mesoderm-like epithelium transitions to mesenchymal progenitor cells. *Tissue Engineering Part a*. 2009;15(8):1897–1907.

Buganim Y, Faddah DA, Cheng AW, et al. Single-cell expression analyses during cellular reprogramming reveal an early stochastic and a late hierarchic phase. *Cell*. 2012;150:1209–22.
Cao, Z., R. Umek, and S. McKnight. Regulated expression of three C/EBP isoforms during adipose conversion of 3T3-L1 cells. *Genes Dev.* 1991;5:1538–1552.

Chen J., Shi Z. D., Ji X., et al. Enhanced osteogenesis of human mesenchymal stem cells by periodic heat shock in self-assembling peptide hydrogel. *Tissue Engineering. Part A*. 2013;19(5-6):716–728.

Chen Y.S., Pelekanos R.A., Ellis R.L., Horne R., Wolvetang E.J., Fisk N.M. Small molecule mesengenic induction of human induced pluripotent stem cells to generate mesenchymal stem/stromal cells. *Stem Cells Transl. Med.* 2012;1:83–95.

Chen, X. et al. Integration of external signalling pathways with the core transcription- al network in embryonic stem cells. *Cell*. 2008;133:1106-1117.

Christman JK. 5-azacytidine and 5-aza-2′-deoxycytidine as inhibitors of DNA methylation: Mechanistic studies and their implications for cancer therapy. *Oncogene*. 2002;21:5483–5495.

Costa-Silva J, Domingues D, Lopes FM. RNA-Seq differential expression analysis: An extended review and a software tool. *PLoS ONE.* 2017;12(12): e0190152.

da Silva Meirelles L, Chagastelles PC, Nardi NB. Mesenchymal stem cells reside in virtually all post- natal organs and tissues. *J. Cell Sci*. 2006; 119:2204–2213.

Dejosez, M. & Zwaka, T. P. Pluripotency and nuclear reprogramming. *Annu Rev Bio- chem.* 2012;81:737-765.

Deyle DR, Khan IF, Ren G, et al. Normal collagen and bone production by gene-targeted human osteogenesis imperfecta iPSCs. *Mol Ther.* 2012; 20: 204–13.

Diederichs S, Tuan RS. Functional comparison of human-induced pluripotent stem cell-derived mesenchymal cells and bone marrow-derived mesenchymal stromal cells from the same donor. Stem Cells Dev 2014;23:1594–1610.

Dominici M, K Le Blanc, I Mueller, I Slaper-Cortenbach, F Marini, D Krause, R Deans, A Keating, D Prockop and E Horwitz. Minimal criteria for defining multi- potent mesenchymal stromal cells. The International So- ciety for Cellular Therapy position statement. *Cytotherapy*. 2006; 8:315–317.

Donovan J., Abraham D., and Norman J. Platelet-derived growth factor signaling in mesenchymal cells. *Front. Biosci. (Landmark Ed.).* 2013;18:106–119.

Draper JS, Pigott C, Thomson JA, Andrews PW. Surface antigens of human embryonic stem cells: Changes upon differentiation in culture. *J Anat.* 2002;200:249–258

Du D.T., Hellen N., Kane C., Terracciano C.M. Action potential morphology of human induced pluripotent stem cell-derived cardiomyocytes does not predict cardiac chamber specificity and is dependent on cell density. *Biophys. J*. 2015;108:1–4.

Dupont C, Armant DR, Brenner CA. Epigenetics: definition, mechanisms and clinical perspective. *Semin Reprod Med*. 2009;27:351-7.

Emre, N., Vidal, J.G., Elia, J., O'Connor, E.D., Paramban, R.I., Hefferan, M.P., Navarro, R., Goldberg, D.S., Varki, N.M., Marsala, M., Carson, C.T., 2010. The ROCK inhibitor Y-27632 improves recovery of human embryonic stem cells after fluorescence- activated cell sorting with multiple cell surfacemarkers. *PLoS One* 5, e12148.

Fatherazi S, Matsa-Dunn D, Foster BL, Rutherford RB, Somerman MJ, Presland RB: Phosphate regulates osteopontin gene transcription. *J Dent Res.* 2009;88:39–44.

Fernandes H.J., Hartfield E.M., Christian H.C., Emmanoulidou E., Zheng Y., Booth H., Bogetofte H., Lang C., Ryan B.J., Sardi S.P. ER stress and autophagic perturbations lead to elevated extracellular α-synuclein in GBA-N370S Parkinson's iPSC-derived dopamine neurons. Stem Cell Reports. 2016, 6:342–356.

Foster BL, Nociti FH Jr, Swanson EC, Matsa-Dunn D, Berry JE, Cupp CJ, Zhang P, Somerman MJ: Regulation of cementoblast gene expression by inorganic phosphate in vitro. *Calcified Tissue Int*. 2006, 78:103–112.

Frobel J, Hemeda H, Lenz M, et al. Epigenetic Rejuvenation of Mesenchymal Stromal Cells Derived from Induced Pluripotent Stem Cells. *Stem Cell Reports*. 2014;3(3):414-422.
Galic S, Oakhill JS, Steinberg GR. Adipose tissue as an endocrine organ. *Mol Cell Endocrinol*. 2010;316(2):129–39.

Gao F, Chiu SM, Motan DA, et al. Mesenchymal stem cells and immunomodulation: current status and future prospects. *Cell Death Dis*. 2016;7:e2062.

Gao WX, et al. Effects of mesenchymal stem cells from human induced pluripotent stem cells on differentiation, maturation, and function of dendritic cells. *Stem Cell Res Ther.* 2017;8(1).

Gładych M, Andrzejewska A, Oleksiewicz U, Estécio MRH. Epigenetic mechanisms of induced pluripotency. *Contemporary Oncology*. 2015;19(1A):A30-A38.

Godini R, Lafta HY, Fallahi H. Epigenetic modifications in the embryonic and induced pluripotent stem cells. *Gene Expression Patterns*. 2018; 1-9.

González, F. et al. Generation of mouse-induced pluripotent stem cells by transient expression of a single nonviral polycistronic vector. *Proc. Natl Acad. Sci. USA.* 2009;106, 8918–8922.

Gonzalez, F., Boue, S., & Izpisua Belmonte, J. C. Methods for making induced pluripotent stem cells: reprogramming à la carte. *Nature Reviews Genetics*. 2011;17(2), 122.

Greenow, K. & Clarke, A. R. Controlling the stem cell compartment and regeneration in vivo: the role of pluripotency pathways. *Physiol Rev*. 2012;92:75-99.

Gu Y., Li T., Ding Y., Sun L., Tu T., Zhu W., Hu J., Sun X. Changes in mesenchymal stem cells following long-term culture in vitro. *Mol. Med. Rep.* 2016;13:5207–5215.

Halfon S., Abramov N., Grinblat B., Ginis I. Markers distinguishing mesenchymal stem cells from fibroblasts are downregulated with passaging. *Stem Cells*. 2011;20:53–66.

Hanrahan K, O'Neill A, Prencipe M, Bugler J, Murphy L, Fabre A, Puhr M, Culig Z, Murphy K, Watson RW. The role of epithelial-mesenchymal transition drivers ZEB1 and ZEB2 in mediating docetaxel-resistant prostate cancer. *Mol Oncol.* 2017;11:251–265.

Hansen, J. B., H. Zhang, T. H. Rasmussen, R. K. Petersen, E. N. Flindt, and K. Kristiansen. Peroxisome proliferator-activated receptor delta (PPARdelta)-mediated regulation of preadipocyte proliferation and gene expression is dependent on cAMP signaling. *J. Biol. Chem.* 2001;276:3175– 3182.

Horwitz EM, LeBlanc K, Dominici M, Mueller I, Slaper-Cortenbach I, Marini FC, et al. International Society for Cellular Therapy. Clarification of the nomenclature for MSC: the International Society for Cellular Therapy position statement. *Cytotherapy.* 2005;7:393-395.

Horwitz EM, Prockop DJ, Fitzpatrick LA, et al. Transplantability and therapeutic effects of bone marrow-derived mesenchymal cells in children with osteogenesis imperfecta. *Nat Med*. 1999; 5:309–313.

Hu Q, AM Friedrich, LV Johnson and DO Clegg. Memory in induced pluripotent stem cells: reprogrammed human retinal-pigmented epithelial cells show tendency for spontaneous redifferentiation. *Stem Cells.* 2010; 28:1981–1991.

Huang,C., Xu,M. and Zhu,B. Epigenetic inheritance mediated by histone lysine methylation: maintaining transcriptional states without the precise restoration of marks? *Philos. Trans. Roy. Soc. B*. 2013;368, 20110332.

Huangfu, D., Maehr, R., Guo, W., Eijkelenboom, A., Snitow, M., Chen, A. E., & Melton, D. A. Induction of pluripotent stem cells by defined factors is greatly improved by small-molecule compounds. *Nature Biotechnology*. 2008;26(7), 795–797.

Ingthorsson, S., Andersen, K., Hilmarsdottir, B., Maelandsmo, G. M., Magnusson, M.K.,&Gudjonsson, T. HER2 induced EMT and tumorigenicity in breast epithelial progenitor cells is inhibited by coexpression of EGFR. *Oncogene*. 2015; *35*, 4244.

International Stem Cell Initiative, Adewumi O, Aflatoonian B, Ahrlund-Richter L, Amit M, Andrews PW, Beighton G, Bello PA, Benvenisty N, Berry LS, Bevan S, et al. Characterization of human embryonic stem cell lines by the International Stem Cell Initiative. *Nat Biotechnol.* 2007;25: 803–816.

Johnson BV, Shindo N, Rathjen PD, Rathjen J, Keough RA. Understanding pluripotency-how embryonic stem cells keep their options open. *Mol Hum Reprod.* 2008;14:513–520.

Johnson C.I., Argyle D.J., Clements D.N. In vitro models for the study of osteoarthritis. *Vet. J.* 2016;209:40–49.

Jones E, Schäfer R. Where is the common ground between bone marrow mesenchymal stem/stromal cells from different donors and species? *Stem Cell Research & Therapy*. 2015;6(1):143.

Joyce N, Annett G, Wirthlin L, et al. Mesenchymal stem cells for the treatment of neurodegenerative disease. *Regen Med*. 2010; 5:933–946.

K. Hynes, D. Menicanin, K. Mrozik, S. Gronthos, and P. M. Bartold. Generation of functional mesenchymal stem cells from different induced pluripotent stem cell lines. *Stem Cells and Development.* 2014;23(10):1084–1096.
Kalluri R. EMT: When epithelial cells decide to become mesenchymal-like cells. 2009;119:1417-1419.

Kaltz N, A Funari, S Hippauf, B Delorme, D Noel, M Riminucci, VR Jacobs, T Haupl, C Jorgensen, et al. In vivo osteoprogenitor potency of human stromal cells from different tissues does not correlate with expression of POU5F1 or its pseudogenes. *Stem Cells.* 2008;26:2419–2424.

Kateřina Štefková, Jiřina Procházková, and Jiří Pacherník. Alkaline Phosphatase in Stem Cells. *Stem Cells International*. 2015.

Kern S, H Eichler, J Stoeve, H Kluter and K Bieback. Comparative analysis of mesenchymal stem cells from bone marrow, umbilical cord blood, or adipose tissue. *Stem Cells*. 2006; 24:1294–1301.

Kim K, A Doi, B Wen, K Ng, R Zhao, P Cahan, J Kim, MJ Aryee, H Ji, et al. Epigenetic memory in induced pluripotent stem cells. Nature 467:285–290.

Kim K, R Zhao, A Doi, K Ng, J Unternaehrer, P Cahan, H Huo, YH Loh, MJ Aryee, et al. Donor cell type can influence the epigenome and differentiation potential of human induced pluripotent stem cells. *Nat Biotechnol.* 2011;29:1117–1119.

Knight M.N., Hankenson K.D. Mesenchymal Stem Cells in Bone Regeneration. *Adv. Wound Care (New Rochelle).* 2013;2:306–316.

Korol A, Taiyab A, West-Mays JA. RhoA/ROCK signaling regulates TGFbeta-induced epithelial-mesenchymal transition of lens epithelial cells through MRTF-A. *Molecular medicine.* 2016:22.

Krabbe C., Zimmer J., Meyer M. Neural transdifferentiation of mesenchymal stem cells - A critical review. *APMIS-Acta Pathologica, Microbiologica et Immunologica Scandinavica*. 2005;113(11-12):831–844.

Kukurba KR, Montgomery SB. RNA Sequencing and Analysis. *Cold Spring Harb Protoc.* 2015;951–69.

Lai MI, Wendy-Yeo WY, Ramasamy R, Nordin N, Rosli R, Veerakumarasivam A, Abdullah S. Advancements in reprogramming strategies for the generation of induced pluripotent stem cells. *J Assist Reprod Genet.* 2011;28:4.

Le Blanc K, Frassoni F, Ball L, et al. Mesenchymal stem cells for treatment of steroid-resistant, severe, acute graft-versus-host disease: a phase II study. *Lancet*. 2008; 371:1579–1586.

Le Blanc K, Tammik L, Sundberg B, Haynesworth SE, Ringden O. Mesenchymal stem cells inhibit and stimulate mixed lymphocyte cultures and mitogenic responses independently of the major histocompatibility complex. *Scand J Immunol.* 200357:11–20.
Lee SB, D Seo, D Choi, KY Park, A Holczbauer, JU Marquardt, EA Conner, VM Factor and SS Thorgeirsson. Contribution of hepatic lineage stage-specific donor memory to the differential potential of induced mouse pluripotent stem cells. *Stem Cells*. 2012; 30:997–1007.

Legzdina D, Romanauska A, Nikulshin S, Kozlovska T, Berzins U. Characterization of senescence of culture-expanded human adipose-derived mesenchymal stem cells. *Intl J Stem Cell.* 2016;9(1):124–136.

Leonel C, Ferreira LC, Borin TF *et al* Inhibition of epithelial-mesenchymal transition in response to treatment with metformin and Y27632 in breast cancer cell lines. *Anticancer Agents Med Chem 2017*; 17.

Li O, Tormin A, Sundberg B, Hyllner J, Le Blanc K, Scheding S. Human embryonic stem cell-derived mesenchymal stroma cells (hES-MSCs) engraft in vivo and support hematopoiesis without suppressing immune function: implications for off-the shelf ES-MSC therapies. *PLoS One.* 2013;8(1).

Lian Q, Lye E, Suan Yeo K et al. Derivation of clinically compliant MSCs from CD105+, CD24- differentiated human ESCs. *STEM CELLS* 2007;25:425–436.

Lin Z, Fateh A, Salem DM, Intini G. Periosteum: biology and applications in craniofacial bone regeneration. *J. Dent. Res.* 2014;93:109–116.

Liu M, Lei H, Dong P, Fu X, Yang Z, Yang Y, et al. Adipose-derived mesenchymal stem cells from the elderly exhibit decreased migration and differentiation abilities with senescent properties. *Cell Transplant.* 2017;26(9):1505–1519.

Liu Y, Goldberg AJ, Dennis JE, et al. One- step derivation of mesenchymal stem cell (MSC)-like cells from human pluripotent stem cells on a fibrillar collagen coating. *PLoS ONE.* 2012; 7: e33225.

Liu Y., Goldberg A. J., Dennis J. E., Gronowicz G. A., Kuhn L. T. One-step derivation of mesenchymal stem cell (MSC)-like cells from human pluripotent stem cells on a 133ibrillary collagen coating. *PloS One*. 2012;7(3, article e33225).

Maldonado M, Luu RJ, Ramos ME, Nam J. ROCK inhibitor primes human induced pluripotent stem cells to selectively differentiate towards mesendodermal lineage via epithelial-mesenchymal transition-like modulation. *Stem Cell Res (Amst)* 2016; 17: 222–227.

Marędziak M, Marycz K, Tomaszewski KA, Kornicka K, Henry BM. The Influence of Aging on the Regenerative Potential of Human Adipose Derived Mesenchymal Stem Cells. *Stem Cells International*. 2016;2152435.

Mohamadnejad M, Alimoghaddam K, Mohyeddin. Phase 1 trial of autologous bone marrow mesenchymal stem cell transplantation in patients with decompensated liver cirrhosis. *Arch Iran Med.* 2007;10:459-466.

Morgillo F, Della Corte CM, Fasano M, Ciardiello F. Mechanisms of resistance to EGFR-targeted drugs: lung cancer. *ESMO Open*. 2016;1(3)
Nakanishi M, Otsu M. Development of Sendai virus vectors and their potential applications in gene therapy and regenerative medicine. *Curr Gene Ther.* 2012, 12(5):410–6.

Ohi Y, H Qin, C Hong, L Blouin, JM Polo, T Guo, Z Qi, SL Downey, PD Manos, et al. Incomplete DNA methylation underlies a transcriptional memory of somatic cells in human iPS cells. *Nat Cell Biol*. 2011;13:541–549.

Okita, K., Nakagawa, M., Hyenjong, H., Ichisaka, T. & Yamanaka, S. Generation of mouse induced pluripotent stem cells without viral vectors. *Science*. 2008;322, 949–953.

Onder TT, Kara N, Cherry A, et al. Chromatin-modifying enzymes as modulators of reprogramming. *Nature*. 2012;483:598–602.

Otto WR, Wright NA. Mesenchymal stem cells: from experiment to clinic. *Fibrogenesis Tissue Repair.* 2011;4:20.

Parekkadan B, Milwid JM. Mesenchymal stem cells as therapeutics. *Annu Rev Biomed Eng*. 2010;12:87–117.

Pauklin S, Vallier L. Activin/Nodal signalling in stem cells. *Development.* 2015;142: 607–619.

Pizzute T, Lynch K, Pei M. Impact of tissue-specific stem cells on lineage-specific differentiation: a focus on the musculoskeletal system. *Stem Cell Rev Rep.* 2015;11(1):119–32.

Polo JM, S Liu, ME Figueroa, W Kulalert, S Eminli, KY Tan, E Apostolou, M Stadtfeld, Y Li, et al. Cell type of origin influences the molecular and functional properties of mouse induced pluripotent stem cells. *Nat Biotechnol*. 2010;28:848–855.

Pomeroy JE, et al. Stem cell surface marker expression defines late stages of reprogramming to pluripotency in human fibroblasts. *Stem Cells Transl. Med.* 2016;5:870–882.

Ripa RS, Haack-Sorensen M, Wang Y, et al. Bone marrow derived mesenchymal cell mobilization by granulocyte-colony stimulating factor after acute myocardial infarction:

results from the stem cells in myocardial infarction (STEMMI) trial. *Circulation*. 2007; 116(11 suppl):I24–I30.

Rojewski MT, Weber BM, Schrezenmeier H. Phenotypic Characterization of Mesenchymal Stem Cells from Various Tissues. *Transfusion Medicine and Hemotherapy*. 2008;35(3):168-184.

Rolandsson Enes, S., Åhrman, E., Palani, A., Hallgren, O., Bjermer, L., Malmström, Westergren-Thorsson, G. (2017). Quantitative proteomic characterization of lung-MSC and bone marrow-MSC using DIA-mass spectrometry. *Scientific Reports*, *7*(1), 9316.

Romito A, Cobellis G. Pluripotent Stem Cells: Current Understanding and Future Directions. *Stem Cells International*. 2016;2016:9451492.
Satomaa T, Heiskanen A, Mikkola M, Olsson C, Blomqvist M, Tiittanen M, Jaatinen T, Aitio O, Olonen A, Helin J, et al. The N-glycome of human embryonic stem cells. *BMC Cell Biol.* 2009;10:42.

Schlaeger, T. M., Daheron, L., Brickler, T. R., Entwisle, S., Chan, K., Cianci, A., … Daley, G. Q. A comparison of non-integrating reprogramming methods. *Nature Biotechnology*. 2014;33(1), 58–63.

Scott MA, Nguyen VT, Levi B, James AW. Current methods of adipogenic differentiation of mesenchymal stem cells. *Stem Cells Dev.* 2011;20(10):1793–1804.

Sharbati J, Hanisch C, Pieper R, Einspanier R, Sharbati S. Small molecule and RNAi induced phenotype transition of expanded and primary colonic epithelial cells. *Scientific Report*s. 2015; 5:12681.

Sokolov MV, Panyutin IV, Onyshchenko MI, et al. Expression of pluripotency-associated genes in the surviving fraction of cultured human embryonic stem cells is not significantly affected by ionizing radiation. *Gene*. 2010;455:8–15.

Soncin F, Ward CM. The Function of E-Cadherin in Stem Cell Pluripotency and Self-Renewal. *Genes*. 2011;2(1):229-259.

Soufi A, Donahue G, Zaret KS. Facilitators and impediments of the pluripotency reprogramming factors' initial engagement with the genome. *Cell*. 2012;151:994–1004.

Sridharan R, Gonzales-Cope M, Chronis C, et al. Proteomic and genomic approaches reveal critical functions of H3K9 methylation and heterochromatin protein-1gamma in reprogramming to pluripotency. *Nat Cell Biol.* 2013;15:872–82.

Stolzing A, E Jones, D McGonagle and A Scutt. Age-related changes in human bone marrow-derived mes- enchymal stem cells: consequences for cell therapies. *Mech Ageing Dev.* 2008;129:163–173.

Styner M, Sen B, Xie Z, Case N, Rubin J. Indomethacin Promotes Adipogenesis of Mesenchymal Stem Cells Through a Cyclooxygenase Independent Mechanism. *Journal of Cellular Biochemistry*. 2010;111:1042–1050.

Sugawara T, Nishino K, Umezawa A, Akutsu H. Investigating cellular identity and manipulating cell fate using induced pluripotent stem cells. *Stem Cell Res. Ther.* 2012;3:8.

Tada H, Nemoto E, Foster BL, Somerman MJ, Shimauchi H: Phosphate increases bone morphogenetic protein-2 expression through cAMP- dependent protein kinase and ERK1/2 pathways in human dental pulp cells. *Bone.* 2011;48:1409–1416.

Takahashi K., Yamanaka S. Induction of pluripotent stem cells from mouse embryonic and adult fibroblast cultures by defined factors. *Cell*. 2006;126:663–676.

Tan, C., P. Costello, J. Sanghera, D. Dominguez, A. Garcia de Harreros, and S. Dedhar. Inhibition of integrin linked kinase (ILK) suppresses beta-catenin-Lef/Tcf-dependent transcription and expression of the E-cadherin suppressor, snail in APC −/− human colon carcinoma cells. *Oncogene*. 2001;20:133–140.

Tang, Q.-Q., M.-S. Jiang, and M. D. Lane. Repressive effect of Sp1 on the C/EBPgene promoter: role in adipocyte differentiation. *Mol. Cell. Biol.* 1999;19:4855–4865.

TheinHan W, Liu J, Tang M, et al. Induced pluripotent stem cell-derived mesenchymal stem cell seeding on biofunctionalized calcium phosphate cements. *Bone Res.* 2013; 4: 371–84.

Turinetto, V., Vitale, E., & Giachino, C. Senescence in Human Mesenchymal Stem Cells: Functional Changes and Implications in Stem Cell-Based Therapy. *International Journal of Molecular Sciences*. 2016;*17*(7), 1164.

Ullah I, Subbarao RB, Rho GJ. Human mesenchymal stem cells—current trends and future prospective. *Biosci Rep.* 2015;35(2).

Venable A, Mitalipova M, Lyons I, Jones K, Shin S, Pierce M, Stice S. Lectin binding profiles of SSEA-4 enriched, pluripotent human embryonic stem cell surfaces. *BMC Dev Biol*. 2005;5:15.

Waddington CH. The epigenotype. *Endeavour* 1942;1:18–20.

Waddington, CH. Towards a Theoretical Biology. Edinburgh, Scotland: Edinburgh University Press; 1968. *The Basic Ideas of Biology*; p. 1-32.

Wagner W, et al. Replicative senescence of mesenchymal stem cells: a continuous and organized process. *PLoS One.* 2008;3:e2213.

Wang, L. T. et al. Differentiation of mesenchymal stem cells from human induced pluripotent stem cells results in downregulation of c-Myc and DNA replication pathways with immunomodulation toward CD4 and CD8 Cells. *Stem Cells* (2018).

Warren, L. et al. Highly efficient reprogramming to pluripotency and directed differentiation of human cells with synthetic modified mRNA. *Cell Stem Cell*. 2010;7,618–630.

Watanabe, K., Ueno,M., Kamiya, D., Nishiyama, A.,Matsumura,M.,Wataya, T., Takahashi, J.B., Nishikawa, S., Muguruma, K., Sasai, Y., 2007. A ROCK inhibitor permits survival of dissociated human embryonic stemcells. *Nat. Biotechnol*. 25, 681–686.

Wearne KA, Winter HC, Goldstein IJ. Temporal changes in the carbohydrates expressed on BG01 human embryonic stem cells during differentiation as embryoid bodies. *Glycoconj J.* 2008;25:121–136.

Wearne KA, Winter HC, O'Shea K, Goldstein IJ. Use of lectins for probing differentiated human embryonic stem cells for carbohydrates. *Glycobiology*. 2006;16:981–990.

Wei, X., Yang, X., Han, Z.P., Qu, F.F., Shao, L. and Shi, Y.F. Mesenchymal stem cells: a new trend for cell therapy. *Acta Pharmacol. Sin.* 2013;34, 747–754.
Whitworth DJ, Frith JE, Frith TJR, Ovchinnikov DA, Cooper-White JJ, Wolvetang EJ. Derivation of mesenchymal stromal cells from canine induced pluripotent stem cells by inhibition of the TGFβ/activin signaling pathway. *Stem Cells Dev.* 2014;23:3021–33.

Wilson HK, Canfield SG, Hjortness MK, Palecek SP, Shusta EV. Exploring the effects of cell seeding density on the differentiation of human pluripotent stem cells to brain microvascular endothelial cells. *Fluids Barriers CNS*. 2015;12:13.

Wright AJ, Andrews PW. Surface marker antigens in the characterization of human embryonic stem cells. *Stem Cell Res*. 2009;3:3–11.

Wu, Ct; Morris, JR. Genes, genetics, and epigenetics: a correspondence. *Science* 2001;293(5532): 1103–1105.

Xu J, Lamouille S, Derynck R. TGF-beta-induced epithelial to mesenchymal transition. *Cell Res.* 2009;19:156–72.

Xu, R. H. et al. Basic FGF and suppression of BMP signaling sustain undifferentiated proliferation of human ES cells. *Nat Methods.* 2005:185-190.

Xue, K., Ng, J. H. & Ng, H. H. Mapping the networks for pluripotency. *Philos Trans R Soc Lond B Biol Sci.* 2011;366:2238-2246.

Yang ZX, Han Z-B, Ji YR, Wang YW, Liang L, Chi Y, Yang SG, Li LN, Luo WF, Li JP, Chen DD, Du WJ, Cao XC, Zhuo GS, Wang T, Han ZC. CD106 identifies a subpopulation of mesenchymal stem cells with unique immunomodulatory properties. *PLoS One*. 2013;8(3).

Yu, J., Shi, J., Zhang, Y., Zhang, Y., Huang, Y., Chen, Z., & Yang, J. The replicative senescent mesenchymal stem / stromal cells defect in DNA damage response and anti-oxidative capacity. *International Journal of Medical Sciences*. 2018;*15*(8), 771–781.

Zhang Z, Zhang Y, Gao F, Han S, Cheah KS, Tse H-F, et al. CRISPR/Cas9 Genome-Editing System in Human Stem Cells: Current Status and Future Prospects. *Mol. Ther. Nucleic Acids*. 2017; 9:230–241.

Zhao L, G Li, KM Chan, Y Wang and PF Tang. Comparison of multipotent differentiation potentials of mu- rine primary bone marrow stromal cells and mesenchymal stem cell line C3H10T1/2. *Calcif Tissue Int.* 2009;84:56–64.

Zhao M, Kong L, Liu Y, Qu H. dbEMT: an epithelial-mesenchymal transition associated gene resource. *Sci Rep.* 2015;5:11459.

Zhao Q, Ren H, Han Z. Mesenchymal stem cells: Immunomodulatory capability and clinical potential in immune diseases. *Journal of Cellular Immunotherapy.* 2016;3-20

Zhou H., Weir M.D., Xu H.H. Effect of cell seeding density on proliferation and osteodifferentiation of umbilical cord stem cells on calcium phosphate cement-fiber scaffold. *Tissue Eng Part A*. 2011;17:2603–2613.

Zhou S, JS Greenberger, MW Epperly, JP Goff, C Adler, MS Leboff and J Glowacki. Age-related intrinsic changes in human bone-marrow-derived mesenchymal stem cells and their differentiation to osteoblasts. *Aging Cell.* 2008; 7:335–343.